Colloquium: Graphene spectroscopy

D. N. Basov* and M. M. Fogler†

Department of Physics, University of California San Diego, 9500 Gilman Drive, La Jolla, California 92093, USA

A. Lanzara and Feng Wang

Department of Physics, University of California at Berkeley, Berkeley, California 94720, USA and Materials Science Division, Lawrence Berkeley National Laboratory, Berkeley, California 94720, USA

Yuanbo Zhang张远波

State Key Laboratory of Surface Physics and Department of Physics, Fudan University, Shanghai 200433, China

(published 23 July 2014)

Spectroscopic studies of electronic phenomena in graphene are reviewed. A variety of methods and techniques are surveyed, from quasiparticle spectroscopies (tunneling, photoemission) to methods probing density and current response (infrared optics, Raman) to scanning probe nanoscopy and ultrafast pump-probe experiments. Vast complimentary information derived from these investigations is shown to highlight unusual properties of Dirac quasiparticles and many-body interaction effects in the physics of graphene.

DOI: 10.1103/RevModPhys.86.959 PACS numbers: 81.05.U−, 73.20.−r, 03.65.Pm, 82.45.Mp

CONTENTS

*dbasov@ucsd.edu
†mfogler@ucsd.edu

I. INTRODUCTION

A. Scope of this review

Graphene is a single atomic layer of sp^2-hybridized carbon atoms arranged in a honeycomb lattice. This two-dimensional (2D) allotrope of carbon is characterized by a number of superlative virtues (Geim, 2009), e.g., a record-high electronic mobility at ambient conditions (Morozov *et al.*, 2008), exceptional mechanical strength (C. Lee *et al.*, 2008), and thermal conductivity (Balandin *et al.*, 2008; Ghosh *et al.*, 2008). Remarkable properties of graphene have ignited tremendous interest that resulted in approximately 50 000 publications at the time of writing. A number of authoritative reviews (Castro Neto *et al.*, 2009; Peres, 2010; Das Sarma *et al.*, 2011; Katsnelson, 2012; Kotov *et al.*, 2012; McCann and Koshino, 2013) have been written to survey this body of literature but no single review can any longer cover the entire topic. The purpose of this Colloquium is to specifically overview the spectroscopic experiments that have helped to shape the modern understanding of the physical properties of graphene. While selected topics in graphene spectroscopy have been discussed [Orlita and Potemski (2010) for optics, Ni, Wang *et al.* (2008) and Dresselhaus *et al.* (2012) for Raman scattering, Li and Andrei (2012) for scanning tunneling spectroscopy (STS), and Connolly and Smith (2010) for other scanned probes], here we present a panoramic view of physical phenomena in graphene emerging from both spectroscopy and imaging [Fig. 1(c)].

Spectroscopic observables can be formally categorized as either quasiparticle or current or density response functions. The former are fermionic, and the latter are bosonic. The

former is traditionally measured by photoemission and tunneling spectroscopy, while the latter can be investigated by, e.g., optical spectroscopy. Yet it may be possible to infer both quasiparticle and collective properties from the same type of measurements. For example, fine anomalies of the quasiparticle spectra seen in photoemission can give information about interactions between quasiparticles and collective modes (Sec. III.D). Conversely, optical conductivity, which is a collective response, enables one to infer, with some approximation, the parameters of a quasiparticle band structure (Secs. II.B, II.C, III.A, and V).

Finding such connections is facilitated by spectacular tunability of graphene. For example, with photoemission or tunneling techniques one can monitor the chemical potential μ of graphene as a function of the electron concentration N and thereby extract the thermodynamic density of states. The same physical quantity can be measured by a very different technique, the scanning single-electron transistor microscopy. In our analysis of such complementary data we focus on what we believe are the most pressing topics in the physics of graphene, e.g., many-body effects. Additionally, our Colloquium covers information obtained by scanned probes and out-of-equilibrium methods that greatly expand available means to study graphene in space and time domains. Finally, we briefly address phenomena that arise when physical properties of graphene are altered via its environment and nanostructuring.

B. Graphene morphology

Graphene can be isolated or fabricated in a number of different forms, which is an important consideration in spectroscopy. Effectiveness of a given spectroscopic tool depends on the accessibility of the sample surface to the incident radiation. The size of the accessible area must normally be larger than the wavelength of the incident beam unless near-field probes are employed (Sec. III.B). Mosaic structure and defects may affect momentum and energy resolution of the measurement. Graphene differs widely in terms of these parameters depending on the preparation method. Mechanical exfoliation of graphite typically produces single, bilayer, and multilayer graphene (SLG, BLG, and MLG, respectively) of a few μm in size, although occasionally samples of dimensions of hundreds of μm can be obtained. Exfoliated samples can be transferred onto insulating substrates, after which they can be gated and subject to transport measurements. The sign and the magnitude of carrier concentration N in gated samples can be precisely controlled over a wide range. The lower bound on $|N| \sim 10^{10}$ cm^{-2} is set by inhomogeneities (Sec. IV.A). The upper bound $|N| \sim 10^{13}$ cm^{-2} is limited by the dielectric breakdown strength of the substrate, although still higher $|N|$ are achievable by electrolytic gating (Mak *et al.*, 2009; Jilin Xia *et al.*, 2009; Efetov and Kim, 2010; Ju *et al.*, 2011; Newaz *et al.*, 2012). The carrier concentration can also be controlled by doping (Chen *et al.*, 2008).

Morphologically, exfoliated samples are single crystals. They hold the record for transport mobility μ_{tr} although it varies much with the type of the substrate. Currently, high-quality hexagonal boron nitride (hBN) substrates enable one to achieve $\mu_{tr} \sim 10^5$ cm^2/V s, which is about an order of magnitude higher than what is typical for graphene on SiO_2 and corresponds to the μm-scale mean-free path (Dean *et al.*, 2010; Mayorov *et al.*, 2011b). The highest mobility $\sim 10^6$ cm^2/V s is demonstrated by exfoliated graphene that is suspended off a substrate and subject to current annealing (Bolotin *et al.*, 2008; Du *et al.*, 2008; Elias *et al.*, 2011). Mechanical instabilities limit the size of suspended devices to 1–2 μm and restrict the maximum $|N|$ to a few times 10^{11} cm^{-2}.

Large-area graphene can be made by another method: epitaxial growth on SiC by thermal desorption of Si (van Bommel, Crombeen, and van Tooren, 1975). Epitaxial graphene may contain a single layer or many dozens of layers. The initial layer (layer number $L = 0$) has strong covalent bonds to the SiC substrate and is electronically different from the ideal SLG (de Heer *et al.*, 2007). The morphology and electron properties of the subsequent layers $L > 0$ depend on which SiC crystal face it is grown: the Si-terminated (0001) face or the C-terminated $(000\bar{1})$ face (Nagashima *et al.*, 1993; Forbeaux, Themlin, and Debever, 1998; Charrier *et al.*, 2002; Berger *et al.*, 2004, 2006; Ohta *et al.*, 2006; Rollings *et al.*, 2006; Emtsev *et al.*, 2009). According to de Heer *et al.* (2011), the Si-face grown graphene is orientationally ordered and has the Bernal stacking (as in graphite). The structure of the C-face epitaxial graphene is consistent with a stacking where every other layer is rotated by approximately $\pm 7°$ with respect to a certain average orientation. The rotations inhibit interlayer tunneling so that the band structure of each layer is similar to SLG (see also Sec. IV.B).

The morphology of the epitaxial graphene after annealing resembles a carpet draping over the staircase (Emtsev *et al.*, 2009). It is characterized by domains a few μm wide and up to 50 μm long that mirror the underlying SiC terraces (Emtsev *et al.*, 2009; de Heer *et al.*, 2011).

The graphene/SiC interface is charged, inducing the n-type doping of about 10^{13} cm^{-2} in the first ($L = 1$) graphene layer. Other layers have much smaller carrier concentration because of screening. The screening length of about one layer was measured by ultrafast infrared (IR) spectroscopy (Dong Sun *et al.*, 2010). The doping of the surface layers can be altered by depositing charged impurities (Ohta *et al.*, 2006; Zhou, Siegel, Fedorov, and Lanzara, 2008a). Relatively low mobility $\mu_{tr} = 500$–$10\,000$ cm^2/V s, the inhomogeneity of the doping profile, and the lack of its *in situ* control can be seen as drawbacks of (the first generation of) epitaxial compared to exfoliated graphene. On the other hand, the much larger surface area of the epitaxial graphene is advantageous for spectroscopic studies and applications (de Heer *et al.*, 2007). An important recent breakthrough is epitaxial growth of graphene on high-quality hBN substrates (Yang *et al.*, 2013).

Graphene samples of strikingly large 30-in. width (Bae *et al.*, 2010) can be produced by the chemical vapor deposition (CVD) on metallic surfaces, e.g., Ru, Ni, or Cu that act as catalysts. CVD graphene can be transferred to insulating substrates making it amenable to gating and transport experiments (Kim *et al.*, 2009; Bae *et al.*, 2010). The microstructure of CVD graphene sensitively depends on the roughness of the metallic substrate and the growth conditions. Typical structural defects of CVD graphene are wrinkles and folds induced

by the transfer process and also by thermal expansion of graphene upon cooling. Grain boundaries are other common defects that have been directly imaged by micro-Raman (Li *et al.*, 2010), transmission electron microscopy (Huang *et al.*, 2011), scanning tunneling microscopy (Tapasztó *et al.*, 2012; Koepke *et al.*, 2013), and near-field microscopy (Fei *et al.*, 2013). The corresponding domain sizes range between 1 and 20 μm. On the other hand, graphene single crystals with dimension ~0.5 mm have been grown on Cu by CVD (Li *et al.*, 2011). Transport mobilities of CVD-grown graphene and epitaxial graphene on SiC are roughly on par.

At the opposite extreme of spatial scales are nanocrystals and nanoribbons. Graphene crystals of nm size can be synthesized by the reduction of graphene oxide [this can be done chemically (Boehm *et al.*, 1962; Dikin *et al.*, 2007) or via IR irradiation (El-Kady *et al.*, 2012)] or by ultrasonic cleavage of graphite in an organic solvent (Hernandez *et al.*, 2008; Nair *et al.*, 2012). Laminates of such crystals can be of macroscopic size amenable to x-ray and Raman spectroscopy. Nanocrystals can also be grown epitaxially on patterned SiC surface (de Heer *et al.*, 2011). Graphene nanoribbons (GNRs) can be produced by lithography, nanoparticle etching, and unzipping of carbon nanotubes. There have been a number of spectroscopic studies of GNRs by scanned probes (Tao *et al.*, 2011), transport (Han *et al.*, 2007; Liu *et al.*, 2009; Stampfer *et al.*, 2009; Todd *et al.*, 2009; Gallagher, Todd, and Goldhaber-Gordon, 2010; Han, Brant, and Kim, 2010; Oostinga *et al.*, 2010), and photoemission (Siegel *et al.*, 2008; Zhou, Siegel, Fedorov, Gabaly *et al.*, 2008), but because of space limitations they could not be covered in this Colloquium.

C. Electronic structure of graphene neglecting interactions

In this section we summarize basic facts about the SLG band structure within the independent electron approximation (Castro Neto *et al.*, 2009). The nearest-neighbor carbon atoms in SLG form sp^2 bonds, which give rise to the π and σ electron bands. The σ bands are relevant mostly for electronic phenomena at energies $\gtrsim 3$ eV. The unique low-energy properties of graphene derive from the π bands whose structure can be understood within the tight-binding model (Wallace, 1947). If only the nearest-neighbor transfer integral $\gamma_0 = 3.0 \pm 0.3$ eV [Fig. 1(b)] is included, the amplitudes ψ_j of the Bloch functions on the two triangular sublattices $j = A$ or B of the full honeycomb lattice can be found by diagonalizing the 2×2 Hamiltonian

$$H_{\mathrm{SLG}} = \begin{pmatrix} E_D & -\gamma_0 S_{\mathbf{k}} \\ -\gamma_0 S_{\mathbf{k}}^* & E_D \end{pmatrix}, \tag{1.1}$$

where E_D is the constant on-site energy, $\mathbf{k} = (k_x, k_y)$ is the in-plane crystal momentum, $S_{\mathbf{k}} = \exp(ik_x a/\sqrt{3}) + 2\exp(-ik_x a/2\sqrt{3})\cos(k_y a/2)$ represents the sum of the hopping amplitudes between a given site and its nearest neighbors, and $a = 2.461$ Å is the lattice constant. The spectrum of H_{SLG} has the form $\varepsilon_\pm(\mathbf{k}) = E_D \pm \gamma_0 |S_{\mathbf{k}}|$ or

$$\varepsilon_\pm = E_D \pm \gamma_0 \sqrt{3 + 2\cos k_y a + 4\cos\frac{\sqrt{3}k_x a}{2}\cos\frac{k_y a}{2}}. \tag{1.2}$$

At energies $|\varepsilon - E_D| \ll \gamma_0$, this dispersion has an approximately conical shape $\varepsilon_\pm(\mathbf{k}) = E_D \pm \hbar v_0 |\mathbf{k} - \mathbf{K}|$ with velocity

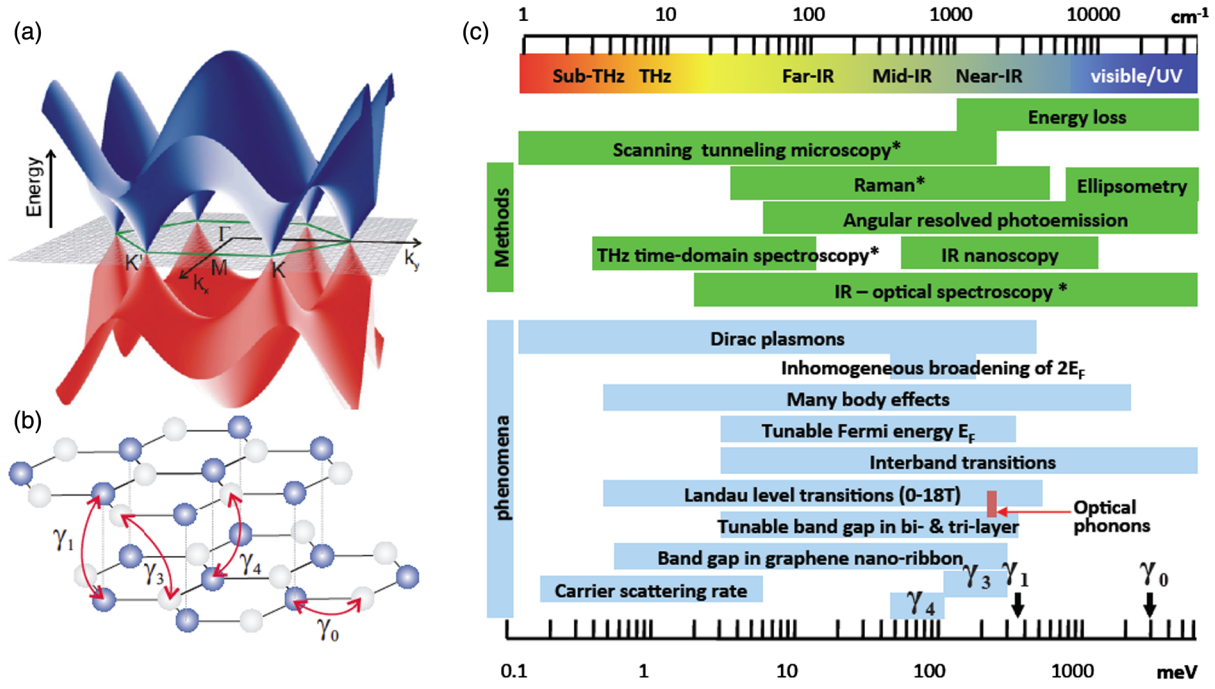

FIG. 1 (color online). (a) Schematic of the π-band dispersion of SLG showing Dirac cones at K and K' points. From Orlita and Potemski, 2010. (b) Definitions of the intralayer (γ_0) and interlayer (γ_1–γ_4) hopping parameters of Bernal-stacked graphene materials. [For their experimental values, see, e.g., L. M. Zhang *et al.* (2008).] (c) The energy scales of electronic phenomena in graphene along with the corresponding frequency ranges and spectroscopic methods. The asterisk denotes compatibility of a method with high magnetic fields.

$$v_0 = \frac{\sqrt{3}}{2}\frac{\gamma_0}{\hbar}a = (0.9\text{–}1.0) \times 10^8 \text{ cm/s}$$

near the corners of the hexagonal Brillouin zone (BZ); see Fig. 1(a). Only two of such corners are inequivalent, e.g., $\mathbf{K}$, $\mathbf{K}' = (2\pi/\sqrt{3}a, \pm 2\pi/3a)$; the other four are obtained via reciprocal lattice translations. Near the $\mathbf{K}$ point, H_{SLG} can be expanded to first order in $q_\parallel$ and $q_\perp$—the components of vector $\mathbf{q} = \mathbf{k} - \mathbf{K}$ parallel and perpendicular to $\mathbf{K}$, respectively. This expansion yields the 2D Dirac Hamiltonian

$$H = E_D + \hbar v_0 (q_\parallel \sigma_x + q_\perp \sigma_y), \tag{1.3}$$

which prompts analogies between graphene and quantum electrodynamics (Katsnelson and Novoselov, 2007). Here σ_x and σ_y are the Pauli matrices. Expansion near $\mathbf{K}'$ points gives a similar expression except for the sign of the $q_\parallel$ term. The eigenvector $\Psi = (\psi_A, \psi_B)^T$ of H can be thought of as a spinor. The direction of the corresponding pseudospin is parallel (antiparallel) for energy ε_+ (ε_-). The definite relation between the pseudospin and momentum directions is referred to as the *chirality*.

The conical dispersion yields the single-particle density of states (DOS) $\nu(E)$ linear in $|E - E_D|$. Accounting for the fourfold degeneracy due to spin and valley, one finds

$$\nu(E) = \frac{2}{\pi\hbar^2 v_0^2}|E - E_D|. \tag{1.4}$$

The frequently needed relations between the zero-temperature chemical potential μ (referenced to the Dirac point energy E_D), Fermi momentum k_F, and the carrier density N are

$$k_F = \sqrt{\pi|N|}, \qquad \mu \equiv E_F - E_D = \mathrm{sgn}(N)\hbar v_0 k_F. \tag{1.5}$$

For $E - E_D$ not small compared to γ_0, deviations from the simplified Dirac model arise. The spectrum exhibits saddle points at energies $E_D \pm \gamma_0$, which are reached at the three inequivalent points of the BZ: $\mathbf{M} = (2\pi/\sqrt{3}a, 0)$ and $\mathbf{M}'$, $\mathbf{M}'' = (-\pi/\sqrt{3}a, \pm\pi/a)$; see Fig. 1(a). The DOS has logarithmic van Hove singularities at these saddle points. In the noninteracting electron picture, direct ($q = 0$) transitions between the conduction and valence band states of a given saddle point would yield resonances at the energy $\hbar\omega = 2\gamma_0 \approx 5.4$ eV. (Actually observed resonances are redshifted due to interaction effects; see Sec. III.)

D. Many-body effects and observables

While the single-electron picture is the basis for our understanding of electron properties of graphene, it is certainly incomplete. One of the goals of this Colloquium is to summarize spectroscopic evidence for many-body effects in graphene. In this section we introduce the relevant theoretical concepts. For simplicity, we assume that the temperature is zero and neglect disorder.

The strength of Coulomb interaction $U(r) = e^2/\kappa r$ in graphene is controlled by the ratio

$$\alpha = \frac{e^2}{\kappa\hbar v_0}, \tag{1.6}$$

where κ is the effective dielectric constant of the environment. Assuming $v_0 \approx 1.0 \times 10^8$ cm/s, for suspended graphene ($\kappa = 1$) one finds $\alpha \approx 2.3$, so that the interaction is quite strong. Somewhat weaker interaction $\alpha \approx 0.9$ is realized for graphene on the common SiO_2 substrate, $\kappa = (1 + \epsilon_{\mathrm{SiO_2}})/2 = 2.45$. For graphene grown on metals the long-range part of the interaction is absent, with only residual short-range interaction remaining.

In general, spectroscopic techniques measure either quasiparticle or current (density) response functions. Within the framework of the Fermi-liquid theory (Nozieres and Pines, 1999), interactions renormalize the quasiparticle properties, meaning they change them quantitatively. The current and density response functions are altered qualitatively due to the emergence of collective modes.

A striking theoretical prediction made two decades ago (González, Guinea, and Vozmediano, 1994) is that Coulomb interaction among electrons should cause a logarithmically divergent renormalization of the Fermi velocity in undoped SLG,

$$\frac{v(q)}{v(k_c)} = 1 + \frac{1}{4}\alpha(k_c)\ln\frac{k_c}{q} \quad \text{at} \quad k_F = 0, \tag{1.7}$$

which implies the negative curvature of the "reshaped" Dirac cones (Elias *et al.*, 2011). Here k_c is the high momentum cutoff and $q = |\mathbf{k} - \mathbf{K}|$ is again the momentum counted from the nearest Dirac point $\mathbf{K}$. The physical reason for the divergence of $v(q)$ is the lack of metallic screening in undoped SLG because of the vanishing thermodynamic density of states (TDOS) $\nu_T = dN/d(\mu + E_D)$.

While Eq. (1.7) can be obtained from the first-order perturbation theory (Barlas *et al.*, 2007; Hwang, Hu, and Das Sarma, 2007; Polini *et al.*, 2007), the renormalization group (RG) approach of González, Guinea, and Vozmediano (1994) indicates that validity of this equation extends beyond the weak-coupling case $\alpha \ll 1$. It remains valid even at $\alpha \sim 1$ albeit in the asymptotic low-q limit where the *running* coupling constant $\alpha(q) \equiv e^2/\kappa\hbar v(q) \ll 1$ is small. The RG flow equation underlying Eq. (1.7),

$$\beta(\alpha) \equiv \frac{d\ln\alpha}{d\ln q} \simeq \frac{\alpha}{4}, \quad \alpha \ll 1, \tag{1.8}$$

is free of nonuniversal quantities κ and k_c, and so in principle it can be used to compare the renormalization effects in different graphene materials. The problem is that the asymptotic low-q regime is hardly accessible in current experiments where one typically deals with the nonperturbative case $\alpha \sim 1$. Theoretical estimates (González, Guinea, and Vozmediano, 1999; Son, 2007; Foster and Aleiner, 2008) of the β function in this latter regime yield

$$\beta \approx 0.2, \qquad \alpha \sim 1. \tag{1.9}$$

The corresponding renormalized velocity scales as

$$v(q) \sim q^{-\beta}. \tag{1.10}$$

Distinguishing this weak power law from the logarithmic one [Eq. (1.7)] still requires a wide range of q.

The gapless Dirac spectrum should become unstable once α exceeds some critical value (Khveshchenko, 2001; Sheehy and Schmalian, 2007; Drut and Lähde, 2009). It is unclear whether this transition may occur in SLG as no experimental evidence for it has been reported.

In doped SLG the RG flow described by Eq. (1.8) is terminated at the Fermi momentum scale. Therefore, velocity renormalization should be described by the same formulas as in the undoped one at $q \gg k_F$ but may have extra features at $q \leq k_F$. This expectation is born out by calculations (Das Sarma, Hwang, and Tse, 2007). The result for the Fermi velocity, written in our notations, is

$$\frac{v_F}{v(k_c)} = 1 + \frac{\alpha}{\pi}\left(\ln\frac{1}{\alpha} - \frac{5}{3}\right) + \frac{\alpha}{4}\ln\frac{k_c}{k_F}, \quad \alpha \ll 1, \tag{1.11}$$

where α should be understood as $\alpha(k_F)$. Comparing with Eq. (1.7), we see that v_F is larger than $v(q)$ in undoped SLG at the same momentum $q = k_F$ by an extra logarithmic term $\sim\alpha|\ln\alpha|$. This logarithmic enhancement of the Fermi velocity is generic for an electron gas with long-range Coulomb interactions in any dimension (Giuliani and Vignale, 2005). As a result, the renormalized dispersion has an inflection point near k_F (Principi *et al.*, 2012; Das Sarma and Hwang, 2013) and a positive (negative) curvature at smaller (larger) q.

Renormalization makes the relation between observables and quasiparticle properties such as $v(q)$ more complicated than in the noninteracting case. For illustration, consider three key spectroscopic observables: the single-particle DOS $\nu(E)$, the TDOS ν_T, and the threshold energy $\hbar\omega_{\text{th}}$ of the interband optical absorption. Since for the case of curved spectrum phase and group velocities are not equal, we must first clarify that by $v(q)$ we mean the latter, i.e., the slope of the dispersion curve $E(q)$. In theoretical literature, $E(q)$ is usually defined by

$$E(q) = \varepsilon(q) + \Sigma_1(q, E(q)), \tag{1.12}$$

where $\Sigma(q,\omega) = \Sigma_1(q,\omega) + i\Sigma_2(q,\omega)$ is the electron self-energy and the subscripts $\pm$ are suppressed to lighten the notations. In experimental practice (Sec. II.A), more directly accessible than $\Sigma(q,\omega)$ is the spectral function

$$A(q,\omega) = \frac{-2\Sigma_2(q,\omega)}{[\omega - \varepsilon(q) - \Sigma_1(q,\omega)]^2 + [\Sigma_2(q,\omega)]^2}, \tag{1.13}$$

and the more convenient definition of $E(q)$ is the energy ω at which $A(q,\omega)$ has a maximum. As long as this maximum is sharp so that the quasiparticles are well defined, the two definitions are equivalent. For the velocity, they entail

$$\frac{v(q)}{v_0} \equiv \frac{1}{\hbar v_0}\frac{dE}{dq} = \left(1 + \frac{\partial_q \Sigma_1}{\hbar v_0}\right) Z(q). \tag{1.14}$$

The three quantities in question, ν, ν_T, and $\hbar\omega_{\text{th}}$, are related to $v(q)$ as follows:

$$\nu(E) \simeq \frac{2}{\pi}\frac{q}{\hbar v(q)} Z(q), \qquad Z(q) \equiv \frac{1}{1 - \partial_E \Sigma_1}, \tag{1.15}$$

$$\nu_T(N) \equiv \frac{dN}{d(\mu + E_D)} = \frac{2}{\pi}\frac{k_F}{\hbar v_F + Z(k_F)\partial_{k_F}\Sigma_1}, \tag{1.16}$$

$$\hbar\omega_{\text{th}} = E_+(k_F) - E_-(k_F) + \Delta_{eh}. \tag{1.17}$$

These formulas contain many-body corrections to the relations given in Sec. I.C that enter through the derivatives of the self-energy, while Eq. (1.17) also has a vertex correction Δ_{eh}. For example, the DOS $\nu(E)$ [Eq. (1.15)], measurable by, e.g., STS is multiplied by the quasiparticle weight Z. Near the Fermi level one usually finds $Z < 1$ (Giuliani and Vignale, 2005), so that the interactions diminish the DOS. Inferring v_F from $\nu(E_F)$ using the formula $v_F \propto k_F/\nu(E_F)$ of the noninteracting theory would cause *overestimation* of the Fermi velocity, e.g., by the factor of $Z^{-1} = 1 + (1/2 + 1/\pi)\alpha$ at $\alpha \ll 1$ (Das Sarma, Hwang, and Tse, 2007). (In practice, the low-bias STS data may be influenced by disorder and a limited momentum resolution; see Sec. II.A.) Away from the Fermi level the interaction may enhance rather than suppress $\nu(E)$. An example is the Dirac point region in a doped SLG where the DOS is predicted to be nonzero (U shaped) (LeBlanc, Carbotte, and Nicol, 2011; Principi *et al.*, 2012) rather than vanishing (V shaped).

Consider next the TDOS $\nu_T(N)$ given by Eq. (1.16), which follows from Eqs. (1.14) and (1.15). The TDOS can be found by measuring capacitance between graphene and metallic gates, either stationary (Ponomarenko *et al.*, 2010; Yu *et al.*, 2013) or scanned (Martin *et al.*, 2008). In the absence of interactions, the TDOS coincides with the DOS at the Fermi level. However, for repulsive Coulomb interactions the second term in the denominator of Eq. (1.16) is negative (Giuliani and Vignale, 2005). (It can be written in terms of the parameter $F_s^0 < 0$ of the Landau Fermi-liquid theory.) Hence, while $\nu(E_F)$ is suppressed, ν_T is enhanced compared to the bare DOS. Extracting v_F from $\nu_T(N)$ (Yu *et al.*, 2013) may lead to *underestimation*.

The third quantity $\hbar\omega_{\text{th}}$ [Eq. (1.17)] stands for the threshold energy required to excite an electron-hole pair with zero total momentum in the process of optical absorption. Without interactions $\hbar\omega_{\text{th}} = 2\mu = 2\hbar v_0 k_F$ (see Fig. 2), and so the bare velocity is equal to $\omega_{\text{th}}/2k_F$. Using the same formula for the interacting system (Li *et al.*, 2008) may lead to underestimation of the renormalized v_F, for two reasons. First, v_F is the *group* velocity at the Fermi momentum while the ratio $[E_+(k_F) - E_-(k_F)]/(2\hbar k_F)$ gives the average *phase* velocity of the electron and hole at $q = k_F$. If the dispersion has the inflection point near k_F, as surmised above, the group velocity must be higher than the phase one. Second, the threshold energy of the electron-hole pair is reduced by the vertex (or excitonic) correction $\Delta_{eh} < 0$ due to their Coulomb attraction.

We now turn to the collective response of SLG at arbitrary ω and $\mathbf{k}$. The simplest type of such a process is excitation of a single particle-hole pair by moving a quasiparticle from an occupied state of momentum $\mathbf{p}$ and energy $E(\mathbf{p}) \leq E_F$ to an empty state of momentum $\mathbf{p} + \mathbf{k}$ and energy $E(\mathbf{p} + \mathbf{k}) \geq E_F$. (The subscripts $\pm$ of all E's are again suppressed.) The particle-hole continuum that consists of all possible $(E(\mathbf{p} + \mathbf{k}) - E(\mathbf{p}), \mathbf{k})$ points is sketched in Fig. 2. If the energy and

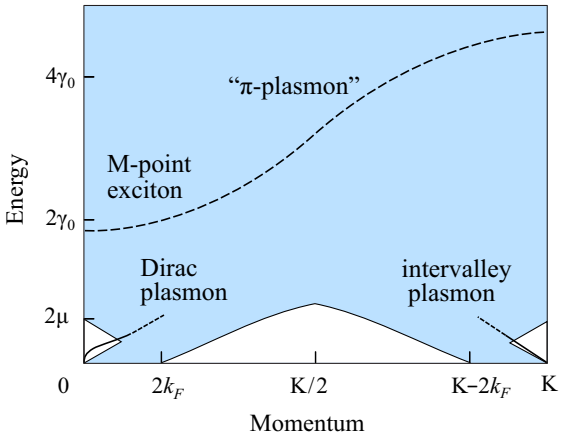

FIG. 2 (color online). Schematic dispersion of electron density excitations in SLG (lines). The horizontal axis corresponds to the Γ-K cut through the Brillouin zone. All excitations experience Landau damping inside the electron-hole pair continuum (shaded).

the in-plane momentum of an electromagnetic excitation falls inside this continuum, it undergoes damping when passing through graphene. The conductivity $\sigma(\mathbf{k},\omega)=\sigma'+i\sigma''$ has a finite real part σ' in this region.

Collective modes can be viewed as superpositions of many interacting particle-hole excitations. A number of such modes have been predicted for graphene. Weakly damped modes exist outside the particle-hole continuum in the three unshaded regions of Fig. 2. At low energy the boundaries of these triangular-shaped regions have the slope $\pm\hbar v_F$. Collective excitations near the Γ point (the left unshaded triangle in Fig. 2) are Dirac plasmons. These excitations, reviewed in Sec. III.B, can be thought of as coherent superpositions of intraband electron-hole pairs from the same valley. The excitations near the K point (the right unshaded triangle) involve electrons and holes of different valleys. Such intervalley plasmons (Tudorovskiy and Mikhailov, 2010) are yet to be seen experimentally. Also shown in Fig. 2 is the "M-point exciton" that originates from mixing of electron and hole states near the M points of the BZ (Sec. I.C) and its finite-momentum extension, which is sometimes called by a potentially confusing term of "π plasmon."

Two other collective modes have been theoretically predicted but not yet observed and are not shown in Fig. 2. One is the excitonic plasmon (Gangadharaiah, Farid, and Mishchenko, 2008)—a single interband electron-hole pair marginally bound by Coulomb attraction. Its dispersion curve is supposed to run near the bottom of the electron-hole continuum. The other mode (Mikhailov and Ziegler, 2007) is predicted to appear in the range $1.66|\mu|<\hbar\omega<2|\mu|$, where $\sigma''<0$. Unlike all the previously mentioned collective modes, which are transverse magnetic (TM) polarized, this one is transverse electric (TE) polarized. It is confined to graphene only weakly, which makes it hardly distinguishable from an electromagnetic wave traveling along graphene. Besides electron density, collective modes may involve electron spin. Further discussion of these and of many other interaction effects in graphene can be found in a recent topical review (Kotov *et al.*, 2012).

II. QUASIPARTICLE PROPERTIES

A. Dirac spectrum and chirality

The first experimental determination of the SLG quasiparticle spectrum was obtained by analyzing the Shubnikov–de Haas oscillations (SdHO) in magnetoresistance (Novoselov, Jiang *et al.*, 2005; Y. Zhang *et al.*, 2005). This analysis yields the cyclotron mass

$$m=\hbar k_F/v_F \tag{2.1}$$

and therefore the Fermi velocity v_F. The lack of dependence of $v_F\approx 1.0\times 10^8$ cm/s on the Fermi momentum k_F in those early measurements was consistent with the linear Dirac spectrum at energies below 0.2 eV.

Direct mapping of the π-band dispersion over a range of several eV (Zhou, Gweon, and Lanzara, 2006; Bostwick, Ohta, Seyller *et al.*, 2007) was achieved soon thereafter by the angle-resolved photoemission spectroscopy (ARPES) experiments. This experimental technique, illustrated by Fig. 3(a), measures the electron spectral function [Eq. (1.13)] weighted by the square of the matrix element $M(\mathbf{k},\nu)$ of interaction between an incident photon of frequency ν and an ejected photoelectron of momentum $\mathbf{k}$; see Eq. (2.2).

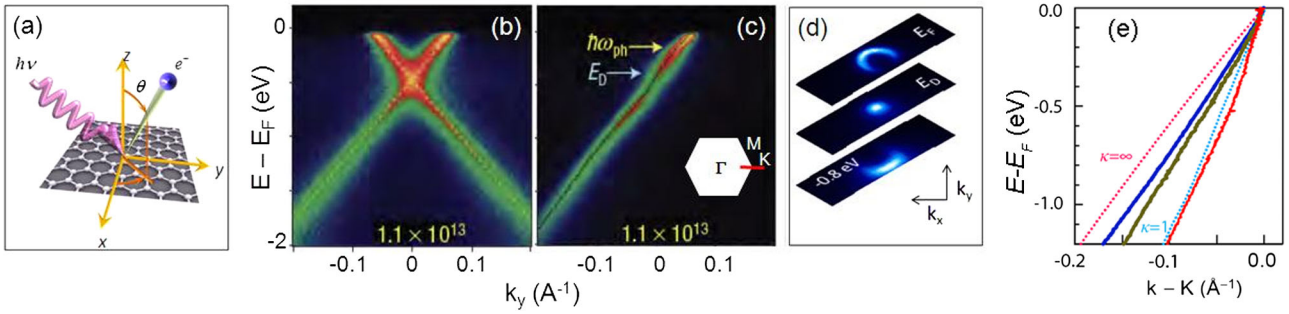

FIG. 3 (color online). (a) The ARPES schematics. (b), (c) The ARPES intensity in the energy-momentum space for a potassium-doped epitaxial graphene on SiC (0001) (Bostwick, Ohta, Seyller *et al.*, 2007). In panel (c) he interval of momenta k_y is indicated by the line segment in the inset. (b) The momentum k_x varies along the orthogonal path through the K point. (d) The ARPES maps for a similar sample taken at the energies (top to bottom) $E=E_F\approx E_D+0.4$ eV, E_D, and $E_F-0.8$ eV (Hwang *et al.*, 2011). (e) Solid lines, left to right: the ARPES dispersions along the Γ-K direction for graphene on SiC$(000\bar{1})$, hBN, and quartz. Dotted lines: results of GW calculations for $\kappa=\infty$ and $\kappa=1$. Adapted from Hwang *et al.*, 2012.

The representative dispersion curves measured for epitaxial graphene on SiC are shown in Figs. 3(b) and 3(c), where bright (dark) color corresponds to high (low) intensity. The "dark corridor" (Gierz *et al.*, 2011) Γ-*K* along which one of the two dispersion lines is conspicuously missing [Fig. 3(c)] occurs due to the selection rules for the matrix element $M(\mathbf{k},\nu)$ known from prior work on graphite (Daimon *et al.*, 1995; Shirley *et al.*, 1995). The full angular dependence of the ARPES intensity is depicted in Fig. 3(d).

The ARPES measurements have been carried out on epitaxial graphene grown on a variety of substrates, on freestanding samples (Knox *et al.*, 2011), and on multilayered samples with weak interlayer interactions (Sprinkle *et al.*, 2009). The tight-binding model (Sec. I.C) accounts for the main features of all these spectra. However, there are also subtle deviations. For example, the slope of the dispersion near the Dirac point varies systematically with the background dielectric constant κ [Fig. 3(d)], which is consistent with the theoretically predicted velocity renormalization; see Secs. I.D and II.B. Certain additional features near the Dirac point (see Fig. 12) have been interpreted (Himpsel *et al.*, 1982; Nagashima, Tejima, and Oshima, 1994; Zhou *et al.*, 2007; Dedkov *et al.*, 2008; Varykhalov *et al.*, 2008; Rader *et al.*, 2009; Sutter *et al.*, 2009; Enderlein *et al.*, 2010; Gao, Guest, and Guisinger, 2010; Walter *et al.*, 2011a; Papagno *et al.*, 2012; Siegel *et al.*, 2012) as evidence for substrate-induced energy gaps; see Sec. IV.B. For graphene on SiC, an alternative explanation invokes electron-plasmon coupling (Bostwick, Ohta, Seyller *et al.*, 2007) (see Fig. 11).

Complimentary evidence for the Dirac dispersion of quasiparticles comes from the tunneling and thermodynamic DOS measurements by means of scanned probes. The Dirac point

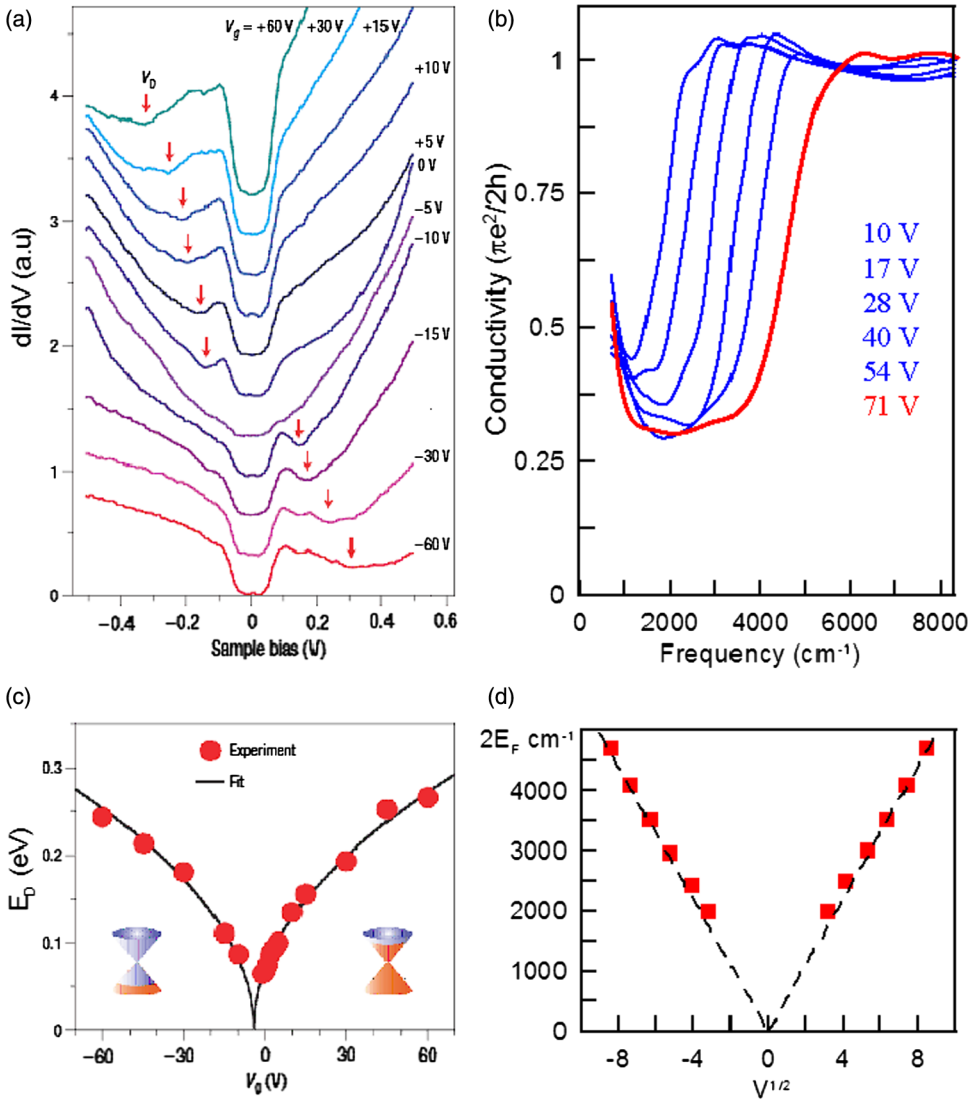

FIG. 4 (color online). Spectroscopic determination of the Dirac dispersion in SLG. (a) The STS tunneling spectra dI/dV taken at the same spatial point and different gate voltages V_g. The curves are vertically displaced for clarity. The arrows indicate the positions of the dI/dV minima V_D. (b) Optical conductivity of SLG at different gate voltages with respect to the neutrality point. (c) The distance $|E_D|$ between the Dirac point and the Fermi level as a function of V_g obtained from the data in (a). The line is the fit to $E_D \propto |V_g|^{1/2}$. The insets are cartoons showing the electron occupation of the Dirac cones. From Yuanbo Zhang *et al.*, 2008. (d) The gate voltage dependence of the interband absorption threshold $2E_F$ obtained from the data in (b). From Li *et al.*, 2008.

manifests itself as a local minimum marked by the arrows in the STS tunneling spectra of Fig. 4(a). The U- rather than the V-shaped form of this minimum (Sec. I.C) is due to disorder smearing. The STS data obtained by Yuanbo Zhang *et al.* (2008) [Fig. 4(a)] also exhibit a prominent suppression at zero bias for all gate voltages. To explain it, Yuanbo Zhang *et al.* (2008) proposed that this feature arises because of a limitation on the possible momentum transfer in tunneling. This limitation is lifted via inelastic tunneling accompanied by the emission of a BZ-boundary acoustic phonon of energy $\hbar\omega_0 = 63$ meV. This energy must be subtracted from the tip-sample bias eV to obtain the tunneling electron energy inside the sample. By tuning the electron density N with a back gate (Yuanbo Zhang *et al.*, 2008; Deshpande *et al.*, 2009; Brar *et al.*, 2010), one can change the Fermi energy E_F with respect to the Dirac point E_D. Taking the former as the reference point (i.e., assuming $E_F \equiv 0$ for now) one obtains the relation $|E_D| = |eV_D| - \hbar\omega_0$. As shown in Fig. 4(c), thus defined $|E_D|$ is proportional to $|N|^{1/2}$, as expected for the linear dispersion, Eq. (1.5). The same zero-bias gap feature is observed in other graphene samples studied by the Berkeley group, e.g., SLG on hBN (Decker *et al.*, 2011a). Yet it is not seen in STS experiments of other groups [see, e.g., Fig. 10(c) and Secs. II.B and II.C] (Deshpande *et al.*, 2009; Song *et al.*, 2010; Xue *et al.*, 2011; Chae *et al.*, 2012; Li and Andrei, 2012; Yankowitz *et al.*, 2012).

The $\mu(N)$ dependence can be more directly inferred from the TDOS $\nu_T(N)$ measured by the scanning single-electron transistor microscopy (SSETM) (Martin *et al.*, 2008). Unlike the STS spectra in Fig. 4(a), the SSETM data are not obscured by the zero-bias feature. They show a finite and position-dependent TDOS at the neutrality point $N = 0$, reflecting once again the presence of disorder in graphene on the SiO_2 substrate; see also Sec. IV.A. The most definitive observation of the Dirac TDOS has been made using exfoliated graphene on hBN (Yankowitz *et al.*, 2012; Yu *et al.*, 2013). Similar to SSETM, the TDOS was extracted from the capacitance measurements, however, it was the capacitance between the sample and the global back gate rather than between the sample and the local probe.

We now turn to the chirality of graphene quasiparticles. Recall that chirality refers to the phase relation between the sublattice amplitudes $\psi_j = \psi_j(\mathbf{k})$, $j = \mathrm{A}, \mathrm{B}$, of the quasiparticle wave functions (Sec. I.C). The chirality has been independently verified by several techniques. First it naturally explains the presence of the special half-filled Landau level (LL) at the Dirac point seen in magnetotransport (Novoselov, Jiang *et al.*, 2005; Y. Zhang *et al.*, 2005). Next in the STS experiments the quasiparticle chirality is revealed by the local DOS features observed near impurities and step edges [see Mallet *et al.* (2007), Rutter *et al.* (2007), Deshpande *et al.* (2009), Zhang, Brar *et al.* (2009), and Sec. IV.A]. The chirality influences the angular distribution of the quasiparticle scattering by these defects, suppressing the backscattering (Brihuega *et al.*, 2008; Xue *et al.*, 2012), in agreement with theoretical predictions (Ando, Zheng, and Suzuura, 2002; Katsnelson, Novoselov, and Geim, 2006).

Finally, in ARPES the chirality manifests itself via the selection rules for the matrix element

$$M(\mathbf{k},\nu) = \frac{e}{c}\int d\mathbf{r}\Psi_f^*(\mathbf{r})(\mathbf{A}\hat{\mathbf{v}})\Psi_i(\mathbf{r}) \tag{2.2}$$

that describes coupling of electrons to the vector potential $\mathbf{A}$ of the photon. Here the Coulomb gauge $\nabla\mathbf{A} = \varphi = 0$ is assumed and $\hat{\mathbf{v}} = -i\hbar\nabla/m$ is the velocity operator. The matrix element $M(\mathbf{k},\nu)$ depends on the relative phase of ψ_A and ψ_B. Based on symmetry considerations, the general form of $M(\mathbf{k},\nu)$ at small $\mathbf{q} = \mathbf{k} - \mathbf{K}$ must be

$$M(\mathbf{k},\nu) = (c_1\mathbf{K} + c_2\mathbf{q})\cdot\mathbf{A}\sum_{j=\mathrm{A,B}} e^{-i\mathbf{K}\boldsymbol{\tau}_j}\psi_j(\mathbf{k}) \tag{2.3}$$

if spin-orbit (SO) interaction effects can be ignored. Here $\boldsymbol{\tau}_j$ are the positions of the jth atom in the unit cell and $\mathbf{K}$ is the nearest Dirac point. The coefficients c_1 and c_2 cannot be obtained solely from symmetry; however, regardless of their values, when $\mathbf{q}$ is parallel (antiparallel) to $\mathbf{K}$ for the states in the conduction (valence) band, the sum over j in Eq. (2.3) vanishes and so does $M(\mathbf{k},\nu)$. This explains the low-intensity dark corridor in the observed ARPES signal [Figs. 3(c) and 3(d)].

The ARPES selection rules are also relevant for BLG. Experimentally, the orientation of the low-intensity directions rotates by $\pm 180°$ ($\pm 90°$) in SLG (BLG) when the photon polarization vector $\mathbf{A}$ is switched between two orientations, parallel and perpendicular to $\mathbf{K}$ (Gierz *et al.*, 2011; Hwang *et al.*, 2011; Liu *et al.*, 2011). Hwang *et al.* (2011) discussed how these rotation angles can be linked to the Berry phase (a quantity closely related to chirality) in SLG and BLG. However, their theoretical model for the matrix element $M(\mathbf{k},\nu)$ has been a subject of controversy, which appears to be rooted in a different assumption about the final-state wave function $\Psi_f(\mathbf{r})$ in Eq. (2.2). At very high energies $h\nu$, the conventional approximation of $\Psi_f(\mathbf{r})$ by a plane wave should be adequate (Shirley *et al.*, 1995; Mucha-Kruczyński *et al.*, 2008). In this case one can replace the velocity operator $\hat{\mathbf{v}}$ by $\hbar\mathbf{k}/m$ leading to $c_1 = c_2$ in Eq. (2.3). On the other hand, Hwang *et al.* (2011) replaced $\hat{\mathbf{v}}$ by the band velocity $v\mathbf{q}/|\mathbf{q}|$. This is perhaps appropriate at low energies $h\nu$ at which $\Psi_f \approx \Psi_i$ near the graphene plane. The corresponding c_1 is equal to zero, which is admissible. However, $c_2 \propto 1/|\mathbf{q}|$ diverges at $\mathbf{q} \to 0$, in contradiction to the $\mathbf{k}\cdot\mathbf{p}$ perturbation theory (Yu and Cardona, 1999). In view of this problem and because other ARPES experiments and calculations (Gierz *et al.*, 2011) indicate a nontrivial ν dependence of $M(\mathbf{k},\nu)$, further study of this question is desirable.

B. Renormalization of Dirac spectrum

Experimental verification of the many-body renormalization of the Dirac spectrum in graphene and its Fermi velocity v_F, in particular, has been sought after in many spectroscopic studies. Some of these studies may be subject to interpretation because v_F usually enters the observables in combination with other quantities; see Sec. I.D. In addition, when the change in v_F is small, one cannot completely exclude single-particle effects.

Probably the first experimental indication for v_F renormalization in graphene came from infrared absorption-transmission spectroscopy (Li *et al.*, 2008) of exfoliated SLG on

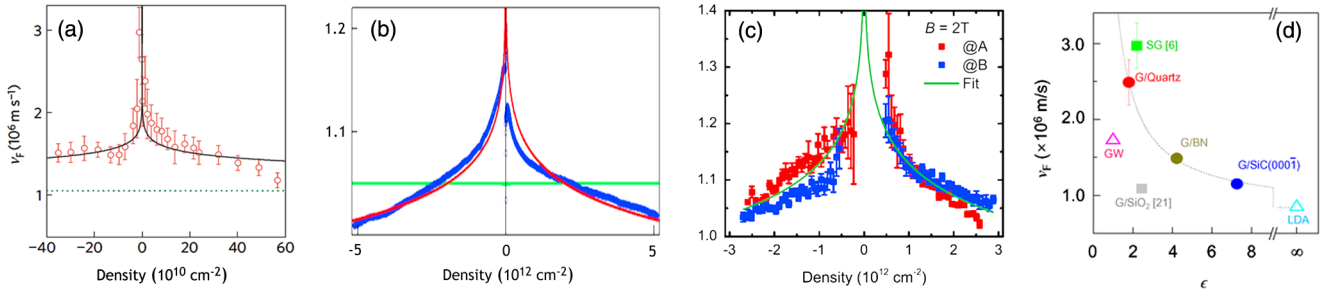

FIG. 5 (color online). (a) The carrier density dependence of v_F in suspended SLG extracted from magnetoresistance oscillations (circles) and a fit to a theory (solid curve). Adapted from Elias *et al.*, 2011. (b) Renormalized velocity determined from the gate capacitance of SLG on hBN (symbols) and a fit to Eq. (1.7) (solid curve). From Yu *et al.*, 2013. (c) Renormalized velocity of SLG on hBN from the STS of Landau levels (symbols). The line is a fit to Eq. (1.11). From Chae *et al.*, 2012. (d) Fermi velocity for SLG as a function of the dielectric constant of the substrate. The filled symbols are the data points obtained from the ARPES spectra. The open symbols and the line are from theoretical modeling. From Siegel *et al.*, 2012.

amorphous SiO_2 (a-SiO_2). This study found that v_F increases from 1.0×10^8 cm/s to a 15% higher value as the carrier density N decreases from 3.0×10^{12} to 0.7×10^{12} cm^{-2}; see Fig. 5(d). Next came an STS study of Landau level spectra (Luican, Li, and Andrei, 2011), which found a 25% enhancement of v_F (fifth row in Table I) in the same range of N.

A much broader range of N has been explored in suspended graphene where N as small as a few times 10^9cm^{-2} can be accessed. Working with such ultraclean suspended samples, Elias *et al.* (2011) were able to carry out the analysis of the SdHO of the magnetoresistance over a two-decade-wide span of the carrier densities. This analysis yields the cyclotron mass [Eq. (2.1)] and thence v_F. The Fermi velocity was shown to reach $v_F \approx 3.0 \times 10^8$ cm/s, the largest value reported to date; cf. Table I. Elias *et al.* (2011) fitted their data [Fig. 5(a)] to Eq. (1.7) for undoped graphene by treating α as an adjustable parameter. Figure 3 of Elias *et al.* (2011) suggests another possible fit to Eq. (1.10) with the exponent $\beta \approx 0.25$, which is close to Eq. (1.9). It would be better to compare the measured v_F with the theoretical predictions for *doped* graphene, i.e., with the extension (or extrapolation) of Eq. (1.11) to the case in hand, $\alpha \sim 1$.

From the measurements of quantum capacitance (the quantity proportional to the TDOS) of SLG on hBN, Yu *et al.* (2013) found that v_F increases by ~15% as N varies from 5×10^{12} down to a few times 10^{10}cm^{-2}; see Fig. 5(b). The vertex corrections were not included when the conversion of the quantum capacitance to v_F was done. Therefore, this number represents the lower bound on v_F; see Sec. I.D.

Using substrates of different dielectric constant $\epsilon_{\rm sub}$ is another approach to study v_F renormalization. An advantage of this approach is that a broad range of N is not necessary in this case. Instead, the renormalization of velocity is driven by the change in the interaction strength $\alpha \propto 1/\kappa$, where $\kappa = (1 + \epsilon_{\rm sub})/2$; see Eq. (1.7). A crude estimate of this effect is as follows. The dielectric screening by the substrate is effective at distances larger than the separation d between graphene and the substrate. Hence, the momentum cutoff in Eqs. (1.7) and (1.11) should be chosen $k_c \sim 1/d$. If $d \lesssim 1$ nm and $k_F^{-1} \sim 6$ nm, then $\ln(k_c/k_F) \lesssim 2$ and Eq. (1.7) entails

$$\delta v_F \lesssim (1.0 \times 10^8 \text{ cm/s}) \times \delta\left(\frac{2}{\epsilon_{\rm sub} + 1}\right), \qquad (2.4)$$

where we use δ to denote a change in a quantity. In a recent ARPES study (Hwang *et al.*, 2012), the smallest $v_F = (0.85 \pm 0.05) \times 10^8$ cm/s was observed on metallic substrates. This value represents presumably the bare quasiparticle velocity in the absence of long-range Coulomb interactions. Note that it is close to the Fermi velocity $v_F = 0.81 \times 10^8$ cm/s measured in carbon nanotubes (Liang *et al.*, 2001). The ARPES results for three other substrates are reproduced in Fig. 5(d). They clearly demonstrate a prominent velocity enhancement near the Fermi level. Thus, graphene on (the carbon face of) SiC has v_F that is only slightly larger than what is observed for metallic substrates (Siegel *et al.*, 2011; Hwang *et al.*, 2012), which can be explained by the high κ. Graphene on hBN has v_F close to that for SLG on a-SiO_2, which is consistent with the effective dielectric constants of hBN and a-SiO_2 being roughly equal (Wang *et al.*, 2012; Yu *et al.*, 2013). A surprisingly large v_F is found for graphene on crystalline SiO_2 (quartz); see Table I and Fig. 5(d).

TABLE I. The Fermi velocity of SLG in excess of the nominal bare value of 0.85×10^8 cm/s.

Substrate	κ	v (10^8 cm/s)	Method	Reference
SiC (0001)	7.26	1.15(2)	ARPES	Hwang *et al.* (2012)
hBN	4.22	2.0	ARPES	Siegel *et al.* (2013)
		1.20(5)	Capacitance	Yu *et al.* (2013)
SiO_2	1.80	2.5(3)	ARPES	Hwang *et al.* (2012)
a-SiO_2	2.45	1.47(5)	STS	Luican, Li, and Andrei (2011)
Vacuum	1.00	3.0(1)	SdH	Elias *et al.* (2011)
		2.6(2)	Transport	Oksanen *et al.* (2014)

As mentioned previously, renormalization of the quasiparticle velocity in SLG can also arise from single-particle physics. One example is the modification of the electron band structure by external periodic potentials (Park *et al.*, 2008a, 2008b; Brey and Fertig, 2009; Guinea and Low, 2010; Wallbank *et al.*, 2013). Such potentials are realized in moiré superlattices that form when graphene is deposited on lattice-matched substrates, which we discuss in Sec. IV.C. Similar effects appear in misoriented graphene bilayers and multilayers that grow on the carbon face of SiC (Hass *et al.*, 2008) (Sec. I.B) and are also common in CVD graphene grown on Ni (Luican *et al.*, 2011). Calculations predict a strong dependence of the velocity on the twist angle (Lopes dos Santos, Peres, and Castro Neto, 2007, 2012; Shallcross *et al.*, 2010; Trambly de Laissardiére, Mayou, and Magaud, 2010; Bistritzer and MacDonald, 2011). The experimental value of v_F reported for twisted graphene layers on the carbon face of SiC is $v_F \approx 1.10 \times 10^8$ cm/s (Miller *et al.*, 2009; Sprinkle *et al.*, 2009; Crassee, Levallois, van der Marel *et al.*, 2011; Siegel *et al.*, 2011). Changes of v_F up to 10% among different layers for graphene on the carbon face of SiC have been deduced from SdH oscillations (de Heer *et al.*, 2007) and magneto-optical measurements (Crassee, Levallois, van der Marel *et al.*, 2011; Crassee, Levallois, Walter *et al.*, 2011). In the latter case these changes have been attributed to electron-hole asymmetry and also to variation of the carrier density and dielectric screening among the graphene layers. No variation of v_F as a function of the twist angle was observed by ARPES and STS (Sadowski *et al.*, 2006; Miller *et al.*, 2009; Sprinkle *et al.*, 2009; Siegel *et al.*, 2011). However, a 14% decrease of v_F at small twist angles was found in the STS study of CVD graphene transferred to the grid of a transmission electron microscope (Luican *et al.*, 2011).

C. Landau quantization

Spectroscopy of LL quantization in a magnetic field is yet another way to probe quasiparticle properties of graphene. The linear dispersion of SLG leads to unequally spaced LLs: $E_n = E_D + \mathrm{sgn}(n) v_0 \sqrt{2e\hbar B|n|}$ [Fig. 6(a)], where $n > 0$ or $n < 0$ represents electrons or holes, respectively (McClure, 1957; Gusynin and Sharapov, 2006; Jiang *et al.*, 2007). Each of the LLs has fourfold degeneracy due to the spin and valley degrees of freedom. Additionally, the electron-hole symmetric $n = 0$ LL gives rise to the extraordinary "half-integer" quantum Hall effect (Novoselov, Geim *et al.*, 2005; Yuanbo Zhang *et al.*, 2005), the observation of which back in 2005 was the watershed event that ignited the widespread interest in graphene.

The LL spectrum of graphene has been probed using STS, IR spectroscopy, and Raman scattering. The STS of graphene LLs was first carried out in graphene on graphite samples, where suspended graphene is isolated from the substrate at macroscopic ridgelike defect in graphite (Li, Luican, and Andrei, 2009). Figure 6(b) displays the differential conductance of graphene versus tip-sample bias at different magnetic fields B normal to the graphene surface. Well-defined LDOS peaks corresponding to discrete LL states appear in the tunneling spectra. These LL peaks become more prominent and shift to higher energies in higher magnetic fields consistent with the expected $\sqrt{B|n|}$ law. Similar LL spectrum was also

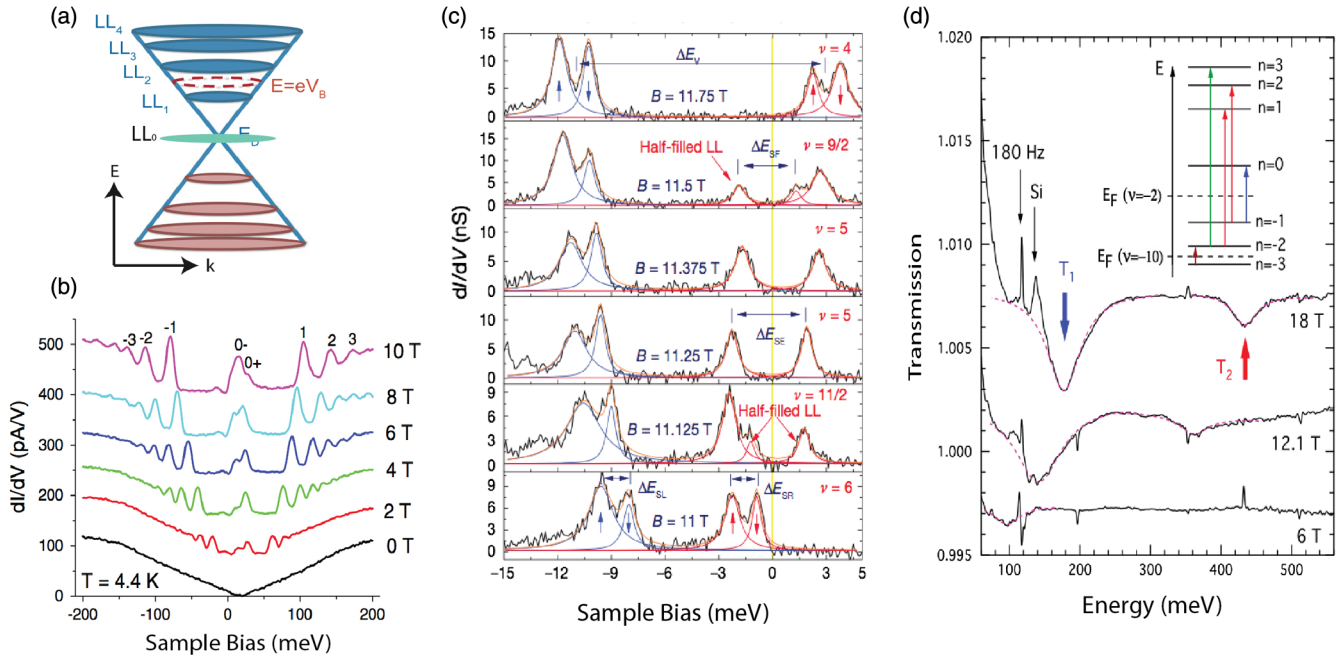

FIG. 6 (color online). (a) The schematics of LLs in SLG. Each LL is fourfold degenerate due to spin and valley degrees of freedom. The neutrality point corresponds to the half filling of the $n = 0$ LL. (b) The STS spectra of graphene on graphite at different magnetic fields (Li, Luican, and Andrei, 2009). (c) A high-resolution STS revealing fourfold states that make up $n = 1$ LL of epitaxial graphene on SiC at different magnetic fields. The energy separations ΔE_v and ΔE_s due to lifting of the valley and spin degeneracies are enhanced when the Fermi level falls between the spin-split levels at filling factor $\nu = 5$. Additional stable states appear at $\nu = 11/2$ and $9/2$ (Song *et al.*, 2010). (d) The IR transmission of a p-doped graphene at $\nu = -2$ normalized to that at $\nu = 10$ at three different magnetic fields. Two LL resonances, T_1 and T_2, are observed. The inset shows the allowed LL transitions (Jiang *et al.*, 2007).

observed in epitaxial grown graphene layers on SiC (Miller *et al.*, 2009).

To examine the fine structure within a LL, Song *et al.* (2010) performed high-resolution STS studies at temperatures as low as 10 mK on epitaxial graphene. Figure 6(c) shows their data for the $n = 1$ LL at the magnetic field range where the LL1 starts to cross the Fermi energy (vertical line). The LL1 level is composed of four separate peaks, indicating that the valley and spin degeneracy is lifted. The larger energy splitting (ΔE_v) is attributed to the lifting of valley degeneracy. It increases monotonically with the applied magnetic field with the effective g factor of 18.4. The smaller splitting (ΔE_s) has an average g factor close to 2, presumably due to the electron spin. Quantitatively, this spin splitting shows a highly unusual dependence on the filling factor. Comparing the spectra at filling factors of 4, 5, and 6, a clear enhancement of the spin splitting is observed at $\nu = 5$, which can be attributed to many-body effects (exchange enhancement). In addition, new stable half-filled Landau levels appear at half fillings such as $9/2$ and $11/2$. Their origin is not yet clear. Landau level spectroscopy of graphene on SiO_2 was presented by Luican, Li, and Andrei (2011) and a similar study for graphene on hBN was reported by Chae *et al.* (2012). In the latter system, which has lower disorder, observation of many LLs was possible over a wide energy range. Deviations of the LL energies by about ~10% from the predictions of the single-particle theory were interpreted in terms of the Fermi velocity renormalization; see Fig. 5(c). This is in line with the results of other measurements discussed above (Table I).

The IR spectroscopy provides another way to study the LL spectra (Sadowski *et al.*, 2006; Jiang *et al.*, 2007; Henriksen *et al.*, 2010). The IR transitions between LLs have to satisfy the selection rule $\Delta|n| = \pm 1$, due to angular momentum conservation. Selection rules also apply to the circular polarization of light. As a result, graphene exhibits strong circular dichroism and Faraday effect (Crassee, Levallois, Walter *et al.*, 2011). Figure 6(d) displays the experimental data of normalized IR transmission spectra through SLG at several magnetic fields (Jiang *et al.*, 2007). The electron density is controlled so that the Fermi energy lies between the $n = -1$ and 0 LL [inset of Fig. 6(d)]. Two transmission minima T_1 and T_2 are readily observable. The T_1 resonance corresponds to the $n = -1$ to $n = 0$ intraband LL transition, and the T_2 resonance arises from the degenerate interband $n = -1$ to $n = 2$ and $n = -2$ to $n = 1$ transitions. The LL transition energies scale linearly with $\sqrt{B}$, as expected from the LL structure described above. A careful examination of the IR transitions as a function of electron filling factor further reveals that at zero filling factor the $n = -1$ to $n = 0$ (or $n = 0$ to $n = 1$) transition is shifted to a higher energy compared to that at the filling factor of 2 and -2 (Henriksen *et al.*, 2010). This shift was again tentatively attributed to interaction effects.

III. CURRENT AND DENSITY RESPONSE AND THE RELATED COLLECTIVE MODES

A. Optical conductivity

Traditionally measured by optical spectroscopy, the "optical" conductivity $\sigma(\omega) = \sigma'(\omega) + i\sigma''(\omega) \equiv \sigma(q = 0, \omega)$ quantifies the response of the current to an external electric field in the low momenta $q \ll \omega/v_F$ region of the q-ω parameter space; see Fig. 2. Both intraband and interband transitions contribute to the optical conductivity; we start with the interband ones.

In a charge-neutral SLG, which is a zero-gap semiconductor with the Fermi energy at the Dirac point, the interband transitions have no threshold. Particularly interesting is the range of (IR) frequencies $\hbar\omega \ll \gamma_0$, where quasiparticles behave as massless Dirac fermions. Since the Dirac spectrum has no characteristic frequency scale and neither does the Coulomb interaction, at zero temperature and in the absence of disorder the conductivity must be of the form $\sigma(\omega) = (e^2/h)f(\alpha)$, where α is defined by Eq. (1.6). [However, $\omega = 0$ is, strictly speaking, a singular point (Ziegler, 2007).] For the noninteracting case, $\alpha = 0$, the theory predicts [see Ludwig *et al.* (1994) for Dirac fermions in general and Ando, Zheng, and Suzuura (2002), Gusynin and Sharapov (2006), Peres, Guinea, and Castro Neto (2006), Falkovsky and Varlamov (2007), Ziegler (2007), and and Stauber, Peres, and Geim (2008) for SLG] $f(0) = \pi/2$, so that $\sigma(\omega)$ is real and has the universal value of

$$\sigma_0 = \frac{\pi}{2}\frac{e^2}{h}. \tag{3.1}$$

The corresponding transmission coefficient $T = 1 - 4\pi\sigma(\omega)/c$ for suspended graphene is expressed solely in terms of the fine-structure constant $T = 1 - \pi(e^2/\hbar c) \approx 0.977$ (Abergel, Russell, and Fal'ko, 2007; Blake *et al.*, 2007; Ni *et al.*, 2007; Roddaro *et al.*, 2007). This prediction matches experimental data surprisingly well, with possible deviations not exceeding 15% throughout the IR and visible spectral region (Li *et al.*, 2008; Mak *et al.*, 2008; Nair *et al.*, 2008). This implies that the interaction correction $f(\alpha) - f(0)$ is numerically small even at $\alpha = 2.3$. At the level of the first-order perturbation theory this remarkable fact is explained by nearly complete cancellations between self-energy and vertex contributions (Mishchenko, 2008; Sheehy and Schmalian, 2009; Sodemann and Fogler, 2012).

Doping of graphene creates an effective threshold $\hbar\omega_{\text{th}}$ for interband absorption by the same mechanism as in the Burstein-Moss effect: the blueshift of the lowest energy of interband transitions in a doped semiconductor (Yu and Cardona, 1999). Because of Pauli blocking, no direct interband transitions exist at $\hbar\omega < 2|\mu|$ in the noninteracting electron picture; see Fig. 2. Experimentally, the existence of such a threshold has been confirmed by IR spectroscopy of gated SLG (Li *et al.*, 2008; Feng Wang *et al.*, 2008; Horng *et al.*, 2011). As shown in Fig. 4, the frequency position of the broadened step in $\sigma'(\omega)$ scales as the square root of the gate voltage V_g and so is proportional to k_F. This is consistent with the linear dispersion $2|\mu| = 2\hbar v_F k_F$ of the Dirac quasiparticles. This behavior is seen in both exfoliated (Li *et al.*, 2008) and CVD-grown graphene (Horng *et al.*, 2011). At the smallest gate voltages, deviations from the square-root law are seen (Li *et al.*, 2008), which may be due to an interplay of many-body effects, the velocity renormalization and the vertex corrections; see Secs. I.D and II.B.

Vertex corrections (which are also referred to as the excitonic effects) play a prominent role also in the optical energy range 4–6 eV. The dominant spectroscopic feature in this region is the interband transition that connects electron and hole states near the M point of the Brillouin zone, where the DOS has van Hove singularities (Sec. I.C). This resonance is seen in both SLG and MLG samples (Fei *et al.*, 2008; Kravets *et al.*, 2010; Chae *et al.*, 2011; Mak, Shan, and Heinz, 2011; Santoso *et al.*, 2011). This resonance has been detected by electron energy loss spectroscopy (EELS) and dubbed π plasmon (Eberlein *et al.*, 2008). We prefer the term "M-point exciton" to avoid confusion with the Dirac plasmon. Electron-electron interactions significantly renormalize the properties of this resonance. The position of the M-point exciton is redshifted from the noninteracting value of $2\gamma_0$ by as much as 600 meV in SLG samples (Yang *et al.*, 2009; Chae *et al.*, 2011; Mak, Shan, and Heinz, 2011). The absorption peak has a Fano line shape indicative of interaction effects.

We now discuss the intraband transitions. The commonly used Drude model assumes that the intraband response of a conductor is a simple fraction:

$$\sigma_{\text{intra}}(\omega) = \frac{i}{\pi}\frac{D}{\omega + i\gamma}. \tag{3.2}$$

For noninteracting electrons with an isotropic Fermi surface one generally finds (Ashcroft and Mermin, 1976)

$$D = \pi e^2 |N|/m, \tag{3.3}$$

where m is defined by Eq. (2.1). For Dirac electrons with $v_F = \text{const}$ and $k_F = \sqrt{\pi|N|}$ both m and D scale as $|N|^{1/2}$. Parameter D is known as the Drude weight. In the Drude model, the relaxation rate γ is frequency independent and can be related to the transport mobility μ_{tr} by $\hbar\gamma = e v_F / k_F \mu_{\text{tr}}$. In exfoliated samples of typical mobility $\mu_{\text{tr}} \sim 10\,000\ \text{cm}^2/\text{V s}$ and carrier density $N \sim 3\times 10^{11}\,\text{cm}^{-2}$ one estimates $\gamma \sim 10$ meV. This is below the low-frequency cutoff of the IR microscopy (Li *et al.*, 2008). One can extend measurements to lower frequency provided larger area samples are used, such as epitaxial (Choi *et al.*, 2009; Hofmann *et al.*, 2011) and CVD-grown graphene (Horng *et al.*, 2011; Ren *et al.*, 2012; Rouhi *et al.*, 2012). In both cases the gross features of the measured frequency dependence of IR conductivity comply with the Drude model. Note that such samples have relatively low mobility (Sec. I.B) and so show wider Drude peaks in $\sigma'(\omega)$.

The intraband response as a function of the carrier density has been studied using a gated CVD-grown graphene (Horng *et al.*, 2011). The experimentally observed Drude weight was found to be 20%–50% smaller than predicted by Eq. (3.3); see Fig. 7. The reduction was larger on the electron ($\mu > 0$) side where the transport mobility was also lower. At the same time, the optical sum rule $\int_0^\infty \sigma'(\omega) d\omega = \text{const}$ was apparently obeyed (Horng *et al.*, 2011). The conservation of the total optical weight was made possible by a residual conductivity in the interval $\gamma \ll \omega \ll 2|\mu| - \gamma$, first observed by Li *et al.* (2008). In this region of frequencies both interband and intraband transitions should be suppressed, yet the conductivity remains no smaller than $\sigma'(\omega) \approx 0.5 e^2/h$; see Fig. 4(b).

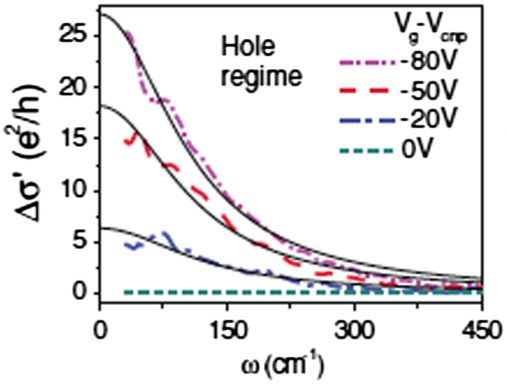

FIG. 7 (color online). Gating-induced change $\Delta\sigma'(\omega) = \sigma'(\omega) - \sigma'_{\text{CNP}}(\omega)$ in the optical conductivity of SLG. Solid lines are the fits assuming the Drude model for both $\sigma(\omega)$ and $\sigma_{\text{CNP}}(\omega)$. The latter is the conductivity at the charge-neutrality point (CNP). Its Drude form is chosen to account for inhomogeneous local doping; cf. Sec. IV.A. From Horng *et al.*, 2011.

Redistribution of the optical weight is common to correlated electron systems (Millis, 2004; Qazilbash *et al.*, 2009; Basov *et al.*, 2011), and so the residual conductivity of graphene is suggestive of interaction effects. Calculation of such effects is more difficult than for the undoped graphene but an extensive theoretical literature already exists on the subject. For example, the role of interaction in the conductivity sum rule was tackled by Sabio, Nilsson, and Castro Neto (2008), and the renormalization of D was discussed by Abedpour *et al.* (2007) and Levitov, Shtyk, and Feigelman (2013). The residual conductivity remains the most challenging problem. So far, theoretical calculations that consider electron-phonon (Peres, Stauber, and Castro Neto, 2008; Stauber, Peres, and Castro Neto, 2008; Hwang, LeBlanc, and Carbotte, 2012; Scharf *et al.*, 2013) or electron-electron (Grushin, Valenzuela, and Vozmediano, 2009; Peres, Ribeiro, and Castro Neto, 2010; Carbotte, LeBlanc, and Nicol, 2012; Hwang, LeBlanc, and Carbotte, 2012; and Principi *et al.*, 2013b) interactions predict relatively small corrections to $\sigma'(\omega)$ inside the interbad-intraband gap $0 < \hbar\omega < 2|\mu|$. Such corrections can, however, be enhanced by disorder (Kechedzhi and Das Sarma, 2013; Principi *et al.*, 2013a).

B. Plasmons

A plasmon is a collective mode of charge-density oscillation in a system with itinerant charge carriers. Plasmons have been extensively investigated in both classical and quantum plasmas. The dispersion relation of plasmons in a 2D conductor is given by

$$q_p(\omega) = \frac{i}{2\pi}\frac{\kappa(\omega)\omega}{\sigma(q_p,\omega)}, \tag{3.4}$$

where $\kappa(\omega)$ is the average of the dielectric functions of the media on the two sides (Fei *et al.*, 2012; Grigorenko, Polini, and Novoselov, 2012). At $q \ll k_F$ the q dependence of $\sigma(q,\omega)$ can be neglected, and so the plasmon dispersion is determined by the optical conductivity $\sigma(\omega)$ discussed above.

This implies that $\sigma(\omega)$, which is usually measured by optical spectroscopy, can also be inferred by studying plasmons (Chen *et al.*, 2012; Fei *et al.*, 2012). (Actually, optics probes transverse rather than a longitudinal response but at $q \ll \omega/v_F$ the two coincide.)

Note that $q_p = q_p{}' + iq_p''$ is a complex number. Its real part determines the plasmon wavelength $\lambda_p = 2\pi/q_p{}'$ and the imaginary part characterizes dissipation. The condition for the propagating plasmon mode to exist is $q_p'' \ll q_p{}'$ or $\sigma' \ll \sigma''$, assuming κ is real. In SLG this condition is satisfied (both in theory and in experiment) at frequencies that are smaller or comparable to $|\mu|/\hbar$. In particular, at $\hbar\omega \ll |\mu|$, one can use Eqs. (3.2) and (3.4) to express the plasmon dispersion in terms of the Drude weight D:

$$\omega_p(q) = \sqrt{\frac{2}{\kappa} Dq}. \tag{3.5}$$

This $\sqrt{q}$ behavior is a well-known property of 2D plasmons. Using Eq. (3.3) for D with Eq. (2.1) for m, one finds

$$\omega_p(q) = \sqrt{\frac{2\sqrt{\pi}e^2}{\kappa\hbar v_F}} v_F |N|^{1/4} q^{1/2}, \quad q \ll k_F. \tag{3.6}$$

The $|N|^{1/4}$ scaling of the plasmon frequency at fixed q should be contrasted with $\omega_p \propto |N|^{1/2}$ scaling well known for the 2D electron gas (2DEG) with a parabolic energy spectrum. The difference is due to the $D \propto N$ dependence in the latter system. Another qualitative difference is the effect of electron interactions on D. In 2DEG, interactions do not change D, which is the statement of Kohn's theorem (Giuliani and Vignale, 2005). In graphene, interactions renormalize the Drude weight (Abedpour *et al.*, 2007; Levitov, Shtyk, and Feigelman, 2013), which causes quantitative deviations from Eq. (3.6). Qualitative deviations from this equation occur, however, only at $q \sim k_F$, where the plasmon dispersion curve enters the particle-hole continuum; see Fig. 2. At such momenta the Drude model (3.2) breaks down and a microscopic approach such as the random-phase approximation (RPA) becomes necessary (Wunsch *et al.*, 2006; Hwang and Das Sarma, 2007; Jablan, Buljan, and Soljačić, 2009). The RPA predicts that inside the particle-hole continuum the plasmon survives as a broad resonance that disperses with velocity that approaches a constant value v_F at large q.

Experimental measurements of the plasmon dispersion over a broad range of q have been obtained by means of EELS. Such experiments (Liu *et al.*, 2008; Koch, Seyller, and Schaefer, 2010; Liu and Willis, 2010; Shin *et al.*, 2011; Tegenkamp *et al.*, 2011) have confirmed the $\omega_p \propto \sqrt{q}$ scaling at small momenta and a kink in the dispersion in the vicinity of the particle-hole continnum. An EELS study carried out by Pfnür *et al.* (2011) reported two distinct plasmon modes, a result yet to be verified through other observations.

The IR spectroscopy of graphene ribbons (Ju *et al.*, 2011; Yan *et al.*, 2013) and disks (Yan, Li *et al.*, 2012; Yan, Xia *et al.*, 2012; Fang *et al.*, 2013) offered a complementary method to probe the plasmon dispersion. The experimental signature of the plasmon mode is the absorption resonance whose frequency $\omega_{\rm res}$ is observed to scale as the inverse square root of the ribbon width W (or disk radius R). This scaling agrees with the theoretical results relating $\omega_{\rm res}$ to the plasmon dispersion in an unbounded graphene sheet [Eq. (3.5)]. For the ribbon, it reads $\omega_{\rm res} \approx \omega_p(2.3/W)$ (Nikitin *et al.*, 2011). The same relation can be deduced from the previous work (Eliasson *et al.*, 1986) on plasmons in 2DEG stripes. In fact, most of the results obtained in the context of plasmons in 2DEG in semiconductors (Demel *et al.*, 1990, 1991; Kukushkin *et al.*, 2003) and also electrons on the surface of a liquid ^{4}He (Glattli *et al.*, 1985; Mast, Dahm, and Fetter, 1985) directly apply to graphene whenever the Drude model holds.

As shown theoretically and experimentally in that earlier work, the spectrum of plasmons in ribbons and stripes is split into a set of discrete modes dispersing as $\omega_l(q_\parallel) \approx \omega_p(\sqrt{q_l^2 + q_\parallel^2})$, as a function of the longitudinal momentum $q_\parallel$ and the mode number $l = 1, 2, \ldots$, with $q_l = (\pi l - \delta_l)/W$ having the meaning of the transverse momentum. Numerical results (Eliasson *et al.*, 1986; Nikitin *et al.*, 2011) suggest that the phase shift parameter is equal to $\delta_l \approx \pi/4$ at $q_\parallel = 0$. The resonance mode detected in graphene ribbons (Ju *et al.*, 2011; Yan *et al.*, 2013) is evidently the $l = 1$ mode. Probing $q_\parallel \neq 0$ modes in ribbons with conventional optics is challenging and has not been done in graphene [It may be possible with a grating coupler (Demel *et al.*, 1991).] On the other hand, working with graphene disks, one can effectively access the quantized values $q_\parallel = m/R$, where m is the azimuthal quantum number. The observed mode (Yan, Li *et al.*, 2012; Yan, Xia *et al.*, 2012; Fang *et al.*, 2013) is evidently the dipolar one $m = l = 1$, which has the highest optical weight. An additional mode that appears in both ribbons and disks is the *edge* plasmon. We discuss it at the end of this section where we discuss the effects of the magnetic field.

The correspondence between the ribbon and bulk plasmon dispersions enables one to also verify the $|N|^{1/4}$ scaling predicted by Eq. (3.6). This has been accomplished by electrostatic gating of graphene microribbons immersed in ionic gel (Ju *et al.*, 2011) and monitoring their resonance frequency.

Plasmons in graphene are believed to strongly interact with electrons. Using the ARPES Bostwick, Ohta, Seyller *et al.* (2007), Bostwick, Ohta, McChesney *et al.* (2007), and Bostwick *et al.* (2010) observed characteristic departure of the quasiparticle dispersion from linearity near the Dirac point energy accompanied by an additional dispersion branch. These features, discussed in more detail in Sec. III.D, were interpreted in terms of plasmarons: bound states of electrons and plasmons (Lundqvist, 1967). Walter *et al.* (2011a, 2011b) demonstrated that the details of the plasmaron spectrum are sensitive to the dielectric environment of graphene. Carbotte, LeBlanc, and Nicol (2012) proposed that plasmaron features can be detected in near-field optical measurements, which allow one to probe the IR response at momenta $q \gg \omega/c$.

Complementary insight on the interaction between plasmons and quasiparticles has been provided by the STS. Based on the gate dependence of the tunneling spectra, Brar *et al.* (2010) distinguished phonon and plasmon effects on the quasiparticle self-energy.

Plasmons in graphene strongly interact with surface phonons of polar substrates such as SiC, SiO_2, and BN. Dispersion of mixed plasmon-phonon modes in graphene on SiC was investigated experimentally using high-resolution EELS (Liu *et al.*, 2008; Koch, Seyller, and Schaefer, 2010; Liu and Willis, 2010) and modeled theoretically by Hwang, Sensarma, and Das Sarma (2010). Theoretical dispersion curves (Fei *et al.*, 2011) for graphene on SiO_2 are shown in the inset of Fig. 8(b). The dispersion characteristic of mixed plasmon-phonon modes in nanoribbons measured via far-field IR spectroscopy was reported by Yan, Xia *et al.* (2012) and Yan *et al.* (2013).

In the near-field IR nanoscopy study of graphene microcrystals on SiO_2 (Fei *et al.*, 2011), the oscillator strength of the plasmon-phonon surface modes was shown to be significantly enhanced by the presence of graphene; see Fig. 8(a). The strength of this effect can be controlled by electrostatic doping, in agreement with theoretical calculations (Fei *et al.*, 2011).

Imaging of plasmon propagation in real space (Chen *et al.*, 2012; Fei *et al.*, 2012) [Fig. 8 (left panel)] has led to the first direct determination of both real and imaginary parts of the plasmon momentum $q_p = q_p' + iq_p''$ as a function of doping. In terms of potential applications of these modes, an important characteristic is the confinement factor λ_p/λ_0, where $\lambda_p = 2\pi/q_p'$ is the plasmon wavelength and $\lambda_0 = 2\pi c/\omega$ is the wavelength of light in vacuum. The experimentally determined confinement factor in exfoliated graphene (Fei *et al.*, 2012) was ~65 in the mid-IR spectral range $\omega \approx 800$ cm^{-1}. According to Eq. (3.6), the scale for the confinement is set by the inverse fine-structure constant $\lambda_0/\lambda_p = (\kappa/2)(\hbar c/e^2)\hbar\omega/|\mu|$ with stronger confinement achieved at higher frequencies. The propagation length of the plasmons $\sim 0.5\lambda_p = 100$–150 nm is consistent with the residual conductivity $\sigma' \approx 0.5e^2/h$ measured by the conventional IR spectroscopy (Li *et al.*, 2008). Possible origins of this residual conductivity have already been discussed in Sec. III.A. In confined structures one additional mechanism of plasmon damping is scattering by the edges (Yan *et al.*, 2013). Despite the observed losses, the plasmonic figures of merits demonstrated by Chen *et al.* (2012) and Fei *et al.* (2012) compare well against the benchmarks set by noble metals. Even though surface plasmons in metals can be confined to scales of the order of tens of nanometers, their propagation length in this regime is plagued by giant losses and does not exceed $0.1\lambda_p \sim 5$ nm for the Ag/Si interface (Jablan, Buljan, and Soljačić, 2009). This consideration was not taken into account in a recent critique of graphene plasmonics (Tassin *et al.*, 2012). Further improvements in the figures of merits are anticipated for graphene with higher

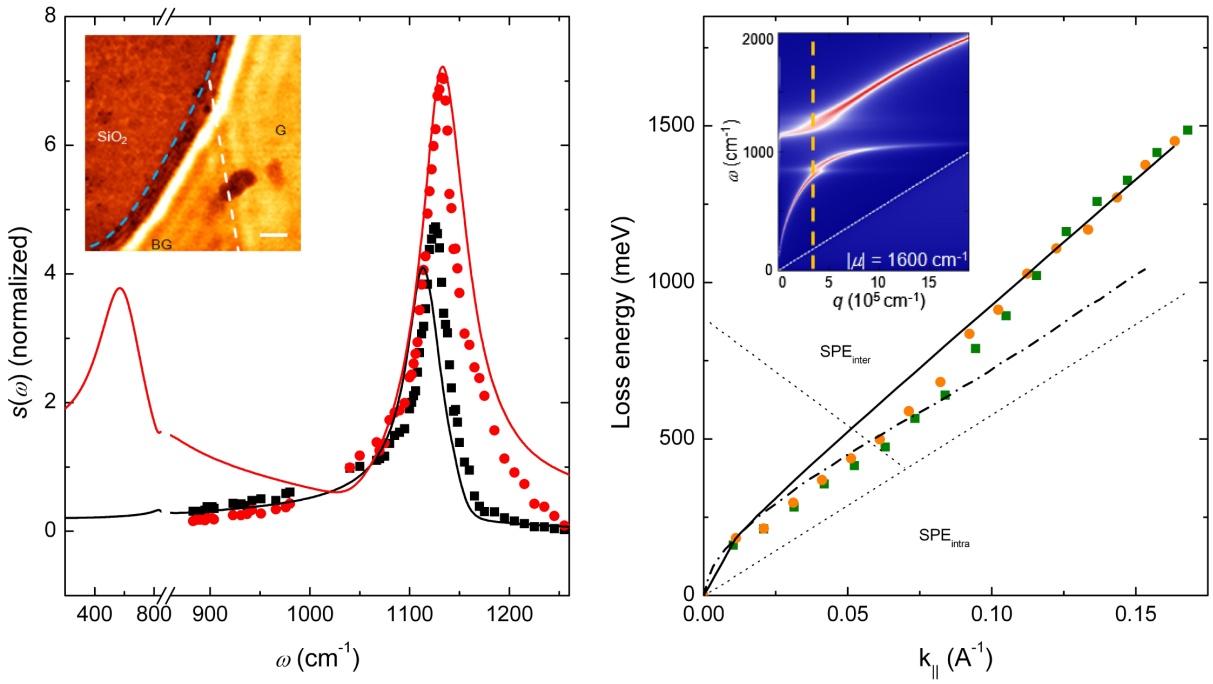

FIG. 8 (color online). Collective modes of graphene on polar substrates originate from hybridization of substrate surface phonons with graphene plasmons. Both modes show up as resonances in the near-field amplitude spectrum $s(\omega)$. The main left panel shows the phonon mode measured for SiO_2 alone (squares) and the phonon-plasmon hybrid mode of SiO_2 covered with SLG (circles). The modeling results are shown by the lines, with the SLG trace revealing the lower hybrid mode of predominantly plasmon character at $\omega \sim 500$ cm^{-1}. From Fei *et al.*, 2011. Direct observation of this plasmonlike mode is achieved by real-space imaging of $s(\omega)$ at a fixed frequency $\omega = 892$ cm^{-1} (inset). The oscillations seen in the image result from interference of plasmon waves (Fei *et al.*, 2012). The bright lines in the right inset depict the calculated mode dispersions for SLG with the chemical potential $\mu/hc = 1600$ cm^{-1} on SiO_2. The experimentally relevant momenta are situated near the vertical dashed line. The diagonal dashed line is the border of the electron-hole continuum (cf. Sec. I.D). The main right panel depicts collective modes of epitaxial graphene on SiC measured with electron energy loss spectroscopy at 300 K (circles) and 80 K (squares). The solid and dash-dotted lines are different theoretical fits. The dotted lines indicate the boundaries of the electron-hole continuum. From Tegenkamp *et al.*, 2011.

electronic mobility. The key forte of graphene in the context of plasmonics is the control over the plasmon frequency and propagation direction (Mishchenko, Shytov, and Silvestrov, 2010; Vakil and Engheta, 2011) by gating.

The properties of graphene plasmons get modified in the presence of a transverse magnetic field B. The magnetoplasmon dispersion is obtained from Eq. (3.4) by replacing σ with the longitudinal conductivity σ_{xx}. For instance, instead of the Drude model (3.2), one would use its finite-B analog, the Drude-Lorentz model (Ashcroft and Mermin, 1976), which yields another well-known dispersion relation (Chiu and Quinn, 1974)

$$\omega_{\mathrm{mp}}(q) = \sqrt{\omega_p^2(q) + \omega_c^2}. \tag{3.7}$$

This magnetoplasmon spectrum is gapped at the cyclotron frequency $\omega_c = eB/mc$ defined through the effective mass m [Eq. (2.1)]. Equation (3.7) is valid at small enough B where Landau quantization can be ignored. At large B, quantum treatment is necessary. In the absence of interactions, the magnetoplasmon gap at $q = 0$ is given by $E_{n+1} - E_n$, the energy difference between the lowest unoccupied $n + 1$ and the highest occupied n Landau levels. Unlike the case of a 2DEG, where Kohn's theorem holds, renormalization of the Fermi velocity by interactions directly affects the cyclotron gap. This many-body effect has been observed by magneto-optical spectroscopy; see Sec. II.C.

Probing finite-q magnetoplasmons optically is possible via the finite-size effects, such as the mode quantization in graphene disks. As known from previous experimental (Glattli *et al.*, 1985; Mast, Dahm, and Fetter, 1985; Demel *et al.*, 1990, 1991; Kukushkin *et al.*, 2003), numerical (Eliasson *et al.*, 1986), and analytical (Volkov and Mikhailov, 1988) studies of other 2D systems, the single plasmon resonance at $B = 0$ splits into two. The upper mode whose frequency increases with B can be regarded as the bulk magnetoplasmon with $q \approx 1/R$, where R is the disk radius. The lower mode whose frequency drops with B can be interpreted as the edge magnetoplasmon, which propagates around the disk in the anticyclotron direction. Both the bulklike and the edgelike modes have been detected by the IR spectroscopy of graphene disk arrays (Yan, Li *et al.*, 2012; Yan, Xia *et al.*, 2012). Additionally, in epitaxial graphene with a random ribbonlike microstructure, the B-field induced splitting of the Drude peak into a high- and a low-frequency branch was observed and interpreted in similar terms (Crassee *et al.*, 2012). The distinguishing property of the edge magnetoplasmon is chirality: the propagation direction is linked to that of the magnetic field. This property has been verified in graphene systems by time-domain spectroscopy (Kumada *et al.*, 2013; Petković *et al.*, 2013), which also allowed extraction of the edge magnetoplasmon velocity.

Other interesting properties of magnetoplasmons, such as splitting of the classical magnetoplasmon dispersion (3.7) into multiple branches, have been predicted theoretically (Roldán, Fuchs, and Goerbig, 2009; Goerbig, 2011) and their similarities and differences with the 2DEG case have been discussed. These effects still await their experimental confirmation.

C. Phonons

Raman spectroscopy is the most widely used tool for probing optical phonons in graphene and related materials (Ferrari *et al.*, 2006; Ferrari, 2007; Dresselhaus *et al.*, 2010, 2012). Quantitative studies of the Raman modes can provide rich information on graphene electron-phonon interaction, electronic structure, as well as on graphene layer thickness, edges, doping, and strain. Because graphene has the same sp^2 bonding and hexagonal carbon lattice, its phonon band structure is almost identical to that in graphite. Figure 9(a) shows a calculated dispersion of the optical phonon branches in graphene (lines) (Piscanec *et al.*, 2004) as well as the experimental data of graphite (symbols) (Maultzsch *et al.*, 2004). One feature of these dispersions is the discontinuity in the frequency derivative at the Γ and K points in the highest optical branches. This discontinuity known as the Kohn

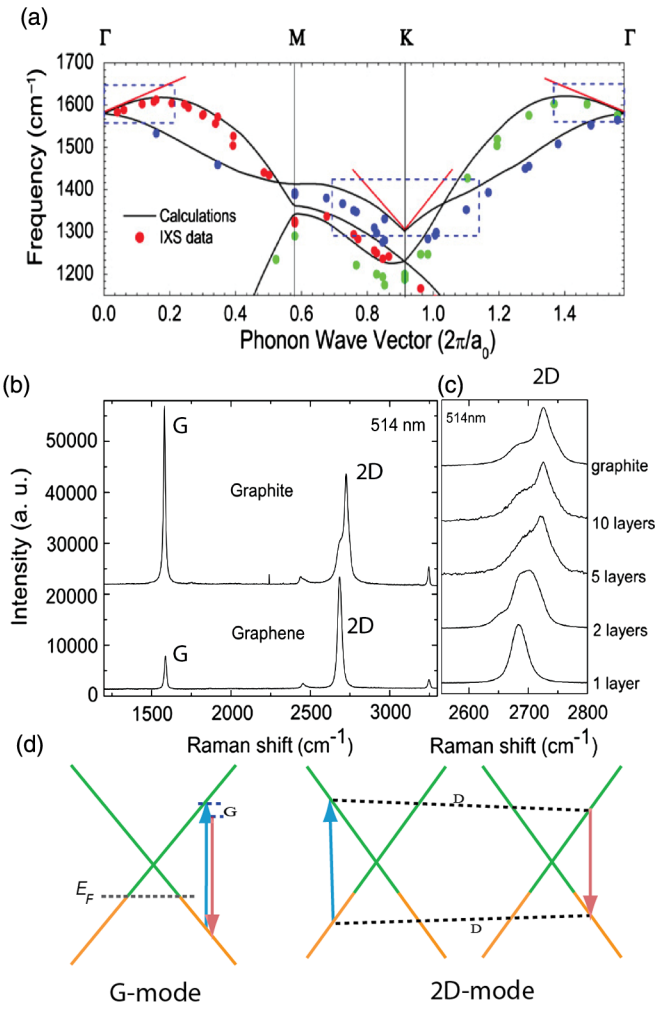

FIG. 9 (color online). Phonon dispersion and Raman spectroscopy of graphene. (a) Calculated phonon dispersion of SLG (Piscanec *et al.*, 2004) (symbols) compared with the experimental data for graphite (Mohr *et al.*, 2007) (lines). (b) Raman spectra of graphene and graphite measured at 514 nm laser excitation showing the G and the $2D$ Raman peaks (Ferrari *et al.*, 2006). (c) The evolution of the $2D$ Raman peak with the number of graphene layers (Ferrari *et al.*, 2006). (d) Schematics of the G-mode and the $2D$-mode Raman scattering processes.

anomaly arises from the unusual electron-phonon coupling in graphitic materials (Piscanec *et al.*, 2004).

Figure 9(b) displays typical Raman spectra of SLG and graphite. They show the same qualitative Raman modes with the two most prominent features being the G mode ($\approx 1580\ \mathrm{cm}^{-1}$) and the $2D$ mode ($\approx 2700\ \mathrm{cm}^{-1}$, also known as the G' mode). The other weak but very informative Raman feature is the D mode ($\approx 1350\ \mathrm{cm}^{-1}$). The line shape of the $2D$ mode is very different in SLG, MLG, and graphite [Fig. 9(c)] (Ferrari *et al.*, 2006). As illustrated in Fig. 9(d), the G peak arises from the Raman scattering of the Γ-point phonon. The $2D$ peak, on the other hand, is a two-phonon process involving emission of two K-point optical phonons. The D peak is a double resonance process similar to the $2D$ peak. It requires structural defects to relax the momentum conservation constraint.

A detailed theory of the G-mode Raman signal was presented by Basko (2008), Basko and Aleiner (2008), Basko, Piscanec, and Ferrari (2009), and Basko (2009). The capability of controlling the electron Fermi energy through electrical gating helped to elucidate electron-phonon interactions (Pisana *et al.*, 2007; Yan *et al.*, 2007; Das *et al.*, 2008; Malard *et al.*, 2008) and the quantum interference between different intermediate excitation pathways (Kalbac *et al.*, 2010; Chen *et al.*, 2011). The frequency and linewidth of the Raman G mode reflect the energy and lifetime of the optical phonon at the Γ point. The Γ-point phonon experiences Landau damping by particle-hole excitations if its energy exceeds $2|\mu|$ (see Fig. 2). As a result, the parameters of the Raman G mode depend on the carrier concentration as demonstrated experimentally (Pisana *et al.*, 2007; Yan *et al.*, 2007). The G-mode Raman shows a reduced damping and a blueshift when the Fermi energy is larger than one-half of the phonon energy, so that the phonon decay pathway into the electron-hole pairs gets blocked. When the Fermi energy in graphene is increased further, some of the intermediate electronic transitions necessary for Raman scattering become blocked. This reduces destructive interference among different pathways and increases the G-mode signal (Chen *et al.*, 2011).

The Raman scattering that gives rise to the $2D$ mode involves emission of two BZ-boundary phonons close to the K point. Being a two-phonon process, it still has large intensity, which is explained by the triple-resonance mechanism [Fig. 9(d)], where every intermediate step involves a resonant electronic excitation (Basko, 2008; Basko, Piscanec, and Ferrari, 2009). Because of smallness of the phonon energy compared with the incident photon energy $\hbar\omega$, the momenta $\mathbf{k}$ of the intermediate electron states are restricted to $\hbar\omega \approx E(\mathbf{k})$, where $E(\mathbf{k})$ is the electron dispersion (Sec. I.C). The phonon momentum (relative to a K-point phonon) then equals $2(\mathbf{k}-\mathbf{K})$. Consequently, phonons and intermediate electronic transitions with specific momentum can be excited by varying incident photon energy for $2D$ Raman modes. This allows one to map the dispersion of both the phonon and the electrons.

Once the phonon dispersion is known, Raman scattering can be used to probe electronic band-structure changes with a fixed laser excitation. For example, it can distinguish SLG, BLG, and MLG due to their different electronic dispersions (Ferrari *et al.*, 2006). In BLG and MLG there are several conduction and valence bands (Sec. V). Hence, valence electrons at more than one momentum $\mathbf{k}$ can satisfy the $\hbar\omega = E(\mathbf{k})$ relation. This leads to an apparent broadening and asymmetry of the $2D$ Raman peaks for BLG and MLG, compared to those for SLG (Ferrari *et al.*, 2006).

The Raman D mode (short for the defect mode) requires the existence of atomically sharp defects to provide the required momentum matching to scatter a zone boundary phonon close to the K point. The intensity of the D peak is used to characterize the sample quality of graphene (Ferrari, 2007; Malard *et al.*, 2009; Dresselhaus *et al.*, 2010). The D mode is also useful for probing graphene edges, which can be considered as line defects. Experiments show that the D peak is indeed the strongest at graphene edges (Graf *et al.*, 2007; Casiraghi *et al.*, 2009; Gupta *et al.*, 2009), and that the D-mode intensity is at maximum for light polarization parallel to the edge and at minimum for the perpendicular polarization (Casiraghi *et al.*, 2009). For ideal edges, theory predicts that the D-mode Raman peak intensity is zero for zigzag edges but large for armchair ones (Casiraghi *et al.*, 2009). In addition to the effects discussed above, the intensity and frequency of Raman peaks also depend on the substrate (Dong Su Lee *et al.*, 2008; Ni, Yu *et al.*, 2008; Ying Ying Wang *et al.*, 2008; Berciaud *et al.*, 2009; Ni, Yu, Lu *et al.*, 2009), temperature (Calizo *et al.*, 2007), and strain (Yu *et al.*, 2008; Huang *et al.*, 2009; Mohiuddin *et al.*, 2009; Proctor *et al.*, 2009) through their effects on the phonon dispersion and electron Fermi energy.

D. Electron-phonon and electron-plasmon interactions

The energies and lifetimes of charge carriers in graphene are significantly affected by interactions with plasmons and phonons. The electron-phonon (el-ph) interaction results in a variety of novel phenomena discussed in Sec. III.C. The ARPES has been used to probe the signature of the el-ph interaction in the electronic spectra of graphene (Bostwick, Ohta, Seyller *et al.*, 2007; McChesney *et al.*, 2007, 2010; Zhou, Siegel, Fedorov, and Lanzara, 2008c) via the measurement of the quasiparticle velocity v. The el-ph coupling constant is usually defined by $\lambda = v_0/v - 1$ (Ashcroft and Mermin, 1976). However, the electron-electron (el-el) interaction also contributes to velocity renormalization (Secs. I.D and II.B). Hence, thus defined λ gives a good estimate of el-ph coupling only if the el-el interaction is screened, which is the case for graphene on a metallic substrate (Siegel *et al.*, 2011).

The el-ph interaction in graphene strongly depends on the carrier concentration, as shown in Figs. 10(a) and 10(b). Siegel *et al.* (2011) reported a large reduction of λ for quasifreestanding graphene with E_F close to the Dirac point E_D. The overall reduction of the el-ph interaction can be reproduced by theoretical calculations (Park *et al.*, 2007). However, to account for the fine features of the quasiparticle dispersion, the el-el interaction has to be included (Lazzeri *et al.*, 2008; Zhou, Siegel, Fedorov, and Lanzara, 2008c; Siegel *et al.*, 2011). At high doping λ appears to be enhanced, reaching values $\lambda \sim 2$, and strongly anisotropic, similar to what is observed in graphite (Zhou, Gweon, and Lanzara, 2006; Leem *et al.*, 2008; Park, Giustino, Cohen, and Louie, 2008) and in the intercalated compound CaC_6 (Valla *et al.*, 1999). Calandra and Mauri (2007b) argued these effects result

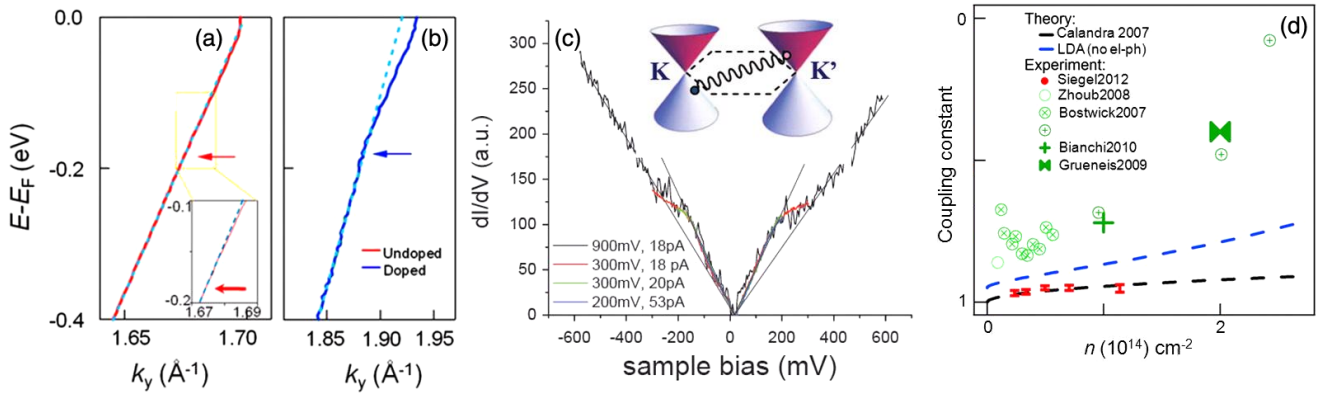

FIG. 10 (color online). The ARPES dispersion along the Γ-K direction for (a) lightly doped (solid line) and (b) heavily doped (solid line) graphene (Siegel *et al.*, 2011). The dashed lines are guides to the eye. The arrows indicate the kinks in the curves due to the el-ph interaction. (c) Zero field STS tunneling spectra (Li, Luican, and Andrei, 2009). The spectra are approximately linear except around the phonon energy. (d) The ARPES electron-phonon coupling constant as a function of the carrier density for graphene grown on different substrates: SiC (Bostwick, Ohta, Seyller *et al.*, 2007; McChesney *et al.*, 2007; Zhou, Siegel, Fedorov, and Lanzara, 2008b; McChesney *et al.*, 2010), Ir (111) (Grüneis *et al.*, 2009; Bianchi *et al.*, 2010), and Cu (Siegel *et al.*, 2012). The results of *ab initio* calculations of Calandra and Mauri (2007a) without (upper dashed line) and with (lower dashed line) el-ph interactions included are shown for comparison.

from distortion of the graphene bands that hybridize with a new Ca-related band. On the other hand, Park, Giustino, McChesney *et al.* (2008) suggested that the anisotropy of λ comes from the nonlinear band dispersion of the graphene bands at high doping.

From a high-resolution ARPES study Zhou, Siegel, Fedorov, and Lanzara (2008b) concluded that the electron-phonon coupling is dominated by the following phonon modes: the A_{1g} phonon at approximately 150 ± 15 meV near the BZ corner, the E_{2g} phonon (~200 meV) at the zone center, and the out-of-plane phonon at 60 meV. Among these, the A_{1g} phonon is the one that mostly contributes to λ and is mainly responsible for the kinks in the ARPES and tunneling spectra (Li, Luican, and Andrei, 2009); see Figs. 11(b) and 11(c). The contribution of a specific phonon mode to λ can also be determined by studying how the Raman signal varies as a function of the applied magnetic field. These magneto-Raman studies focused on the E_{2g} phonon (Faugeras *et al.*, 2009, 2011), as the A_{1g} phonon is Raman inactive in high-quality graphene samples.

The origin of the large discrepancy [Fig. 10(d)] between theoretically predicted and experimentally measured values of λ is debated (Bostwick, Ohta, McChesney *et al.*, 2007; Calandra and Mauri, 2007a; McChesney *et al.*, 2007, 2008, 2010; Park *et al.*, 2007; Zhou, Siegel, Fedorov, and Lanzara, 2008b; Park, Giustino, McChesney *et al.*, 2008; Filleter *et al.*, 2009; Grüneis *et al.*, 2009; Bianchi *et al.*, 2010). Siegel *et al.* (2012) found a good agreement with the theory [Fig. 10(d)] using the bare velocity v_0 measured for graphene grown on Cu where the el-el interaction is expected to be screened.

Electron-plasmon interaction is also believed to play an important role in renormalizing the band structure of graphene. Bostwick, Ohta, Seyller *et al.* (2007), Bostwick, Ohta, McChesney *et al.* (2007), and Bostwick *et al.* (2010) argued that this interaction is responsible for the anomalous departure from the linear dispersion observed in epitaxial graphene grown on the Si face of SiC. Bostwick *et al.* (2010) provided evidence (Fig. 11) for a well-resolved plasmaron band in the ARPES spectra of a "freestanding" graphene sample in which hydrogen has been intercalated between graphene and SiC to make negligible the interaction between the two. The plasmaron of momentum $\mathbf{k}$ is a bound state of a hole with momentum $\mathbf{k}+\mathbf{q}$ and a plasmon of momentum $-\mathbf{q}$ (Lundqvist, 1967). Theoretical calculations (Polini *et al.*, 2008) within the *GW* approximation predict that the plasmaron band appears at finite charge densities. Its energy separation from the primary quasiparticle band is proportional to μ with a coefficient that depends on the Coulomb interaction strength α, which in turn depends on the dielectric environment of graphene. Quantitative aspects of these calculations were disputed by Lischner, Vigil-Fowler, and Louie (2013) who included vertex corrections neglected in the *GW* scheme. Compared to Polini *et al.* (2008), for the same α Lischner, Vigil-Fowler, and Louie (2013) found a broader plasmaron peak at a smaller separation from the primary band, which appears to be in better agreement with the experiments of Bostwick *et al.* (2010).

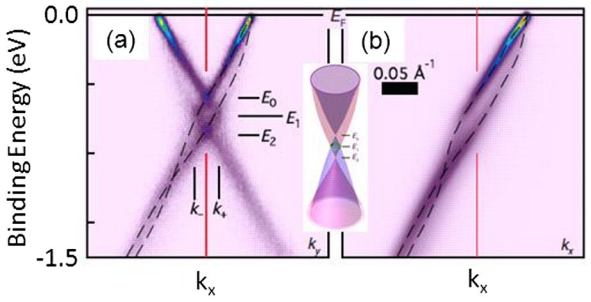

FIG. 11 (color online). The ARPES dispersion of doped ($N = 8 \times 10^{10}$ cm^{-2}) graphene (a) perpendicular and (b) parallel to the Γ-K direction (Bostwick *et al.*, 2010). The dashed lines are guides to the eye for the dispersion of the hole and plasmaron bands; the vertical solid line goes through the Dirac point. The inset shows a schematic of the renormalized spectrum in the presence of plasmarons.

No evidence of the plasmaron band has been reported in samples where decoupling of graphene from the buffer later was achieved by either gold or fluorine intercalation (Starodub *et al.*, 2011; Walter *et al.*, 2011c). This has been attributed to a stronger dielectric screening by the buffer layer. An alternative interpretation of the apparent nonlinearity of the Dirac spectrum of graphene on SiC invokes a substrate-induced band gap (Zhou *et al.*, 2007; Benfatto and Cappelluti, 2008; Kim *et al.*, 2008; Zhou, Siegel, Fedorov, Gabaly *et al.*, 2008; Zhou, Siegel, Fedorov, and Lanzara, 2008b); see Sec. IV.B below.

IV. INDUCED EFFECTS

A. Inhomogeneities and disorder

Intentional and unintentional doping by charged impurities plays a very important role in the electronic phenomena of graphene. It is unclear if there is a single dominant source of unintentional doping even for the most studied type of samples: exfoliated graphene on SiO_2. In addition to adsorbates from the ambient atmosphere, doping could also result from charged defects in SiO_2 (Adam *et al.*, 2007; Schedin *et al.*, 2007; Wehling *et al.*, 2008; Zhou, Siegel, Fedorov, and Lanzara, 2008a; Coletti *et al.*, 2010), lithographic residues (Dan *et al.*, 2009), and metal contacts (Connolly *et al.*, 2010).

The dopants introduce not only a change in the average carrier concentration but also charge inhomogeneities and scattering. Near the graphene neutrality point inhomogeneities of either sign can arise, which are often referred to as the electron-hole puddles (Geim and Novoselov, 2007). Thus, even at the neutrality point the graphene is always locally doped. This is a qualitative explanation for nonvanishing conductivity (Geim and Novoselov, 2007; Tan *et al.*, 2007; Chen *et al.*, 2008) and TDOS (Martin *et al.*, 2008). A more detailed model (Adam *et al.*, 2007; Hwang, Adam, and Das Sarma, 2007; Shklovskii, 2007; Rossi and Sarma, 2008) invokes a system of conducting electron-rich and hole-rich regions separated by *p*-*n* junctions (Cheianov, Fal'ko, and Altshuler, 2007; Zhang and Fogler, 2008). The transport involves percolation through the *p* and *n* regions aided by tunneling across the junctions (Cheianov *et al.*, 2007; Das Sarma *et al.*, 2011). Many elements of this semiclassical model hark back to the earlier studies of two-dimensional (Efros, Pikus, and Burnett, 1993; Fogler, 2004) and three-dimensional (Efros and Shklovskii, 1984) electron systems in semiconductors. However, the puddle model may not be quantitatively reliable for graphene. The correlation length of the density inhomogeneities is typically very short. For SLG on SiO_2 it was consistently estimated to be of the order of 20 nm using several complementary scanned probe microscopy techniques (Martin *et al.*, 2008; Berezovsky *et al.*, 2010; Deshpande *et al.*, 2011; Luican, Li, and Andrei, 2011). A typical electron-hole "puddle" is also too small to contain even a single charge (Martin *et al.*, 2008). Therefore, the inhomogeneities in question may be better described as quantum interference patterns of disorder-scattered electron waves rather than large semiclassical puddles. The situation may change if Coulomb interactions among electrons and impurities are screened. The crossover to the semiclassical regime is predicted to occur (Fogler, 2009) for graphene on a substrate of high dielectric constant $\kappa \gg 1$. Suppression of density inhomogeneities in one graphene layer due to screening by a nearby second layer has been invoked to explain the observed localization transition in graphene-hBN-graphene structures (Ponomarenko *et al.*, 2011).

The inhomogeneities may also be induced by elastic strain and ripples (Brey and Palacios, 2008; Guinea, Katsnelson, and Vozmediano, 2008; Gibertini *et al.*, 2010). Electron density inside the highly strained graphene bubbles (Bunch *et al.*, 2008; Levy *et al.*, 2010; Georgiou *et al.*, 2011) is undoubtedly inhomogeneous. However, the relation between strain and electron density is nonlocal. Indeed, no local correlations between the carrier density in graphene and the roughness of SiO_2 substrate is evident in scanned probe images (Martin *et al.*, 2008; Zhang, Brar *et al.*, 2009; Deshpande *et al.*, 2011).

The hypothesis that unintentional doping is caused by impurities trapped under graphene is supported by some micro-Raman experiments showing that proximity to the SiO_2 substrate results in an increase of carrier density (Berciaud *et al.*, 2009; Ni, Yu, Luo *et al.*, 2009; Bukowska *et al.*, 2011). Yet other micro-Raman measurements (Casiraghi *et al.*, 2009) have not observed such correlations.

Charge inhomogeneities can be reduced by either removing the substrate (Du *et al.*, 2008; Knox *et al.*, 2011) or using a high-quality hBN substrate (Dean *et al.*, 2010). The random charge fluctuations of exfoliated graphene on hBN are at least 2 orders of magnitude smaller than those on SiO_2 according to the scanning tunneling microscopy (STM) studies (Decker *et al.*, 2011b; Xue *et al.*, 2011). (However, in such structures periodic charge oscillations may appear instead of random ones; see Sec. IV.C.) These random fluctuations are on par with the values estimated from transport data for freestanding graphene (Du *et al.*, 2008). The electronic mobility of graphene on hBN approaches $\sim 10^5$ $cm^2/V\,s$ implying the mean-free path of several hundred nanometers (Du *et al.*, 2008; Dean *et al.*, 2010).

Although detrimental for transport properties, impurities can play the role of elementary perturbations that help reveal useful physical information. We give two examples. First, disorder-induced LDOS fluctuations seen in STS (Rutter *et al.*, 2007; Zhang, Brar *et al.*, 2009) reveal the dominant momenta for intervalley and intravalley scattering and therefore shed light on chirality and the energy spectrum of the quasiparticles. Second, by utilizing ionized Co adatoms one can study screening properties of graphene. The screening cloud surrounding the adatoms was shown to have a qualitatively different profile depending on the total charge of the adatom cluster. In the subcritical case this profile is governed essentially by the linear response dielectric constant of graphene. Theoretical modeling of the STS spectra (Brar *et al.*, 2011; Wang *et al.*, 2012) suggests the enhanced value $\epsilon \approx 3.0$ of this constant, which is indicative of many-body interactions (Sodemann and Fogler, 2012). In the supercritical case (Wang *et al.*, 2013) sharp resonances in the local DOS appear, which is the hallmark of a nonlinear screening with intriguing analogy to "atomic collapse" of superheavy elements.

B. Substrate-induced doping

Metallic substrates induce a strong doping of graphene, which is readily seen by the ARPES [Fig. 12(a)]. The

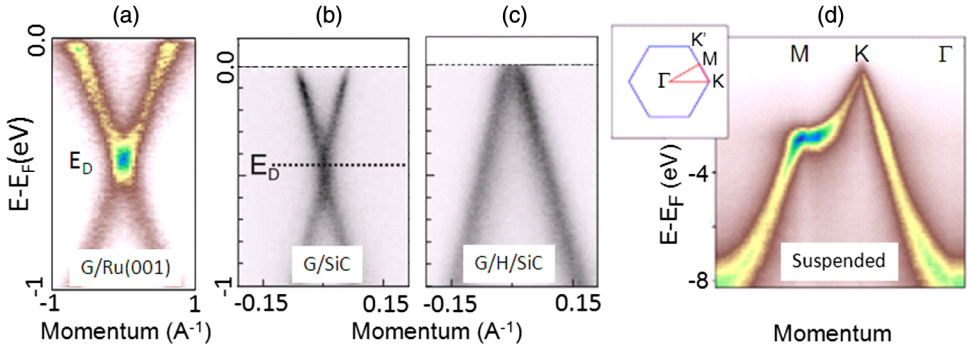

FIG. 12 (color online). The ARPES intensity along (a)–(c) the direction orthogonal to Γ-*K*, (d) the path Γ-*M*-*K*-Γ. (a) Adapted from Enderlein *et al.*, 2010. (b), (c) Adapted from Riedl *et al.*, 2009. (d) Adapted from Knox *et al.*, 2011.

chemical potential $\mu = E_F - E_D$ measured with respect to the Dirac point ranges from approximately 0.5 eV for Cu(111) (Gao, Guest, and Guisinger, 2010) and Cu films (Walter *et al.*, 2011a; Siegel *et al.*, 2012) to 2 eV for other transition metals, such as Ni(111) (Nagashima, Tejima, and Oshima, 1994; Dedkov *et al.*, 2008; Varykhalov *et al.*, 2008), Ru(0001) (Himpsel *et al.*, 1982; Sutter *et al.*, 2009; Enderlein *et al.*, 2010), and Co(0001) (Rader *et al.*, 2009). An exception to this is graphene on Ir(111) (N'Diaye *et al.*, 2006; Pletikosić *et al.*, 2009), where the surface states of the substrate cause pinning of μ near zero.

Naively, graphene is n doped if $W_G > W_M$ and p doped otherwise, where $W_G = 4.5$ eV is the work function of pristine graphene and W_M is that of the metal. In fact, the charge transfer is affected by chemical interaction between graphene and the metal and by their equilibrium separation (Giovannetti *et al.*, 2008). The amount of charge transfer can be modified by intercalation. Fluorine intercalation yields a large p-type doping of graphene (Walter *et al.*, 2011c). Hydrogen intercalation leads to decoupling of graphene from the substrate (Riedl *et al.*, 2009), as evidenced by the ARPES dispersions [Figs. 12(b) and 12(c)], typical of suspended graphene; cf. Fig. 12(d). Similar effects can be obtained by Au intercalation (Gierz *et al.*, 2008). When gold atoms are intercalated between graphene and a Ni(111) substrate (Varykhalov *et al.*, 2008), μ drops down to 25 meV, corresponding to the 2 orders of magnitude decrease in the carrier concentration.

C. Moiré patterns and energy gaps

When the lattice constants of the graphene layer and the substrate differ by a small relative amount δ and/or are misoriented by an angle ϕ a moiré supelattice arises (N'Diaye *et al.*, 2006; Marchini, Günther, and Wintterlin, 2007; B. Wang *et al.*, 2008; Wintterlin and Bocquet, 2009). The electron dispersion in the presence of the moiré superlattice gets modified as a result of hybridization of the original Dirac cones with their replicas folded into a superlattice Brillouin zone (sBZ). Such replicas have been seen in the ARPES spectra of graphene on Ir(111) (Pletikosić *et al.*, 2009) although they may also be due to the final-state diffraction (Sutter *et al.*, 2009).

The most striking experimental manifestations of the moiré superlattice effects have recently been observed in SGL on hBN. This system has $\delta = 1.8\%$, so that the moiré period can be as long as 14 nm, which can be easily imaged by scanned probes (Fig. 13, insets). Dependence of the moiré period on the misorientation angle ϕ is very sharp [Fig. 13(a)], so achieving a large period requires precise alignment.

It has been predicted theoretically that at the intersections of the replica and the main bands new Dirac points appear; see Fig. 13(c). For the practical case of a weak superlattice potential, these points have energy

$$E_D^m \simeq E_D \pm \frac{2\pi}{\sqrt{3}} \frac{\hbar v}{\Lambda}, \tag{4.1}$$

where Λ is the moiré period. [For the opposite limit of strong modulation, see Brey and Fertig (2009).] The extra Dirac points are characterized by a modified and generally, anisotropic quasiparticle velocity (Park *et al.*, 2008a; Guinea and Low, 2010; Wallbank *et al.*, 2013). The original Dirac point at the center of the sBZ remains gapless, at least, within the scope of generic theoretical models of the moiré superlattice which preserve sublattice symmetry.

First attempts to identify extra Dirac points in the SLG and hBN structures were unsuccessful because these points were outside the experimental energy window (Xue *et al.*, 2011). In more recent experiments, which utilized precisely aligned ($\phi < 0.5°$) structures, the new Dirac points are clearly evidenced by additional minima of the DOS measured by STS (Yankowitz *et al.*, 2012); see Fig. 13(b). The unmistakable signatures of the second-generation Dirac points in transport include peaks in longitudinal resistance and the sign change of the Hall resistance (Yankowitz *et al.*, 2012; Dean *et al.*, 2013; Ponomarenko *et al.*, 2013; Yang *et al.*, 2013); see Figs. 13(c) and 13(d). Additional LL fans emerging from these extra Dirac points are seen in magnetotransport (Dean *et al.*, 2013; Hunt *et al.*, 2013; Ponomarenko *et al.*, 2013) and the gate capacitance measurements. The detailed structure of such LLs is predicted to be fractal, as illustrated by the iconic image of the "Hofstadter butterfly" (Hofstadter, 1976). Experiments (Hunt *et al.*, 2013) in strong fields $B > 20$ T demonstrate additional quantum Hall plateaus and a large gap (tens of meV) at the neutrality point, the physical origin of which remains to be understood.

Opening a band gap at the Dirac point is indeed the most often cited effect that can enable wider applications of graphene. Inducing gap by confinement in various graphene superstructures such as quantum dots, ribbons, etc., has

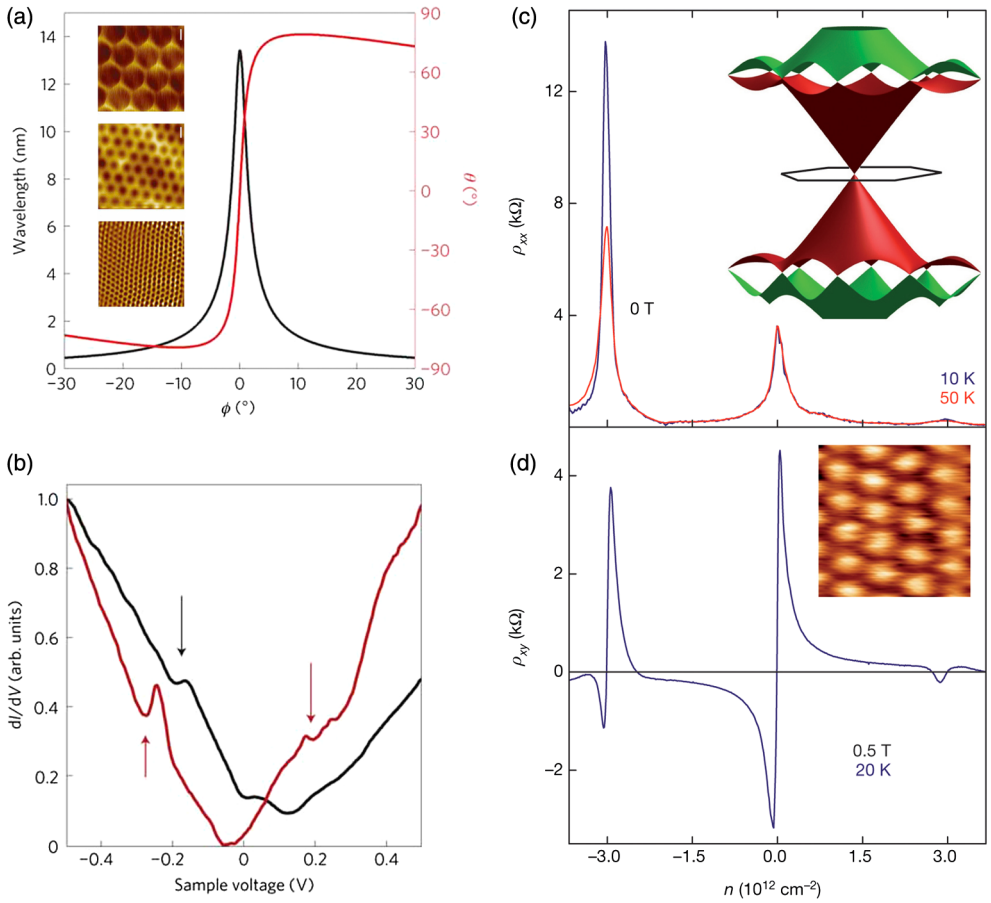

FIG. 13 (color online). (a) Moiré superlattice wavelength (left axis) and rotation (right axis) as a function of the angle between the SLG and hBN lattices. Inset: STM topography images showing (top to bottom) 2.4, 6.0, and 11.5 nm moiré patterns. The scale bars in all the images are 5 nm tall. (b) The tunneling dI/dV curves for samples with moiré wavelengths 9.0 nm (right curve) and 13.4 nm (left curve). The dips in the dI/dV curves marked by arrows occur at secondary Dirac points. (c) Longitudinal resistivity ρ_{xx} of SLG on hBN as a function of carrier density. Inset: One possible reconstruction of SLG spectrum. (d) The Hall resistivity ρ_{xy} changes sign at high electron and hole doping, revealing well-isolated secondary Dirac points. Inset: Conductive atomic force microscope image of the moiré pattern. The separation between the white spots is 11 nm. (a), (b) Adapted from Yankowitz *et al.*, 2012. (c), (d) Adapted from Ponomarenko *et al.*, 2013.

proved to be problematic due to disorder effects. Inducing a gap through the graphene-substrate interaction seems to be an attractive alternative. The most straightforward mechanism of the gap generation is breaking the sublattice symmetry of graphene (Nakada *et al.*, 1996; Brey and Fertig, 2006; Giovannetti *et al.*, 2007; Nilsson *et al.*, 2007; Trauzettel *et al.*, 2007). For a hypothetical commensurate SLG-hBN structure, a band gap ~50 meV was predicted (Giovannetti *et al.*, 2007; Sławińska, Zasada, and Klusek, 2010). Theoretically, the gap can also be induced by hybridization of the two valleys (Mañes, Guinea, and Vozmediano, 2007). A small band gap in graphene can also be induced by a spin-orbit coupling of the Rashba type (Kane and Mele, 2005). The curvature of the graphene sheet is predicted to enhance the Rashba splitting (Huertas-Hernando, Guinea, and Brataas, 2006; Kuemmeth *et al.*, 2008).

The existence of substrate-induced gaps has been indicated by many ARPES experiments. A wide spread of gap values has been reported, which remains unexplained. One of the earliest ARPES studies (Oshima and Nagashima, 1997) claimed the largest gap so far, 1.3 eV, for a "soft" SLG on TaC(111). Large gaps have also been reported for graphene on certain metallic substrates. Brugger *et al.* (2009) found an ~1 eV gap for SLG on Ru(0001). Nagashima, Tejima, and Oshima (1994) observed 0.7–1.3 eV gaps in SLG on Ni(111) intercalated with alkaline metals. For Ru(0001) covered with a monolayer of gold (Enderlein *et al.*, 2010) and for Ir(111) substrates (Starodub *et al.*, 2011) the gap is 0.2 eV. The effect of intercalants is counterintuitive because these are metals to which graphene interacts weakly. The gap for SLG on Cu is 0.3–0.4 eV. Zhou *et al.* (2007) made a case for the 0.26 eV gap in epitaxial graphene on SiC. As discussed in Sec. III.D, a competing interpretation of these data is in terms of plasmarons (Bostwick, Ohta, Seyller *et al.*, 2007; Bostwick, Ohta, McChesney *et al.*, 2007; Bostwick *et al.*, 2010). Comparable gaps were found for other semiconducting substrates (Siegel *et al.*, 2011; Walter *et al.*, 2011a). For graphene on graphite the gap of 20 meV (Li, Luican, and Andrei, 2009; Siegel *et al.*, 2011) was reported. The STS (Kawasaki *et al.*, 2002) observed a 0.5 eV for the SLG–single-layer hBN/Ni(111) structure.

The largest Rashba splitting 13 ± 3 meV has been reported for graphene on magnetic substrate Ni(111) intercalated by Au (Varykhalov *et al.*, 2008). The mechanism behind this

enhancement is still unknown. No Rashba splitting has been observed on another magnetic substrate, Co(0001) intercalated by Au (Rader *et al.*, 2009). Although intrinsic SO coupling is also responsible for the opening of a band gap Δ_{SO}, in pure SLG it is predicted to be extremely small, e.g., 10^{-3}–10^{-2} meV (Kane and Mele, 2005). A broken symmetry at the interface of two SLG can somewhat amplify this gap (Schmidt and Loss, 2010). Impurities in graphene resulting in sp^3-type deformation of the flat graphene are also predicted to enhance Δ_{SO} up to 7 meV (Castro Neto and Guinea, 2009). In fact, a recent experimental study on hydrogenated graphene revealed a drastically enhanced Δ_{SO} of 2.5 meV (Balakrishnan *et al.*, 2013). Alternatively, the interactions of charge carriers in graphene with heavy atoms such as In and Tl adsorbed on graphene are predicted to enhance Δ_{SO} up to 7 and 21 meV, respectively (Weeks *et al.*, 2011).

D. Elastic strain

A controlled uniaxial strain can be readily introduced into graphene by stretching the flexible substrate. The strain modifies the graphene phonon energy spectrum, which is effectively probed by Raman spectroscopy. Under uniaxial strain the G and $2D$ phonon bands display significant redshift proportional to the applied strain: a result of the anharmonicity of the interatomic potentials in graphene (Ni, Yu *et al.*, 2008; Huang *et al.*, 2009; Mohiuddin *et al.*, 2009; Ni, Yu, Lu *et al.*, 2009; Tsoukleri *et al.*, 2009). Meanwhile the sp^2 bonds of graphene lengthen or shorten in the direction parallel or perpendicular to the strain axis. This reduces the C_6 symmetry of the honeycomb lattice to C_2, and splits the doubly degenerate G band into two singlet bands, G^+ and G^-, with normal modes perpendicular and parallel to the strain axis, respectively. The polarization of Raman scattered light for the G^+ and G^- modes is thus expected to depend on the direction of the strain axis relative to the crystal orientation: a conjecture verified by Huang *et al.* (2009) and Mohiuddin *et al.* (2009).

Strain also introduces profound modifications to the graphene electronic structure. The defining topology feature of the graphene electronic band, namely, the degeneracy of conical electron and hole bands at Dirac points, is protected by the inversion symmetry of graphene lattice (Hasegawa *et al.*, 2006; Kishigi, Takeda, and Hasegawa, 2008; Wunsch, Guinea, and Sols, 2008). A small perturbation in the form of mechanical strain does not lift the degeneracy, but deforms the energy bands and shifts the Dirac points in both the energy and the momentum space. The former is equivalent to a scalar potential also known as the deformation potential. A general nonuniform strain generates a spatially varying dilation of the graphene lattice and therefore local ion density. The deformation potential arises because the corresponding Coulomb potential is only partially screened by electrons (Suzuura and Ando, 2002; Guinea, Horovitz, and Le Doussal, 2008; Kim and Castro Neto, 2008). Next, shifting the Dirac point in the k space away from the K (K') points (Dietl, Piéchon, and Montambaux, 2008; Ni, Yu *et al.*, 2008; Farjam and Rafii-Tabar, 2009; Ni, Yu, Lu *et al.*, 2009; Pereira and Castro Neto, 2009) is analogous to the effect induced by an external magnetic field applied perpendicular to the graphene plane. One can parametrize the mechanical strain by a gauge field $\mathbf{A}$ (Iordanskii and Koshelev, 1985; Kane and Mele, 1997; Sasaki, Kawazoe, and Saito, 2005; Morpurgo and Guinea, 2006; Katsnelson and Novoselov, 2007; Fogler, Guinea, and Katsnelson, 2008) and define the pseudomagnetic field $B_s = \nabla \times \mathbf{A}$. The strain-induced $\mathbf{A}$ and B_s have opposite

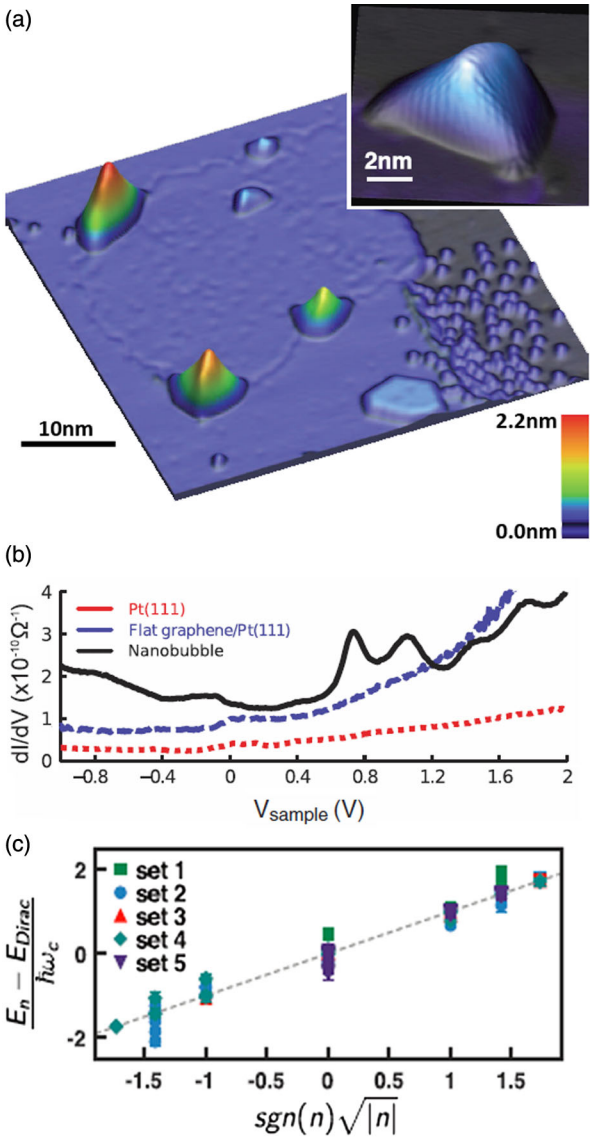

FIG. 14 (color online). STM images and STS spectra taken at 7.5 K. (a) Graphene monolayer patch on Pt(111) with four nanobubbles at the graphene-Pt border and one in the patch interior. Residual ethylene molecules and a small hexagonal graphene patch can be seen in the lower right (3D z scale enhanced 4.6×). (Inset) High-resolution image of a graphene nanobubble showing distorted honeycomb lattice resulting from strain in the bubble (max $z = 1.6$ nm, 3D z scale enhanced 2×). (b) STS spectra of bare Pt(111), flat graphene on Pt(111) (shifted upward by $3 \times 10^{-11}\,\Omega^{-1}$), and the center of a graphene bubble (shifted upward by $9 \times 10^{-11}\,\Omega^{-1}$). The peaks in the graphene bubble spectrum indicate the formation of pseudo-Landau levels. (c) Normalized peak energy vs $\mathrm{sgn}(n)\sqrt{|n|}$ for peaks observed on five different nanobubbles follow expected scaling behavior (see text). Adapted from Levy *et al.*. 2010.

signs at two valleys K and K', so that the time-reversal symmetry is preserved.

It is possible to engineer a special nonuniform strain for which B_s is approximately constant in a finite-size region. If such pseudomagnetic field is strong enough, it can lead to Landau quantization and quantum Hall-like states (Guinea, Katsnelson, and Geim, 2010; Guinea *et al.*, 2010). In a recent experiment (Levy *et al.*, 2010), such an unusual Landau quantization has been observed in highly strained graphene nanobubbles. The strain arises upon cooling because of a mismatch in the thermal expansion coefficients of graphene and the Pt substrate [Fig. 14(a)]. The pseudo-Landau levels, manifested as local density of states peaks, are probed by STS [Figs. 14(b) and 14(c)]. Their energies follow the theoretically predicted $\mathrm{sgn}(n)\sqrt{|n|}$ behavior with a gigantic $B_s \sim 300$ T; see Fig. 14(c).

E. Photoinduced effects

Optical spectroscopy with ultrafast laser excitation pulses provides a unique tool to probe the dynamic evolution of electrons and phonons in graphene, including the cooling of the nonequilibrium quasiparticle plasma through electron-electron and electron-phonon interactions and the relaxation of hot optical phonons. These processes are not only of fundamental interest due to the unusual electronic structure in graphene, but also important for technological applications of high-field electronics and nonlinear photonic devices (Bao *et al.*, 2009; Fengnian Xia *et al.*, 2009; Bonaccorso *et al.*, 2010; Zhipei Sun *et al.*, 2010; Zhang *et al.*, 2010).

The response of graphene to a pulsed laser excitation has been studied by several complementary ultrafast spectroscopy techniques. For example, pump-probe IR-visible spectroscopy (Dawlaty *et al.*, 2008; Sun *et al.*, 2008; Newson *et al.*, 2009; Huang *et al.*, 2010) and pump-probe THz spectroscopy (George *et al.*, 2008) has been employed to track the time evolution of optical absorption and transmission by graphene. Ultrafast photoluminescence (Liu *et al.*, 2010, 2010; Stöhr *et al.*, 2010) has been used to monitor light emission by nonequilibrium electron gas. Time-resolved Raman spectroscopy (Yan *et al.*, 2009; Chatzakis *et al.*, 2011) has explored the generation and decay of hot optical phonons. Breusing, Ropers, and Elsaesser (2009) studied graphite using 7 fs, 1.55 eV pump pulses and broadband probe pulses with energy spectrum from 1.2 to 2 eV. Figure 15(a) shows the observed increase of transmission during the first 150 eV with sub-10 fs time resolution. This phenomenon is attributed to partial Pauli blocking of the optical transition by photoexcited electron-hole pairs. The change in transmission scales linearly with the pump influence and decays with two time constants of 13 and 100 fs. The former characterizes electron-electron interactions, which cause energy redistribution within the conduction and valence bands, as well as relaxation of occupation factors by Auger processes. The second time constant describes interaction of quasiparticles with optical phonons. The emission of optical phonons with energy ≈ 0.2 eV cools down electron-hole plasma. Once its temperature drops below this number, emission of optical phonons becomes ineffective. Eventual equilibration of the electron and lattice temperatures

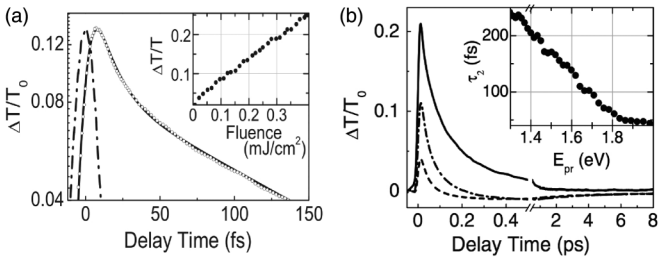

FIG. 15. Ultrafast dynamics of excited electrons in graphene. (a) Spectrally integrated transmission change as a function of pump-probe delay (open circles). The solid line is the numerical fit, and the dash-dotted line is the cross correlation of pump and probe pulses. The inset shows linear dependence of the maximum transmission change on the absorbed pump fluence. The transmission increase is due to photoinduced Pauli blocking of interband transitions. The ultrafast decay is due to thermalization between the electrons and holes and optical phonons. (b) Transient transmission changes at probe photon energies of 1.24 eV (solid), 1.55 eV (dash-dotted), and 1.77 eV (dashed) for short and long delays. The slower decay at the picosecond time scale is due to equilibration with acoustic phonons. From Breusing, Ropers, and Elsaesser, 2009.

is achieved by emission of acoustic phonons on a time scale of $\sim$2 ps.

The decay dynamics of graphene in the 8 ps temporal range is shown in Fig. 15(b) with three different probe photon energies. In addition to the fast decay processes described above, it shows a slower relaxation process with a time constant of 1.4 ps. This picosecond time scale reflects partial thermalization between the hot electron and holes and optical phonons with the acoustic phonons in graphene. We note that the photoinduced transmission change can become negative at certain probe photon energies at longer delay. This is because optical excitation not only leads to Pauli blocking of interband transitions, but also increased high frequency absorption from intraband transitions. At longer pump-probe delay, the intraband absorption can dominate over the Pauli blocking effects at some probe photon energies. Similar photoinduced transmission decreases have also been observed in optical pump-THz probe measurements, where photoinduced intraband transitions always dominate (George *et al.*, 2008; Wright *et al.*, 2009; Strait *et al.*, 2011).

Ultrafast photoluminescence monitors the light emission from the highly nonequilibrium electrons after femtosecond pump excitations (Liu *et al.*, 2010, 2010; Stöhr *et al.*, 2010). Broad light emission across the visible spectral range (1.7–3.5 eV) was observed with femtosecond near-IR laser excitation, where the incident photon has an energy of 1.5 eV. This unusual blueshifted photoluminescence exhibits a nonlinear dependence on the laser fluence, and it has a dominant relaxation time within 100 fs. This nonlinear blueshifted luminescence was attributed to a recombination of hot electron-hole plasma generated right after the femtosecond excitation.

In addition to the electron dynamics, researchers were able to probe the phonon dynamics specifically using time-resolved Raman spectroscopy (Yan *et al.*, 2009; Chatzakis *et al.*, 2011). Such studies show a decay lifetime of 2.5 ps

for the BZ-center G-mode phonons. This time scale corresponds to the cooling of the optical phonons through anharmonic coupling to acoustic phonons, and the 2.5 ps time constant is similar to that obtained in pump-probe transmission spectroscopy.

V. BILAYER AND MULTILAYER GRAPHENE

There has been a rapidly increasing interest in graphene systems with more than one layer [for an early review, see Nilsson *et al.* (2008)]. The electronic structure of BLG and MLG is distinctly different from that of SLG. These differences give rise to many new phenomena, ranging from a tunable band gap (McCann, 2006; McCann and Fal'ko, 2006; Castro *et al.*, 2007; Oostinga *et al.*, 2007; Zhang, Tang *et al.*, 2009) to strongly correlated ground states (Feldman, Martin, and Yacoby, 2009; Bao *et al.*, 2010; Weitz *et al.*, 2010; Mayorov *et al.*, 2011a; Velasco *et al.*, 2012). Unfortunately, space limitations and the open debate on the nature of these low-energy states (Nilsson *et al.*, 2006; Min *et al.*, 2008; Barlas *et al.*, 2010; Nandkishore and Levitov, 2010a, 2010b, 2011; Vafek and Yang, 2010) do not permit us to describe them in any detail. Here we confine ourselves to discussing "higher" energy properties of these materials that have been measured by ARPES and by optical spectroscopy.

We begin by discussing the quasiparticle dispersion of BLG. For the Bernal-stacked BLG, which is the most energetically favorable structure, it is conventionally described by means of five parameters. They include four hopping integrals $\gamma_0 = 3.0$, $\gamma_1 = 0.41$, $\gamma_3 = 0.3$, $\gamma_4 = 0.15$ eV, and also the on-site energy shift $\Delta' = 0.018$ eV [Fig. 1(b)]. [For a discussion of these numerical values and comparison with graphite, see L. M. Zhang *et al.* (2008), Kuzmenko, Benfatto *et al.* (2009), Kuzmenko, van Heumen *et al.* (2009), and Li *et al.* (2009).] When BLG is subject to an electric field due to external gates or charged impurities, the sixth parameter, a scalar potential $\pm\Delta/2$ on the two layers must be included. The interlayer bias $\Delta = eEd$ is given by the product of the layer separation $d = 0.335$ nm and the electric field E between the layers.

The BLG has four atoms in the unit cell, and so the electron spectrum consists of four bands. The two outer (lowest and highest energy) bands are hyperbolic, with the extremal values at approximately $\pm\gamma_1$ reached at the BZ corners. The shape of the two inner bands is more intricate. At high energies they are nested with the outer bands. At low energies their dispersion depends on the relation between the gap Δ and the hopping integral γ_3, which causes the trigonal warping. At $\Delta \gg \gamma_3/\gamma_0\gamma_1$, the trigonal warping is a small effect. The bands are shaped as sombreros, e.g., the conduction band has a local maximum at energy $\Delta/2$ at $q = 0$ and a local minimum—the bottom of the sombrero—at the ring $|\mathbf{q}| \approx \Delta/\sqrt{2}\hbar v_0$; see Fig. 16(d), right panel (McCann and Fal'ko, 2006). As Δ is decreased, the trigonal warping of the bottom of the sombrero becomes more and more pronounced. In the absence of the interlayer bias, $\Delta = 0$, the parabolic extrema split into the four conical Dirac points. This reconstruction is an example of the Lifshitz transition. The linear rather than parabolic shape of the bands in the symmetric BLG is supported by the linear-T dependence of low-temperature electric conductivity in extremely clean suspended BLG (Mayorov *et al.*, 2011a). However, in less perfect samples, the quadruple Dirac cones structure is smeared by disorder. It is therefore common to approximate the inner bands by hyperboloids touching at a point; see Fig. 16(d), left panel.

In order to vary Δ, one has to apply an external electric field to BLG. This can be achieved experimentally through electrostatic gating or doping. If D_t and D_b are electric displacement fields on the two sides of BLG [Fig. 16(c)], then the interlayer electric field E is determined by their mean $\bar{D} = (D_b + D_t)/2$. Notably, E is smaller than $\bar{D}$ due to screening effects. Calculations within the self-consistent Hartree approximation (McCann and Fal'ko, 2006) predict a factor of 2 or so reduction in typical experimental conditions.

The difference $D = D_b - D_t$ of the displacement fields produces a net carrier doping, and so the Fermi energy shift [Fig. 16(d)]. Unless D_t and D_b are precisely equal or precisely opposite, the modification of the band gap Δ and the shift of the Fermi energy E_F occur simultaneously (McCann, 2006; McCann and Fal'ko, 2006; Castro *et al.*, 2007).

The control of the electronic structure of BLG was first revealed in ARPES studies of potassium-doped epitaxial graphene on SiC (Ohta *et al.*, 2006). Figures 16(e)–16(g) display the evolution of the ARPES spectra with doping. As prepared, BLG is n-type doped. This corresponds to a finite D_b and zero D_t, leading to a nonzero band gap [Fig. 16(e)]. Potassium adsorption generates a finite D_t. When its value is the same as D_b, one obtains an electron doped gapless BLG [Fig. 16(f)]. With further increase in potassium doping, the band gap reappears [Fig. 16(g)]. Tuning of the BLG electron structure can also be achieved via coupling to different substrates (Siegel *et al.*, 2010).

Complimentary insight on the band structure of BLG has been provided through IR spectroscopy. There is a total of six interband optical transitions possible in this material. The near-perfect nesting of two conductions bands results in a strong absorption peak at mid-IR energy γ_1, when the transition between them is activated by n-type doping. A refined estimate of $\gamma_1 = 0.40 \pm 0.01$ eV has been obtained by monitoring the line shape and position of this peak in a gated BLG structure as a function of the gate voltage and modeling these spectra theoretically (Zhang, Tang *et al.*, 2009). Similarly, the p-type doping activates transition between the two valence bands. From slight differences of p- and n-type spectra, the electron-hole symmetry breaking parameters γ_4 and Δ' have been inferred. The parameters obtained from the IR experiments are corroborated by those derived from the Raman spectroscopy (Malard *et al.*, 2007) and the capacitance measurements of the TDOS (Henriksen and Eisenstein, 2010).

The band gap tuning by electrical gating was demonstrated using IR spectroscopy through monitoring the gate-induced change in other three transitions shown in Fig. 16(d) by arrows (Kuzmenko, Crassee *et al.*, 2009; Mak *et al.*, 2009; Zhang, Tang *et al.*, 2009). The dependence on the band gap on the mean displacement field $\bar{D}$ [Fig. 16(h)] was found to be in agreement with theory (McCann and Fal'ko, 2006).

On the other hand, observing the predicted band gap value from electrical transport measurements has been challenging

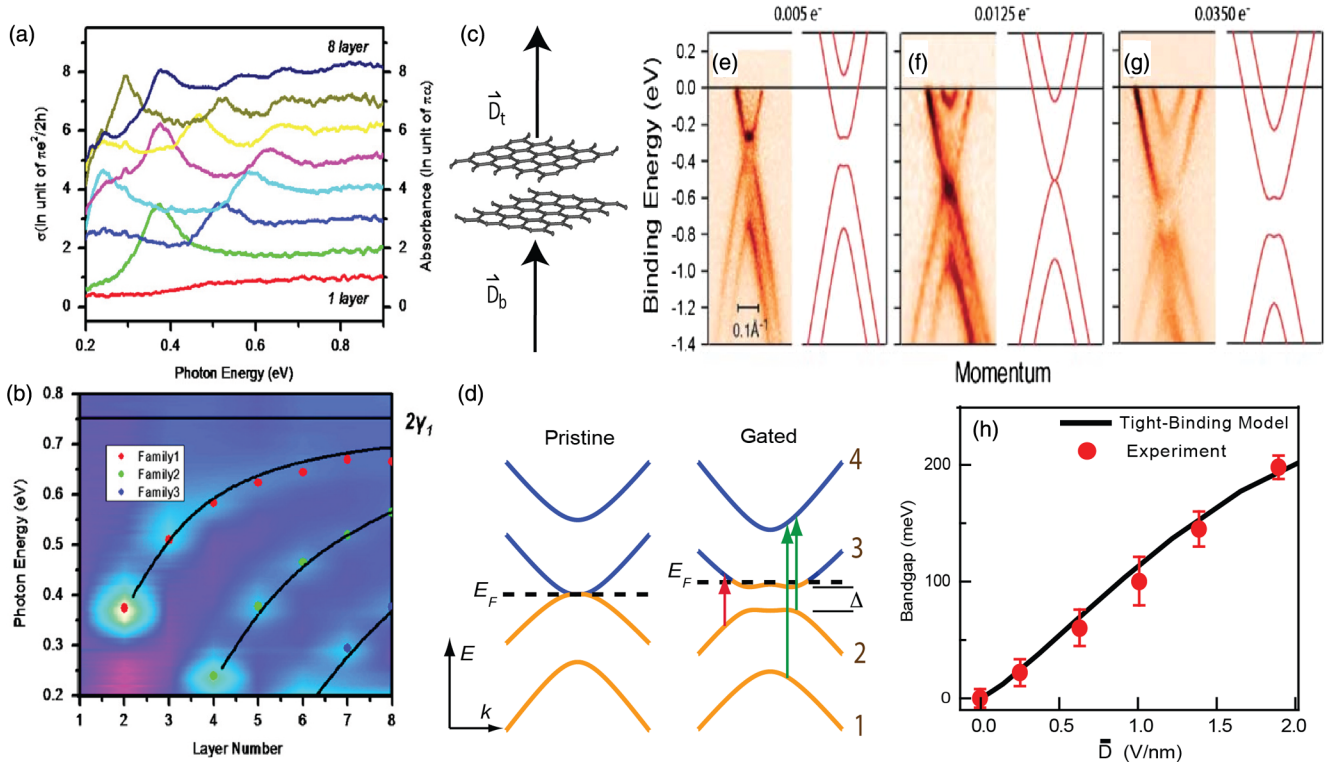

FIG. 16 (color online). (a) IR conductivity spectra of MLG with layer number $L = 1, 2, \ldots, 8$. (b) A contour plot of the IR conductivity per layer as a function of photon energy and L. The dots identify the position of the peaks in experimental IR conductivity. These transition energies follow well-defined energy-scaling relations predicted by the zone-folding model (solid curves). From Mak *et al.*, 2010. (c) An illustration of the Bernal-stacked BLG with electrical field above and below it. (d) Electronic structure of a pristine and a gated BLG. Arrows indicate allowed optical transitions. (e)–(g) ARPES data showing the evolution of an induced band gap in electronic structure of epitaxial BLG on SiC with chemical adsorbed Ca atoms. From Ohta *et al.*, 2006. (h) Electrical field dependence of the induced band gap in BLG measured through IR absorption spectroscopy (symbols). From Zhang, Tang *et al.*, 2009.

(Castro *et al.*, 2007; Oostinga *et al.*, 2007; Szafranek *et al.*, 2010; Xia *et al.*, 2010). Gated BLG typically exhibits an insulating behavior only at $T < 1$ K, suggesting a very narrow gap (Oostinga *et al.*, 2007). This is because electrical transport is extremely sensitive to defects and impurities, and a very high-quality graphene is required to reach the intrinsic BLG behavior. Recent transport studies (Xia *et al.*, 2010), however, demonstrate transport gaps closer to those obtained through IR spectroscopy.

Electron-phonon coupling in gated BLG shows up in tunable electron-phonon Fano resonances (Kuzmenko, Benfatto *et al.*, 2009; Cappelluti, Benfatto, and Kuzmenko, 2010; Tang *et al.*, 2010). There is a host of other effects that originate from unique gate-tunable electronic structures in BLG that have been predicted theoretically and are amenable to spectroscopic studies, e.g., a rich Landau level spectrum structure (Zhang, Fogler, and Arovas, 2011). However, we must leave this topic now to at least briefly discuss MLG.

The electronic structure of MLG has been investigated experimentally using optical spectroscopy. Figure 16(a) displays a set of IR absorption spectra from $L = 1$ to 8 layer graphene over the photon-energy range of 0.2–0.9 eV (Mak *et al.*, 2010). At energies in the range $\gamma_1 \ll \hbar\omega \ll \gamma_0$ the MLG is expected to behave in the first approximation as a stack of uncoupled SLG, each possessing the universal optical conductivity σ_0, Eq. (3.1). Indeed, at energies above 0.8 eV, the measured optical absorption scales linearly with L. However, at lower energies, the absorption becomes highly structured and distinct for different L. The evolution of the absorption spectra as a function of L can be visualized from the false color plot of Fig. 16(b) in which the principle transition energies are marked by the solid curves. The shape of these curves can be understood through zone folding of the graphite band structure. In particular, a gapless band is present if L is odd and absent if it is even (Mak *et al.*, 2010).

VI. OUTLOOK

A wealth of spectroscopic data analyzed in this Colloquium has provided a panoramic picture of electronic phenomena in graphene. The concept of 2D Dirac quasiparticles offers a unifying description of the gross features revealed in all spectroscopic and transport probes. At the same time, pronounced and reproducible deviations from the predictions of noninteracting models of graphene have been documented. An outstanding challenge for future research is probing these many-body effects using specimens of record-high electron mobility where the role of disorder is further reduced.

Because of space limitations, we have not been able to cover some topics, e.g., nanostructured graphene, spin phenomena, graphene at ultrahigh doping, or fractional quantum Hall effect in graphene (Goerbig, 2011). We also

covered some others, e.g., BLG and MLG, in insufficient detail. These topics are being actively explored, and the consensus is still being reached (McCann and Koshino, 2013). In addition, a particularly interesting class of materials for future research is hybrid multilayer structures and superlattices assembled from graphene and other ultrathin atomic crystals, such as hBN, MoS_2, etc. (Geim and Grigorieva, 2013).

Besides fundamental research, graphene and its spectroscopy have inspired a number of applications. For example, the spectroscopic studies motivated the development of novel experimental tools and methods compatible with the architecture of gatable devices. Novel scanning spectroscopies have advanced by exploiting the unique aspect of graphene that graphene is unobstructed by other interfaces. Controlled modification of graphene properties has been demonstrated through using elastic strain, interactions with the substrate, adatoms, and/or other graphene layers. These new experimental approaches are expected to find applications in other areas of condensed matter physics. Examples of viable device concepts spawned by photon-based spectroscopies include compact (passive) optical components, photodetectors and bolometers, and saturable absorbers. In addition, standard plasmonics figures of merit show competitiveness or even superiority of graphene as a plasmonic medium compared to more seasoned metal-based technologies. An unresolved question is whether graphene is suitable for achieving population inversion and lasing.

ACKNOWLEDGMENTS

D. B., M. F., and F. W. acknowledge support from ONR under Grant No. N0014-13-0464. The work at UCSD is also supported by DOE-BES under Contract No. DE-FG02-00ER45799, by AFOSR Grant No. FA9550-09-1-0566, by NSF Grant No. DMR-1337356, by ARO Grant No. W911NF-13-1-0210, and also by UCOP and FENA. Additionally, F. W. is supported by DOE-BES under Contracts No. DE-SC0003949 and No. DE-AC02-05CH11231. A. L. acknowledges support from the Novel sp^2-bonded Materials Program at Lawrence Berkeley National Laboratory, funded by the DOE Office of Basic Energy Sciences, Materials Sciences and Engineering Division under Contract No. DE-AC02-05CH11231. Y. Z is supported by NSF of China through Grant No. 11034001 and MOST of China through Grant No. 2011CB921802.

REFERENCES

Abedpour, N., M. Neek-Amal, Reza Asgari, F. Shahbazi, N. Nafari, and M. Reza Rahimi Tabar, 2007, "Roughness of undoped graphene and its short-range induced gauge field," Phys. Rev. B **76**, 195407.

Abergel, D. S. L., A. Russell, and Vladimir I. Fal'ko, 2007, "Visibility of graphene flakes on a dielectric substrate," Appl. Phys. Lett. **91**, 063125.

Adam, S., E. H. Hwang, V. M. Galitski, and S. Das Sarma, 2007, "A self-consistent theory for graphene transport," Proc. Natl. Acad. Sci. U.S.A. **104**, 18 392.

Ando, Tsuneya, Yisong Zheng, and Hidekatsu Suzuura, 2002, "Dynamical Conductivity and Zero-Mode Anomaly in Honeycomb Lattices," J. Phys. Soc. Jpn. **71**, 1318.

Ashcroft, N. W., and N. D. Mermin, 1976, *Solid State Physics* (Saunders College, Philadelphia).

Bae, Sukang, *et al.*, 2010, "Roll-to-roll production of 30-inch graphene films for transparent electrodes," Nat. Nanotechnol. **5**, 574.

Balakrishnan, Jayakumar, Gavin Kok Wai Koon, Manu Jaiswal, A. H. Castro Neto, and Barbaros Özyilmaz, 2013, "Colossal enhancement of spin-orbit coupling in weakly hydrogenated graphene," Nat. Phys. **9**, 284.

Balandin, Alexander A., Suchismita Ghosh, Wenzhong Bao, Irene Calizo, Desalegne Teweldebrhan, Feng Miao, and Chun Ning Lau, 2008, "Superior Thermal Conductivity of Single-Layer Graphene," Nano Lett. **8**, 902.

Bao, Qiaoliang, Han Zhang, Yu Wang, Zhenhua Ni, Yongli Yan, Ze Xiang Shen, Kian Ping Loh, and Ding Yuan Tang, 2009, "Atomic-Layer Graphene as a Saturable Absorber for Ultrafast Pulsed Lasers," Adv. Funct. Mater. **19**, 3077.

Bao, Wenzhong, Zeng Zhao, Hang Zhang, Gang Liu, Philip Kratz, Lei Jing, Jairo Velasco, Dmitry Smirnov, and Chun Ning Lau, 2010, "Magnetoconductance Oscillations and Evidence for Fractional Quantum Hall States in Suspended Bilayer and Trilayer Graphene," Phys. Rev. Lett. **105**, 246601.

Barlas, Yafis, R. Côté, J. Lambert, and A. H. MacDonald, 2010, "Anomalous Exciton Condensation in Graphene Bilayers," Phys. Rev. Lett. **104**, 096802.

Barlas, Yafis, T. Pereg-Barnea, Marco Polini, Reza Asgari, and A. H. MacDonald, 2007, "Chirality and Correlations in Graphene," Phys. Rev. Lett. **98**, 236601.

Basko, D. M., 2008, "Theory of resonant multiphonon Raman scattering in graphene," Phys. Rev. B **78**, 125418.

Basko, D. M., 2009, "Calculation of the Raman G peak intensity in monolayer graphene: role of Ward identities," New J. Phys. **11**, 095011.

Basko, D. M., and I. L. Aleiner, 2008, "Interplay of Coulomb and electron-phonon interactions in graphene," Phys. Rev. B **77**, 041409(R).

Basko, D. M., S. Piscanec, and A. C. Ferrari, 2009, "Electron-electron interactions and doping dependence of the two-phonon Raman intensity in graphene," Phys. Rev. B **80**, 165413.

Basov, D. N., Richard D. Averitt, Dirk van der Marel, Martin Dressel, and Kristjan Haule, 2011, "Electrodynamics of correlated electron materials," Rev. Mod. Phys. **83**, 471.

Benfatto, L., and E. Cappelluti, 2008, "Spectroscopic signatures of massless gap opening in graphene," Phys. Rev. B **78**, 115434.

Berciaud, Stéphane, Sunmin Ryu, Louis E. Brus, and Tony F. Heinz, 2009, "Probing the Intrinsic Properties of Exfoliated Graphene: Raman Spectroscopy of Free-Standing Monolayers," Nano Lett. **9**, 346.

Berezovsky, J., M. F. Borunda, E. J. Heller, and R. M. Westervelt, 2010, "Imaging coherent transport in graphene (part I): mapping universal conductance fluctuations," Nanotechnology **21**, 274013.

Berger, Claire, *et al.*, 2004, "Ultrathin Epitaxial Graphite: 2D Electron Gas Properties and a Route toward Graphene-based Nanoelectronics," J. Phys. Chem. B **108**, 19 912.

Berger, Claire, *et al.*, 2006, "Electronic Confinement and Coherence in Patterned Epitaxial Graphene," Science **312**, 1191.

Bianchi, M., E. D. L. Rienks, S. Lizzit, A. Baraldi, R. Balog, L. Hornekær, and Ph. Hofmann, 2010, "Electron-phonon coupling in potassium-doped graphene: Angle-resolved photoemission spectroscopy," Phys. Rev. B **81**, 041403(R).

Bistritzer, Rafi, and Allan H. MacDonald, 2011, "Moiré bands in twisted double-layer graphene," Proc. Natl. Acad. Sci. U.S.A. **108**, 12 233.

Blake, P., E. W. Hill, A. H. Castro Neto, K. S. Novoselov, D. Jiang, R. Yang, T. J. Booth, and A. K. Geim, 2007, "Making graphene visible," Appl. Phys. Lett. **91**, 063124.

Boehm, H. P., A. Clauss, G. O. Fischer, and U. Hofmann, 1962, "Das Adsorptionsverhalten sehr dünner Kohlenstoff-Folien," Z. Anorg. Allg. Chem. **316**, 119.

Bolotin, K. I., K. J. Sikes, Z. Jiang, M. Klima, G. Fudenberg, J. Hone, P. Kim, and H. L. Stormer, 2008, "Ultrahigh electron mobility in suspended graphene," Solid State Commun. **146**, 351.

Bonaccorso, F., Z. Sun, T. Hasan, and A. C. Ferrari, 2010, "Graphene photonics and optoelectronics," Nat. Photonics **4**, 611.

Bostwick, Aaron, Taisuke Ohta, Jessica L. McChesney, Thomas Seyller, Karsten Horn, and Eli Rotenberg, 2007, "Renormalization of graphene bands by many-body interactions," Solid State Commun. **143**, 63.

Bostwick, Aaron, Taisuke Ohta, Thomas Seyller, Karsten Horn, and Eli Rotenberg, 2007, "Quasiparticle dynamics in graphene," Nat. Phys. **3**, 36.

Bostwick, Aaron, Florian Speck, Thomas Seyller, Karsten Horn, Marco Polini, Reza Asgari, Allan H. MacDonald, and Eli Rotenberg, 2010, "Observation of Plasmarons in Quasi-Freestanding Doped Graphene," Science **328**, 999.

Brar, Victor W., *et al.*, 2010, "Observation of Carrier-Density-Dependent Many-Body Effects in Graphene via Tunneling Spectroscopy," Phys. Rev. Lett. **104**, 036805.

Brar, Victor W., *et al.*, 2011, "Gate-controlled ionization and screening of cobalt adatoms on a graphene surface," Nat. Phys. **7**, 43.

Breusing, Markus, Claus Ropers, and Thomas Elsaesser, 2009, "Ultrafast Carrier Dynamics in Graphite," Phys. Rev. Lett. **102**, 086809.

Brey, L., and H. A. Fertig, 2006, "Electronic states of graphene nanoribbons studied with the Dirac equation," Phys. Rev. B **73**, 235411.

Brey, L., and H. A. Fertig, 2009, "Emerging Zero Modes for Graphene in a Periodic Potential," Phys. Rev. Lett. **103**, 046809.

Brey, L., and J. J. Palacios, 2008, "Exchange-induced charge inhomogeneities in rippled neutral graphene," Phys. Rev. B **77**, 041403(R).

Brihuega, I., P. Mallet, C. Bena, S. Bose, C. Michaelis, L. Vitali, F. Varchon, L. Magaud, K. Kern, and J. Y. Veuillen, 2008, "Quasiparticle Chirality in Epitaxial Graphene Probed at the Nanometer Scale," Phys. Rev. Lett. **101**, 206802.

Brugger, Thomas, Sebastian Günther, Bin Wang, J. Hugo Dil, Marie-Laure Bocquet, Jürg Osterwalder, Joost Wintterlin, and Thomas Greber, 2009, "Comparison of electronic structure and template function of single-layer graphene and a hexagonal boron nitride nanomesh on Ru(0001)," Phys. Rev. B **79**, 045407.

Bukowska, H., F. Meinerzhagen, S. Akcöltekin, O. Ochedowski, M. Neubert, V. Buck, and M. Schleberger, 2011, "Raman spectra of graphene exfoliated on insulating crystalline substrates," New J. Phys. **13**, 063018.

Bunch, J. Scott, Scott S. Verbridge, Jonathan S. Alden, Arend M. van der Zande, Jeevak M. Parpia, Harold G. Craighead, and Paul L. McEuen, 2008, "Impermeable Atomic Membranes from Graphene Sheets," Nano Lett. **8**, 2458.

Calandra, Matteo, and Francesco Mauri, 2007a, "Electron-phonon coupling and electron self-energy in electron-doped graphene: Calculation of angular-resolved photoemission spectra," Phys. Rev. B **76**, 205411.

Calandra, Matteo, and Francesco Mauri, 2007b, "Electronic structure of heavily doped graphene: The role of foreign atom states," Phys. Rev. B **76**, 161406.

Calizo, I., A. A. Balandin, W. Bao, F. Miao, and C. N. Lau, 2007, "Temperature Dependence of the Raman Spectra of Graphene and Graphene Multilayers," Nano Lett. **7**, 2645.

Cappelluti, E., L. Benfatto, and A. B. Kuzmenko, 2010, "Phonon switching and combined Fano-Rice effect in optical spectra of bilayer graphene," Phys. Rev. B **82**, 041402(R).

Carbotte, J. P., J. P. F. LeBlanc, and E. J. Nicol, 2012, "Emergence of Plasmaronic Structure in the Near Field Optical Response of Graphene," Phys. Rev. B **85**, 201411(R).

Casiraghi, C., A. Hartschuh, H. Qian, S. Piscanec, C. Georgi, A. Fasoli, K. S. Novoselov, D. M. Basko, and A. C. Ferrari, 2009, "Raman Spectroscopy of Graphene Edges," Nano Lett. **9**, 1433.

Castro, Eduardo V., K. S. Novoselov, S. V. Morozov, N. M. R. Peres, J. M. B. Lopes dos Santos, Johan Nilsson, F. Guinea, A. K. Geim, and A. H. Castro Neto, 2007, "Biased Bilayer Graphene: Semiconductor with a Gap Tunable by the Electric Field Effect," Phys. Rev. Lett. **99**, 216802.

Castro Neto, A. H., and F. Guinea, 2009, "Impurity-Induced Spin-Orbit Coupling in Graphene," Phys. Rev. Lett. **103**, 026804.

Castro Neto, A. H., F. Guinea, N. M. R. Peres, K. S. Novoselov, and A. K. Geim, 2009, "The electronic properties of graphene," Rev. Mod. Phys. **81**, 109.

Chae, Dong-Hun, Tobias Utikal, Siegfried Weisenburger, Harald Giessen, Klaus v. Klitzing, Markus Lippitz, and Jurgen Smet, 2011, "Excitonic Fano Resonance in Free-Standing Graphene," Nano Lett. **11**, 1379.

Chae, Jungseok, *et al.*, 2012, "Renormalization of the Graphene Dispersion Velocity Determined from Scanning Tunneling Spectroscopy," Phys. Rev. Lett. **109**, 116802.

Charrier, A., A. Coati, T. Argunova, F. Thibaudau, Y. Garreau, R. Pinchaux, I. Forbeaux, J.-M. Debever, M. Sauvage-Simkin, and J.-M. Themlin, 2002, "Solid-state decomposition of silicon carbide for growing ultra-thin heteroepitaxial graphite films," J. Appl. Phys. **92**, 2479.

Chatzakis, Ioannis, Hugen Yan, Daohua Song, Stéphane Berciaud, and Tony F. Heinz, 2011, "Temperature dependence of the anharmonic decay of optical phonons in carbon nanotubes and graphite," Phys. Rev. B **83**, 205411.

Cheianov, V. V., V. I. Fal'ko, B. L. Altshuler, and I. L. Aleiner, 2007, "Random Resistor Network Model of Minimal Conductivity in Graphene," Phys. Rev. Lett. **99**, 176801.

Cheianov, Vadim V., Vladimir Fal'ko, and B. L. Altshuler, 2007, "The Focusing of Electron Flow and a Veselago Lens in Graphene *p-n* Junctions," Science **315**, 1252.

Chen, Chi-Fan, *et al.*, 2011, "Controlling inelastic light scattering quantum pathways in graphene," Nature (London) **471**, 617.

Chen, J.-H., C. Jang, S. Adam, M. S. Fuhrer, E. D. Williams, and M. Ishigami, 2008, "Charged-impurity scattering in graphene," Nat. Phys. **4**, 377.

Chen, Jianing, *et al.*, 2012, "Optical nano-imaging of gate-tunable graphene plasmons," Nature (London) **487**, 77.

Chiu, K. W., and J. J. Quinn, 1974, "Plasma oscillations of a two-dimensional electron gas in a strong magnetic field," Phys. Rev. B **9**, 4724.

Choi, H., F. Borondics, D. A. Siegel, S. Y. Zhou, M. C. Martin, A. Lanzara, and R. A. Kaindl, 2009, "Broadband electromagnetic response and ultrafast dynamics of few-layer epitaxial graphene," Appl. Phys. Lett. **94**, 172102.

Coletti, C., C. Riedl, D. S. Lee, B. Krauss, L. Patthey, K. von Klitzing, J. H. Smet, and U. Starke, 2010, "Charge neutrality and

band-gap tuning of epitaxial graphene on SiC by molecular doping," Phys. Rev. B **81**, 235401.
Connolly, M. R., K. L. Chiou, C. G. Smith, D. Anderson, G. A. C. Jones, A. Lombardo, A. Fasoli, and A. C. Ferrari, 2010, "Scanning gate microscopy of current-annealed single layer graphene," Appl. Phys. Lett. **96**, 113501.
Connolly, M. R., and C. G. Smith, 2010, "Nanoanalysis of graphene layers using scanning probe techniques," Phil. Trans. R. Soc. A **368**, 5379.
Crassee, I., J. Levallois, D. van der Marel, A. L. Walter, Th. Seyller, and A. B. Kuzmenko, 2011, "Multicomponent magneto-optical conductivity of multilayer graphene on SiC," Phys. Rev. B **84**, 035103.
Crassee, I., M. Orlita, M. Potemski, A. L. Walter, M. Ostler, Th. Seyller, I. Gaponenko, J. Chen, and A. B. Kuzmenko, 2012, "Intrinsic Terahertz Plasmons and Magnetoplasmons in Large Scale Monolayer Graphene," Nano Lett. **12**, 2470.
Crassee, Iris, Julien Levallois, Andrew L. Walter, Markus Ostler, Aaron Bostwick, Eli Rotenberg, Thomas Seyller, Dirk van der Marel, and Alexey B. Kuzmenko, 2011, "Giant Faraday rotation in single- and multilayer graphene," Nat. Phys. **7**, 48.
Daimon, H., S. Imada, H. Nishimoto, and S. Suga, 1995, "Structure factor in photoemission from valence band," J. Electron Spectrosc. Relat. Phenom. **76**, 487.
Dan, Yaping, Ye Lu, Nicholas J. Kybert, Zhengtang Luo, and A. T. Charlie Johnson, 2009, "Intrinsic Response of Graphene Vapor Sensors," Nano Lett. **9**, 1472.
Das, A., *et al.*, 2008, "Monitoring dopants by Raman scattering in an electrochemically top-gated graphene transistor," Nat. Nanotechnol. **3**, 210.
Das Sarma, S., Shaffique Adam, E. H. Hwang, and Enrico Rossi, 2011, "Electronic transport in two-dimensional graphene," Rev. Mod. Phys. **83**, 407.
Das Sarma, S., and E. H. Hwang, 2013, "Velocity renormalization and anomalous quasiparticle dispersion in extrinsic graphene," Phys. Rev. B **87**, 045425.
Das Sarma, S., E. H. Hwang, and Wang-Kong Tse, 2007, "Many-body interaction effects in doped and undoped graphene: Fermi liquid versus non-Fermi liquid," Phys. Rev. B **75**, 121406(R).
Dawlaty, Jahan M., Shriram Shivaraman, Mvs Chandrashekhar, Farhan Rana, and Michael G. Spencer, 2008, "Measurement of ultrafast carrier dynamics in epitaxial graphene," Appl. Phys. Lett. **92**, 042116.
Dean, C. R., *et al.*, 2013, "Hofstadter's butterfly and the fractal quantum Hall effect in moiré superlattices," Nature (London) **497**, 598.
Dean, C. R., *et al.*, 2010, "Boron nitride substrates for high-quality graphene electronics," Nat. Nanotechnol. **5**, 722.
Decker, Régis, Yang Wang, Victor W. Brar, William Regan, Hsin-Zon Tsai, Qiong Wu, William Gannett, Alex Zettl, and Michael F. Crommie, 2011a, "Local Electronic Properties of Graphene on a BN Substrate via Scanning Tunneling Microscopy," Nano Lett. **11**, 2291.
Decker, Régis, Yang Wang, Victor W. Brar, William Regan, Hsin-Zon Tsai, Qiong Wu, William Gannett, Alex Zettl, and Michael F. Crommie, 2011b, "Local Electronic Properties of Graphene on a BN Substrate via Scanning Tunneling Microscopy," Nano Lett. **11**, 2291.
Dedkov, Yu. S., M. Fonin, U. Rüdiger, and C. Laubschat, 2008, "Rashba Effect in the Graphene/Ni(111) System," Phys. Rev. Lett. **100**, 107602.
de Heer, Walt A., Claire Berger, Ming Ruan, Mike Sprinkle, Xuebin Li, Yike Hu, Baiqian Zhang, John Hankinson, and Edward Conrad, 2011, "Large area and structured epitaxial graphene produced by confinement controlled sublimation of silicon carbide," Proc. Natl. Acad. Sci. U.S.A. **108**, 16 900.
de Heer, Walt A., *et al.*, 2007, "Epitaxial graphene," Solid State Commun. **143**, 92.
Demel, T., D. Heitmann, P. Grambow, and K. Ploog, 1990, "Nonlocal dynamic response and level crossings in quantum-dot structures," Phys. Rev. Lett. **64**, 788.
Demel, T., D. Heitmann, P. Grambow, and K. Ploog, 1991, "One-dimensional plasmons in AlGaAs/GaAs quantum wires," Phys. Rev. Lett. **66**, 2657.
Deshpande, A., W. Bao, F. Miao, C. N. Lau, and B. J. LeRoy, 2009, "Spatially resolved spectroscopy of monolayer graphene on SiO_2," Phys. Rev. B **79**, 205411.
Deshpande, A., W. Bao, Z. Zhao, C. N. Lau, and B. J. LeRoy, 2011, "Imaging charge density fluctuations in graphene using Coulomb blockade spectroscopy," Phys. Rev. B **83**, 155409.
Dietl, Petra, Frédéric Piéchon, and Gilles Montambaux, 2008, "New Magnetic Field Dependence of Landau Levels in a Graphene-like Structure," Phys. Rev. Lett. **100**, 236405.
Dikin, Dmitriy A., Sasha Stankovich, Eric J. Zimney, Richard D. Piner, Geoffrey H. B. Dommett, Guennadi Evmenenko, SonBinh T. Nguyen, and Rodney S. Ruoff, 2007, "Preparation and characterization of graphene oxide paper," Nature (London) **448**, 457.
Dresselhaus, M. S., A. Jorio, L. G. Cançado, G. Dresselhaus, and R. Saito, 2012, "Raman Spectroscopy: Characterization of Edges, Defects, and the Fermi Energy of Graphene and sp^2 Carbons," in *Graphene Nanoelectronics: Metrology, Synthesis, Properties and Applications*, edited by Hasan Reza (Springer, Berlin), Chap. 2, p. 15.
Dresselhaus, Mildred S., Ado Jorio, Mario Hofmann, Gene Dresselhaus, and Riichiro Saito, 2010, "Perspectives on Carbon Nanotubes and Graphene Raman Spectroscopy," Nano Lett. **10**, 751.
Drut, Joaquín E., and Timo A. Lähde, 2009, "Is Graphene in Vacuum an Insulator?" Phys. Rev. Lett. **102**, 026802.
Du, Xu, Ivan Skachko, Anthony Barker, and Eva Y. Andrei, 2008, "Approaching ballistic transport in suspended graphene," Nat. Nanotechnol. **3**, 491.
Eberlein, T., U. Bangert, R. R. Nair, R. Jones, M. Gass, A. L. Bleloch, K. S. Novoselov, A. Geim, and P. R. Briddon, 2008, "Plasmon spectroscopy of free-standing graphene films," Phys. Rev. B **77**, 233406.
Efetov, Dmitri K., and Philip Kim, 2010, "Controlling Electron-Phonon Interactions in Graphene at Ultrahigh Carrier Densities," Phys. Rev. Lett. **105**, 256805.
Efros, A. L., F. G. Pikus, and V. G. Burnett, 1993, "Density of states of a two-dimensional electron gas in a long-range random potential," Phys. Rev. B **47**, 2233.
Efros, A. L., and B. I. Shklovskii, 1984, *Electronic Properties of Doped Semiconductors* (Springer-Verlag, New York).
Elias, D. C., *et al.*, 2011, "Dirac cones reshaped by interaction effects in suspended graphene," Nat. Phys. **7**, 701.
Eliasson, G., Ji-Wei Wu, P. Hawrylak, and J. J. Quinn, 1986, "Magnetoplasma modes of a spatially periodic two-dimensional electron gas," Solid State Commun. **60**, 41.
El-Kady, Maher F., Veronica Strong, Sergey Dubin, and Richard B. Kaner, 2012, "Laser Scribing of High-Performance and Flexible Graphene-Based Electrochemical Capacitors," Science **335**, 1326.
Emtsev, Konstantin V., *et al.*, 2009, "Towards wafer-size graphene layers by atmospheric pressure graphitization of silicon carbide," Nat. Mater. **8**, 203.

Enderlein, C, Y. S Kim, A. Bostwick, E. Rotenberg, and K. Horn, 2010, "The formation of an energy gap in graphene on ruthenium by controlling the interface," New J. Phys. **12**, 033014.

Falkovsky, L. A., and A. A. Varlamov, 2007, "Space-time dispersion of graphene conductivity," Eur. Phys. J. B **56**, 281.

Fang, Zheyu, Sukosin Thongrattanasiri, Andrea Schlather, Zheng Liu, Lulu Ma, Yumin Wang, Pulickel M. Ajayan, Peter Nordlander, Naomi J. Halas, and F. Javier García de Abajo, 2013, "Gated Tunability and Hybridization of Localized Plasmons in Nanostructured Graphene," ACS Nano **7**, 2388.

Farjam, M., and H. Rafii-Tabar, 2009, "Comment on "Band structure engineering of graphene by strain: First-principles calculations"," Phys. Rev. B **80**, 167401.

Faugeras, C., M. Amado, P. Kossacki, M. Orlita, M. Kühne, A. A. L. Nicolet, Yu. I. Latyshev, and M. Potemski, 2011, "Magneto-Raman Scattering of Graphene on Graphite: Electronic and Phonon Excitations," Phys. Rev. Lett. **107**, 036807.

Faugeras, C., M. Amado, P. Kossacki, M. Orlita, M. Sprinkle, C. Berger, W. A. de Heer, and M. Potemski, 2009, "Tuning the Electron-Phonon Coupling in Multilayer Graphene with Magnetic Fields," Phys. Rev. Lett. **103**, 186803.

Fei, Z., *et al.*, 2012, "Gate-tuning of graphene plasmons revealed by infrared nano-imaging," Nature (London) **487**, 82.

Fei, Z., *et al.*, 2013, "Electronic and plasmonic phenomena at grain boundaries in chemical vapor deposited graphene," Nat. Nanotechnol. **8**, 821.

Fei, Zhe, Yi Shi, Lin Pu, Feng Gao, Yu Liu, L. Sheng, Baigeng Wang, Rong Zhang, and Youdou Zheng, 2008, "High-energy optical conductivity of graphene determined by reflection contrast spectroscopy," Phys. Rev. B **78**, 201402.

Fei, Zhe, *et al.*, 2011, "Infrared Nanoscopy of Dirac Plasmons at the Graphene-SiO_2 Interface," Nano Lett. **11**, 4701.

Feldman, Benjamin E., Jens Martin, and Amir Yacoby, 2009, "Broken-symmetry states and divergent resistance in suspended bilayer graphene," Nat. Phys. **5**, 889.

Ferrari, A. C., *et al.*, 2006, "Raman Spectrum of Graphene and Graphene Layers," Phys. Rev. Lett. **97**, 187401.

Ferrari, Andrea C., 2007, "Raman spectroscopy of graphene and graphite: Disorder, electron-phonon coupling, doping and non-adiabatic effects," Solid State Commun. **143**, 47.

Filleter, T., J. L. McChesney, A. Bostwick, E. Rotenberg, K. V. Emtsev, Th. Seyller, K. Horn, and R. Bennewitz, 2009, Phys. Rev. Lett. **102**, 086102.

Fogler, M. M., F. Guinea, and M. I. Katsnelson, 2008, "Pseudomagnetic Fields and Ballistic Transport in a Suspended Graphene Sheet," Phys. Rev. Lett. **101**, 226804.

Fogler, Michael M., 2004, "Nonlinear screening and percolative transition in a two-dimensional electron liquid," Phys. Rev. B **69**, 121409.

Fogler, Michael M., 2009, "Neutrality Point of Graphene with Coplanar Charged Impurities," Phys. Rev. Lett. **103**, 236801.

Forbeaux, I., J.-M. Themlin, and J.-M. Debever, 1998, "Heteroepitaxial graphite on $6H-\mathrm{SiC}(0001)$: Interface formation through conduction-band electronic structure," Phys. Rev. B **58**, 16 396.

Foster, Matthew S., and Igor L. Aleiner, "Graphene via large N: A renormalization group study, 2008," Phys. Rev. B **77**, 195413.

Gallagher, Patrick, Kathryn Todd, and David Goldhaber-Gordon, 2010, "Disorder-induced gap behavior in graphene nanoribbons," Phys. Rev. B **81**, 115409.

Gangadharaiah, S., A. M. Farid, and E. G. Mishchenko, 2008, "Charge Response Function and a Novel Plasmon Mode in Graphene," Phys. Rev. Lett. **100**, 166802.

Gao, Li, Jeffrey R. Guest, and Nathan P. Guisinger, 2010, "Epitaxial Graphene on Cu(111)," Nano Lett. **10**, 3512.

Geim, A. K., 2009, "Graphene: Status and Prospects," Science **324**, 1530.

Geim, A. K., and I. V. Grigorieva, 2013, "Van der Waals heterostructures," Nature (London) **499**, 419.

Geim, A. K., and K. S. Novoselov, 2007, "The rise of graphene," Nat. Mater. **6**, 183.

George, Paul A., Jared Strait, Jahan Dawlaty, Shriram Shivaraman, Mvs Chandrashekhar, Farhan Rana, and Michael G. Spencer, 2008, "Ultrafast Optical-Pump Terahertz-Probe Spectroscopy of the Carrier Relaxation and Recombination Dynamics in Epitaxial Graphene," Nano Lett. **8**, 4248.

Georgiou, T., L. Britnell, P. Blake, R. V. Gorbachev, A. Gholinia, A. K. Geim, C. Casiraghi, and K. S. Novoselov, 2011, "Graphene bubbles with controllable curvature," Appl. Phys. Lett. **99**, 093103.

Ghosh, S., I. Calizo, D. Teweldebrhan, E. P. Pokatilov, D. L. Nika, A. A. Balandin, W. Bao, F. Miao, and C. N. Lau, 2008, "Extremely high thermal conductivity of graphene: Prospects for thermal management applications in nanoelectronic circuits," Appl. Phys. Lett. **92**, 151911.

Gibertini, Marco, Andrea Tomadin, Marco Polini, A. Fasolino, and M. I. Katsnelson, 2010, "Electron density distribution and screening in rippled graphene sheets," Phys. Rev. B **81**, 125437.

Gierz, Isabella, Jürgen Henk, Hartmut Höchst, Christian R. Ast, and Klaus Kern, 2011, "Illuminating the dark corridor in graphene: Polarization dependence of angle-resolved photoemission spectroscopy on graphene," Phys. Rev. B **83**, 121408.

Gierz, Isabella, Christian Riedl, Ulrich Starke, Christian R. Ast, and Klaus Kern, 2008, "Atomic Hole Doping of Graphene," Nano Lett. **8**, 4603.

Giovannetti, G., P. A. Khomyakov, G. Brocks, V. M. Karpan, J. van den Brink, and P. J. Kelly, 2008, "Doping Graphene with Metal Contacts," Phys. Rev. Lett. **101**, 026803.

Giovannetti, Gianluca, Petr A. Khomyakov, Geert Brocks, Paul J. Kelly, and Jeroen van den Brink, 2007, "Substrate-induced band gap in graphene on hexagonal boron nitride: *Ab initio* density functional calculations," Phys. Rev. B **76**, 073103.

Giuliani, G., and G. Vignale, 2005, *Quantum Theory of the Electron Liquid* (Cambridge University Press, New York).

Glattli, D. C., E. Y. Andrei, G. Deville, J. Poitrenaud, and F. I. B. Williams, 1985, "Dynamical Hall Effect in a Two-Dimensional Classical Plasma," Phys. Rev. Lett. **54**, 1710.

Goerbig, M. O., 2011, "Electronic properties of graphene in a strong magnetic field," Rev. Mod. Phys. **83**, 1193.

González, J., F. Guinea, and M. A. H. Vozmediano, 1994, "Non-Fermi liquid behavior of electrons in the half-filled honeycomb lattice (A renormalization group approach)," Nucl. Phys. **B424**, 595.

González, J., F. Guinea, and M. A. H. Vozmediano, 1999, "Marginal-Fermi-liquid behavior from two-dimensional Coulomb interaction," Phys. Rev. B **59**, R2474.

Graf, D., F. Molitor, K. Ensslin, C. Stampfer, A. Jungen, C. Hierold, and L. Wirtz, 2007, "Spatially Resolved Raman Spectroscopy of Single- and Few-Layer Graphene," Nano Lett. **7**, 238.

Grigorenko, A. N., M. Polini, and K. S. Novoselov, 2012, "Graphene plasmonics," Nat. Photonics **6**, 749.

Grüneis, A., C. Attaccalite, A. Rubio, D. V. Vyalikh, S. L. Molodtsov, J. Fink, R. Follath, W. Eberhardt, B. Büchner, and T. Pichler, 2009, "Electronic structure and electron-phonon coupling of doped graphene layers in KC_8," Phys. Rev. B **79**, 205106.

Grushin, Adolfo G., Belén Valenzuela, and María A. H. Vozmediano, 2009, "Effect of Coulomb interactions on the optical properties of doped graphene," Phys. Rev. B **80**, 155417.

Guinea, F., A. K. Geim, M. I. Katsnelson, and K. S. Novoselov, 2010, "Generating quantizing pseudomagnetic fields by bending graphene ribbons," Phys. Rev. B **81**, 035408.

Guinea, F., Baruch Horovitz, and P. Le Doussal, 2008, "Gauge field induced by ripples in graphene," Phys. Rev. B **77**, 205421.

Guinea, F., M. I. Katsnelson, and A. K. Geim, 2010, "Energy gaps and a zero-field quantum Hall effect in graphene by strain engineering," Nat. Phys. **6**, 30.

Guinea, F., M. I. Katsnelson, and M. A. H. Vozmediano, 2008, "Midgap states and charge inhomogeneities in corrugated graphene," Phys. Rev. B **77**, 075422.

Guinea, F., and Tony Low, 2010, "Band structure and gaps of triangular graphene superlattices," Phil. Trans. R. Soc. A **368**, 5391.

Gupta, Awnish K., Timothy J. Russin, Humberto R. Gutiérrez, and Peter C. Eklund, 2009, "Probing Graphene Edges via Raman Scattering," ACS Nano **3**, 45.

Gusynin, V. P., and S. G. Sharapov, 2006, "Transport of Dirac quasiparticles in graphene: Hall and optical conductivities," Phys. Rev. B **73**, 245411.

Han, Melinda Y., Juliana C. Brant, and Philip Kim, 2010, "Electron Transport in Disordered Graphene Nanoribbons," Phys. Rev. Lett. **104**, 056801.

Han, Melinda Y., Barbaros Özyilmaz, Yuanbo Zhang, and Philip Kim, 2007, "Energy Band-Gap Engineering of Graphene Nanoribbons," Phys. Rev. Lett. **98**, 206805.

Hasegawa, Yasumasa, Rikio Konno, Hiroki Nakano, and Mahito Kohmoto, 2006, "Zero modes of tight-binding electrons on the honeycomb lattice," Phys. Rev. B **74**, 033413.

Hass, J., F. Varchon, J. E. Millán-Otoya, M. Sprinkle, N. Sharma, W. A. de Heer, C. Berger, P. N. First, L. Magaud, and E. H. Conrad, 2008, "Why Multilayer Graphene on $4H-\mathrm{SiC}(000\bar{1})$ Behaves Like a Single Sheet of Graphene," Phys. Rev. Lett. **100**, 125504.

Henriksen, E. A., P. Cadden-Zimansky, Z. Jiang, Z. Q. Li, L.-C. Tung, M. E. Schwartz, M. Takita, Y.-J. Wang, P. Kim, and H. L. Stormer, 2010, "Interaction-Induced Shift of the Cyclotron Resonance of Graphene Using Infrared Spectroscopy," Phys. Rev. Lett. **104**, 067404.

Henriksen, E. A., and J. P. Eisenstein, 2010, "Measurement of the electronic compressibility of bilayer graphene," Phys. Rev. B **82**, 041412(R).

Hernandez, Yenny, *et al.*, 2008, "High-yield production of graphene by liquid-phase exfoliation of graphite," Nat. Nanotechnol. **3**, 563.

Himpsel, F. J., K. Christmann, P. Heimann, D. E. Eastman, and Peter J. Feibelman, 1982, "Adsorbate band dispersions for C on Ru (0001)," Surf. Sci. Lett. **115**, L159.

Hofmann, T., A. Boosalis, P. Kühne, C. M. Herzinger, J. A. Woollam, D. K. Gaskill, J. L. Tedesco, and M. Schubert, 2011, "Hole-channel conductivity in epitaxial graphene determined by terahertz optical-Hall effect and midinfrared ellipsometry," Appl. Phys. Lett. **98**, 041906.

Hofstadter, Douglas R., 1976, "Energy levels and wave functions of Bloch electrons in rational and irrational magnetic fields," Phys. Rev. B **14**, 2239.

Horng, Jason, *et al.*, 2011, "Drude conductivity of Dirac fermions in graphene," Phys. Rev. B **83**, 165113.

Huang, Libai, Gregory V. Hartland, Li-Qiang Chu, Luxmi, Randall M. Feenstra, Chuanxin Lian, Kristof Tahy, and Huili Xing, 2010, "Ultrafast Transient Absorption Microscopy Studies of Carrier Dynamics in Epitaxial Graphene," Nano Lett. **10**, 1308.

Huang, Mingyuan, Hugen Yan, Changyao Chen, Daohua Song, Tony F. Heinz, and James Hone, 2009, "Phonon softening and crystallographic orientation of strained graphene studied by Raman spectroscopy," Proc. Natl. Acad. Sci. U.S.A. **106**, 7304.

Huang, Pinshane Y., *et al.*, 2011, "Grains and grain boundaries in single-layer graphene atomic patchwork quilts," Nature (London) **469**, 389.

Huertas-Hernando, Daniel, F. Guinea, and Arne Brataas, 2006, "Spin-orbit coupling in curved graphene, fullerenes, nanotubes, and nanotube caps," Phys. Rev. B **74**, 155426.

Hunt, B., *et al.*, 2013, "Massive Dirac Fermions and Hofstadter Butterfly in a van der Waals Heterostructure," Science **340**, 1427.

Hwang, Choongyu, Cheol-Hwan Park, David A. Siegel, Alexei V. Fedorov, Steven G. Louie, and Alessandra Lanzara, 2011, "Direct measurement of quantum phases in graphene via photoemission spectroscopy," Phys. Rev. B **84**, 125422.

Hwang, Choongyu, David A. Siegel, Sung-Kwan Mo, William Regan, Ariel Ismach, Yuegang Zhang, Alex Zettl, and Alessandra Lanzara, 2012, "Fermi velocity engineering in graphene by substrate modification," Sci. Rep. **2**, 590.

Hwang, E. H., S. Adam, and S. Das Sarma, 2007, "Carrier Transport in Two-Dimensional Graphene Layers," Phys. Rev. Lett. **98**, 186806.

Hwang, E. H., and S. Das Sarma, 2007, "Dielectric Function, Screening, and Plasmons in Two-Dimensional Graphene," Phys. Rev. B **75**, 205418.

Hwang, E. H., Ben Yu-Kuang Hu, and S. Das Sarma, 2007, "Density Dependent Exchange Contribution to d mu / d n and Compressibility in Graphene," Phys. Rev. Lett. **99**, 226801.

Hwang, E. H., Rajdeep Sensarma, and S. Das Sarma, 2010, "Plasmon-phonon coupling in graphene," Phys. Rev. B **82**, 195406.

Hwang, J., J. P. F. LeBlanc, and J. P. Carbotte, 2012, "Optical self-energy in graphene due to correlations," J. Phys. Condens. Matter **24**, 245601.

Iordanskii, S. V., and A. E. Koshelev, 1985, "Dislocations and localization effects in multivalley conductors," JETP Lett. **41**, 574 [http://www.jetpletters.ac.ru/ps/1469/article_22404.shtml].

Jablan, Marinko, Hrvoje Buljan, and Marin Soljačić, 2009, "Plasmonics in graphene at infrared frequencies," Phys. Rev. B **80**, 245435.

Jiang, Z., E. A. Henriksen, L. C. Tung, Y.-J. Wang, M. E. Schwartz, M. Y. Han, P. Kim, and H. L. Stormer, 2007, "Infrared Spectroscopy of Landau Levels of Graphene," Phys. Rev. Lett. **98**, 197403.

Ju, Long, *et al.*, 2011, "Graphene plasmonics for tunable terahertz metamaterials," Nat. Nanotechnol. **6**, 630.

Kalbac, Martin, Alfonso Reina-Cecco, Hootan Farhat, Jing Kong, Ladislav Kavan, and Mildred S. Dresselhaus, 2010, "The Influence of Strong Electron and Hole Doping on the Raman Intensity of Chemical Vapor-Deposition Graphene," ACS Nano **4**, 6055.

Kane, C. L., and E. J. Mele, 1997, "Size, Shape, and Low Energy Electronic Structure of Carbon Nanotubes," Phys. Rev. Lett. **78**, 1932.

Kane, C. L., and E. J. Mele, 2005, "Quantum Spin Hall Effect in Graphene," Phys. Rev. Lett. **95**, 226801.

Katsnelson, M. I., and K. S. Novoselov, 2007, "Graphene: New bridge between condensed matter physics and quantum electrodynamics," Solid State Commun. **143**, 3.

Katsnelson, M. I., K. S. Novoselov, and A. K. Geim, 2006, "Chiral tunnelling and the Klein paradox in graphene," Nat. Phys. **2**, 620.

Katsnelson, Mikhail I., 2012, *Graphene: Carbon in Two Dimensions* (Cambridge, New York).

Kawasaki, T., T. Ichimura, H. Kishimoto, A. A. Akbar, T. Ogawa, and C. Oshima, 2002, "Double Atomic Layers of Graphene/

Monolayer h-BN on Ni(111) Studied by Scanning Tunneling Microscopy and Scanning Tunneling Spectroscopy," Surf. Rev. Lett. **09**, 1459.

Kechedzhi, K., and S. Das Sarma, 2013, "Plasmon anomaly in the dynamical optical conductivity of graphene," Phys. Rev. B **88**, 085403.

Khveshchenko, D. V., 2001, "Ghost Excitonic Insulator Transition in Layered Graphite," Phys. Rev. Lett. **87**, 246802.

Kim, Eun-Ah, and A. H. Castro Neto, 2008, "Graphene as an electronic membrane," Europhys. Lett. **84**, 57 007.

Kim, Keun Soo, Yue Zhao, Houk Jang, Sang Yoon Lee, Jong Min Kim, Kwang S. Kim, Jong-Hyun Ahn, Philip Kim, Jae-Young Choi, and Byung Hee Hong, 2009, "Large-scale pattern growth of graphene films for stretchable transparent electrodes," Nature (London) **457**, 706.

Kim, Seungchul, Jisoon Ihm, Hyoung Joon Choi, and Young-Woo Son, 2008, "Origin of Anomalous Electronic Structures of Epitaxial Graphene on Silicon Carbide," Phys. Rev. Lett. **100**, 176802.

Kishigi, Keita, Ryuichi Takeda, and Yasumasa Hasegawa, 2008, "Energy gap of tight-binding electrons on generalized honeycomb lattice," J. Phys. Conf. Ser. **132**, 012005.

Knox, Kevin R., Andrea Locatelli, Mehmet B. Yilmaz, Dean Cvetko, Tevfik Onur Menteş, Miguel Ángel Niño, Philip Kim, Alberto Morgante, and Richard M. Osgood, 2011, "Making angle-resolved photoemission measurements on corrugated monolayer crystals: Suspended exfoliated single-crystal graphene," Phys. Rev. B **84**, 115401.

Koch, R. J., Th. Seyller, and J. A. Schaefer, 2010, "Strong phonon-plasmon coupled modes in the graphene/silicon carbide heterosystem," Phys. Rev. B **82**, 201413.

Koepke, Justin C., Joshua D. Wood, David Estrada, Zhun-Yong Ong, Kevin T. He, Eric Pop, and Joseph W. Lyding, 2013, "Atomic-Scale Evidence for Potential Barriers and Strong Carrier Scattering at Graphene Grain Boundaries: A Scanning Tunneling Microscopy Study," ACS Nano **7**, 75.

Kotov, Valeri N., Bruno Uchoa, Vitor M. Pereira, F. Guinea, and A. H. Castro Neto, 2012, "Electron-Electron Interactions in Graphene: Current Status and Perspectives," Rev. Mod. Phys. **84**, 1067.

Kravets, V. G., A. N. Grigorenko, R. R. Nair, P. Blake, S. Anissimova, K. S. Novoselov, and A. K. Geim, 2010, "Spectroscopic ellipsometry of graphene and an exciton-shifted van Hove peak in absorption," Phys. Rev. B **81**, 155413.

Kuemmeth, F., S. Ilani, D. C. Ralph, and P. L. McEuen, 2008, "Coupling of spin and orbital motion of electrons in carbon nanotubes," Nature (London) **452**, 448.

Kukushkin, I. V., J. H. Smet, S. A. Mikhailov, D. V. Kulakovskii, K. von Klitzing, and W. Wegscheider, 2003, "Observation of Retardation Effects in the Spectrum of Two-Dimensional Plasmons," Phys. Rev. Lett. **90**, 156801.

Kumada, N., S. Tanabe, H. Hibino, H. Kamata, M. Hashisaka, K. Muraki, and T. Fujisawa, 2013, "Plasmon transport in graphene investigated by time-resolved electrical measurements," Nat. Commun. **4**, 1363.

Kuzmenko, A. B., L. Benfatto, E. Cappelluti, I. Crassee, D. van der Marel, P. Blake, K. S. Novoselov, and A. K. Geim, 2009, "Gate Tunable Infrared Phonon Anomalies in Bilayer Graphene," Phys. Rev. Lett. **103**, 116804.

Kuzmenko, A. B., I. Crassee, D. van der Marel, P. Blake, and K. S. Novoselov, 2009, "Determination of the gate-tunable band gap and tight-binding parameters in bilayer graphene using infrared spectroscopy," Phys. Rev. B **80**, 165406.

Kuzmenko, A. B., E. van Heumen, D. van der Marel, P. Lerch, P. Blake, K. S. Novoselov, and A. K. Geim, 2009, "Infrared spectroscopy of electronic bands in bilayer graphene," Phys. Rev. B **79**, 115441.

Lazzeri, Michele, Claudio Attaccalite, Ludger Wirtz, and Francesco Mauri, 2008, "Impact of the electron-electron correlation on phonon dispersion: Failure of LDA and GGA DFT functionals in graphene and graphite," Phys. Rev. B **78**, 081406(R).

LeBlanc, J. P. F., J. P. Carbotte, and E. J. Nicol, 2011, "Effect of electron-phonon coupling on energy and density of states renormalizations of dynamically screened graphene," Phys. Rev. B **84**, 165448.

Lee, C., X. Wei, J. W. Kysar, and J. Hone, 2008, "Measurement of the Elastic Properties and Intrinsic Strength of Monolayer Graphene," Science **321**, 385.

Lee, Dong Su, Christian Riedl, Benjamin Krauss, Klaus von Klitzing, Ulrich Starke, and Jurgen H. Smet, 2008, "Raman Spectra of Epitaxial Graphene on SiC and of Epitaxial Graphene Transferred to SiO_2," Nano Lett. **8**, 4320.

Leem, C. S., *et al.*, 2008, "Effect of Linear Density of States on the Quasiparticle Dynamics and Small Electron-Phonon Coupling in Graphite," Phys. Rev. Lett. **100**, 016802.

Levitov, L. S., A. V. Shtyk, and M. V. Feigelman, 2013, "Electron-Electron Interactions and Plasmon Dispersion in Graphene," unpublished (arXiv:1302.5036).

Levy, N., S. A. Burke, K. L. Meaker, M. Panlasigui, A. Zettl, F. Guinea, A. H. Castro Neto, and M. F. Crommie, 2010, "Strain-Induced Pseudo-Magnetic Fields Greater Than 300 Tesla in Graphene Nanobubbles," Science **329**, 544.

Li, Guohong, and Eva Y. Andrei, 2012, "Scanning Tunneling Microscopy and Spectroscopy of Graphene," in *Graphene Nanoelectronics: Metrology, Synthesis, Properties and Applications*, edited by Hasan Reza (Springer, Berlin), Chap. 3, pp. 57–91.

Li, Guohong, Adina Luican, and Eva Y. Andrei, 2009, "Scanning Tunneling Spectroscopy of Graphene on Graphite," Phys. Rev. Lett. **102**, 176804.

Li, Xuesong, Carl W. Magnuson, Archana Venugopal, Rudolf M. Tromp, James B. Hannon, Eric M. Vogel, Luigi Colombo, and Rodney S. Ruoff, 2011, "Large-Area Graphene Single Crystals Grown by Low-Pressure Chemical Vapor Deposition of Methane on Copper," J. Am. Chem. Soc. **133**, 2816.

Li, Xuesong, *et al.*, 2010, "Graphene Films with Large Domain Size by a Two-Step Chemical Vapor Deposition Process," Nano Lett. **10**, 4328.

Li, Z. Q., E. A. Henriksen, Z. Jiang, Z. Hao, M. C. Martin, P. Kim, H. L. Stormer, and D. N. Basov, 2008, "Dirac charge dynamics in graphene by infrared spectroscopy," Nat. Phys. **4**, 532.

Li, Z. Q., E. A. Henriksen, Z. Jiang, Z. Hao, M. C. Martin, P. Kim, H. L. Stormer, and D. N. Basov, 2009, "Band Structure Asymmetry of Bilayer Graphene Revealed by Infrared Spectroscopy," Phys. Rev. Lett. **102**, 037403.

Liang, Wenjie, Marc Bockrath, Dolores Bozovic, Jason H. Hafner, M. Tinkham, and Hongkun Park, 2001, "Fabry-Perot interference in a nanotube electron waveguide," Nature (London) **411**, 665.

Lischner, Johannes, Derek Vigil-Fowler, and Steven G. Louie, 2013, "Physical Origin of Satellites in Photoemission of Doped Graphene: An *Ab Initio GW* Plus Cumulant Study," Phys. Rev. Lett. **110**, 146801.

Liu, Wei-Tao, S. W. Wu, P. J. Schuck, M. Salmeron, Y. R. Shen, and F. Wang, 2010, "Nonlinear broadband photoluminescence of graphene induced by femtosecond laser irradiation," Phys. Rev. B **82**, 081408(R).

Liu, Xinglan, Jeroen B. Oostinga, Alberto F. Morpurgo, and Lieven M. K. Vandersypen, 2009, "Electrostatic confinement of electrons in graphene nanoribbons," Phys. Rev. B **80**, 121407.

Liu, Y., G. Bian, T. Miller, and T.-C. Chiang, 2011, "Visualizing Electronic Chirality and Berry Phases in Graphene Systems Using Photoemission with Circularly Polarized Light," Phys. Rev. Lett. **107**, 166803.

Liu, Yu, and R. F. Willis, 2010, "Plasmon-phonon strongly coupled mode in epitaxial graphene," Phys. Rev. B **81**, 081406.

Liu, Yu, R. F. Willis, K. V. Emtsev, and Th. Seyller, 2008, "Plasmon dispersion and damping in electrically isolated two-dimensional charge sheets," Phys. Rev. B **78**, 201403.

Lopes dos Santos, J. M. B., N. M. R. Peres, and A. H. Castro Neto, 2007, "Graphene Bilayer with a Twist: Electronic Structure," Phys. Rev. Lett. **99**, 256802.

Lopes dos Santos, J. M. B., N. M. R. Peres, and A. H. Castro Neto, 2012, "Continuum model of the twisted graphene bilayer," Phys. Rev. B **86**, 155449.

Ludwig, Andreas W. W., Matthew P. A. Fisher, R. Shankar, and G. Grinstein, 1994, "Integer quantum Hall transition: An alternative approach and exact results," Phys. Rev. B **50**, 7526.

Lui, Chun Hung, Kin Fai Mak, Jie Shan, and Tony F. Heinz, 2010, "Ultrafast Photoluminescence from Graphene," Phys. Rev. Lett. **105**, 127404.

Luican, A., Guohong Li, A. Reina, J. Kong, R. R. Nair, K. S. Novoselov, A. K. Geim, and E. Y. Andrei2011, "Single-Layer Behavior and Its Breakdown in Twisted Graphene Layers," Phys. Rev. Lett. **106**, 126802.

Luican, Adina, Guohong Li, and Eva Y. Andrei, 2011, "Quantized Landau level spectrum and its density dependence in graphene," Phys. Rev. B **83**, 041405.

Lundqvist, B., 1967, "Single-particle spectrum of the degenerate electron gas," Phys. Kondens. Mater. **6**, 193.

Mak, Kin Fai, Chun Hung Lui, Jie Shan, and Tony F. Heinz, 2009, "Observation of an Electric-Field-Induced Band Gap in Bilayer Grapheneby Infrared Spectroscopy," Phys. Rev. Lett. **102**, 256405.

Mak, Kin Fai, Matthew Y. Sfeir, James A. Misewich, and Tony F. Heinz, 2010, "The evolution of electronic structure in few-layer graphene revealed by optical spectroscopy," Proc. Natl. Acad. Sci. U.S.A. **107**, 14 999.

Mak, Kin Fai, Matthew Y. Sfeir, Yang Wu, Chun Hung Lui, James A. Misewich, and Tony F. Heinz, 2008, "Measurement of the Optical Conductivity of Graphene," Phys. Rev. Lett. **101**, 196405.

Mak, Kin Fai, Jie Shan, and Tony F. Heinz, 2011, "Seeing Many-Body Effects in Single- and Few-Layer Graphene: Observation of Two-Dimensional Saddle-Point Excitons," Phys. Rev. Lett. **106**, 046401.

Malard, L. M., D. C. Elias, E. S. Alves, and M. A. Pimenta, 2008, "Observation of Distinct Electron-Phonon Couplings in Gated Bilayer Graphene," Phys. Rev. Lett. **101**, 257401.

Malard, L. M., J. Nilsson, D. C. Elias, J. C. Brant, F. Plentz, E. S. Alves, A. H. Castro Neto, and M. A. Pimenta, 2007, "Probing the electronic structure of bilayer graphene by Raman scattering," Phys. Rev. B **76**, 201401(R).

Malard, L. M., M. A. Pimenta, G. Dresselhaus, and M. S. Dresselhaus, 2009, "Raman spectroscopy in graphene," Phys. Rep. **473**, 51.

Mallet, P., F. Varchon, C. Naud, L. Magaud, C. Berger, and J.-Y. Veuillen, 2007, "Electron states of mono- and bilayer graphene on SiC probed by scanning-tunneling microscopy," Phys. Rev. B **76**, 041403(R).

Mañes, J. L., F. Guinea, and María A. H. Vozmediano, 2007, "Existence and topological stability of Fermi points in multilayered graphene," Phys. Rev. B **75**, 155424.

Marchini, S., S. Günther, and J. Wintterlin, 2007, "Scanning tunneling microscopy of graphene on Ru(0001)," Phys. Rev. B **76**, 075429.

Martin, J., N. Akerman, G. Ulbricht, T. Lohmann, J. H. Smet, K. von Klitzing, and A. Yacoby, 2008, "Observation of electron-hole puddles in graphene using a scanning single-electron transistor," Nat. Phys. **4**, 144.

Mast, D. B., A. J. Dahm, and A. L. Fetter, 1985, "Observation of Bulk and Edge Magnetoplasmons in a Two-Dimensional Electron Fluid," Phys. Rev. Lett. **54**, 1706.

Maultzsch, J., S. Reich, C. Thomsen, H. Requardt, and P. Ordejón, 2004, "Phonon Dispersion in Graphite," Phys. Rev. Lett. **92**, 075501.

Mayorov, A. S., *et al.*, 2011a, "Interaction-Driven Spectrum Reconstruction in Bilayer Graphene," Science **333**, 860.

Mayorov, Alexander S., *et al.*, 2011b, "Micrometer-Scale Ballistic Transport in Encapsulated Graphene at Room Temperature," Nano Lett. **11**, 2396.

McCann, Edward, 2006, "Asymmetry gap in the electronic band structure of bilayer graphene," Phys. Rev. B **74**, 161403.

McCann, Edward, and Vladimir I. Fal'ko, 2006, "Landau-Level Degeneracy and Quantum Hall Effect in a Graphite Bilayer," Phys. Rev. Lett. **96**, 086805.

McCann, Edward, and Mikito Koshino, 2013, "The electronic properties of bilayer graphene," Rep. Prog. Phys. **76**, 056503.

McChesney, J. L., A. Bostwick, T. Ohta, K. Emtsev, T. Seyller, K. Horn, and E. Rotenberg, 2008, "Self-consistent analysis of electron-phonon coupling parameters of graphene," unpublished (arXiv:0809.4046).

McChesney, J. L., A. Bostwick, T. Ohta, K. V. Emtsev, T. Seyller, K. Horn, and E. Rotenberg, 2007, "Massive enhancement of electron-phonon coupling in doped graphene by an electronic singularity," unpublished (arXiv:0705.3264).

McChesney, J. L., Aaron Bostwick, Taisuke Ohta, Thomas Seyller, Karsten Horn, J. González, and Eli Rotenberg, 2010, "Extended van Hove Singularity and Superconducting Instability in Doped Graphene," Phys. Rev. Lett. **104**, 136803.

McClure, J. W., 1957, "Band Structure of Graphite and de Haas-van Alphen Effect," Phys. Rev. **108**, 612.

Mikhailov, S. A., and K. Ziegler, 2007, "New Electromagnetic Mode in Graphene," Phys. Rev. Lett. **99**, 016803.

Miller, David L., Kevin D. Kubista, Gregory M. Rutter, Ming Ruan, Walt A. de Heer, Phillip N. First, and Joseph A. Stroscio, 2009, "Observing the Quantization of Zero Mass Carriers in Graphene," Science **324**, 924.

Millis, A., 2004, "Optical conductivity and correlated electron physics," in *Strong interactions in low dimensions*, Physics and Chemistry of Materials with Low-Dimensional Structures, Vol. 25, edited by D. Baeriswyl, L. Degiorgi, F. Lévy, and E. Mooser (Kluwer, Dordrecht), Chap. 7, pp. 195–235.

Min, Hongki, Giovanni Borghi, Marco Polini, and A. H. MacDonald, 2008, "Pseudospin magnetism in graphene," Phys. Rev. B **77**, 041407(R).

Mishchenko, E. G., 2008, "Minimal conductivity in graphene: Interaction corrections and ultraviolet anomaly," Europhys. Lett. **83**, 17 005.

Mishchenko, E. G., A. V. Shytov, and P. G. Silvestrov, 2010, "Guided Plasmons in Graphene *p-n* Junctions," Phys. Rev. Lett. **104**, 156806.

Mohiuddin, T. M. G., *et al.*, 2009, "Uniaxial strain in graphene by Raman spectroscopy: *G* peak splitting, Grüneisen parameters, and sample orientation," Phys. Rev. B **79**, 205433.

Mohr, M., J. Maultzsch, E. Dobardžić, S. Reich, I. Milošević, M. Damnjanović, A. Bosak, M. Krisch, and C. Thomsen, 2007, "Phonon dispersion of graphite by inelastic x-ray scattering," Phys. Rev. B **76**, 035439.

Morozov, S. V., K. S. Novoselov, M. I. Katsnelson, F. Schedin, D. C. Elias, J. A. Jaszczak, and A. K. Geim, 2008, "Giant Intrinsic Carrier Mobilities in Graphene and Its Bilayer," Phys. Rev. Lett. **100**, 016602.

Morpurgo, A. F., and F. Guinea, 2006, "Intervalley Scattering, Long-Range Disorder, and Effective Time-Reversal Symmetry Breaking in Graphene," Phys. Rev. Lett. **97**, 196804.

Mucha-Kruczyński, M., O. Tsyplyatyev, A. Grishin, E. McCann, Vladimir I. Fal'ko, Aaron Bostwick, and Eli Rotenberg, 2008, "Characterization of graphene through anisotropy of constant-energy maps in angle-resolved photoemission," Phys. Rev. B **77**, 195403.

Nagashima, A., N. Tejima, and C. Oshima, 1994, "Electronic states of the pristine and alkali-metal-intercalated monolayer graphite/Ni (111) systems," Phys. Rev. B **50**, 17 487.

Nagashima, Ayato, Kenji Nuka, Hiroshi Itoh, Takeo Ichinokawa, Chuhei Oshima, and Shigeki Otani, 1993, "Electronic states of monolayer graphite formed on TiC(111) surface," Surf. Sci. **291**, 93.

Nair, R. R., P. Blake, A. N. Grigorenko, K. S. Novoselov, T. J. Booth, T. Stauber, N. M. R. Peres, and A. K. Geim, 2008, "Fine Structure Constant Defines Visual Transparency of Graphene," Science **320**, 1308.

Nair, R. R., M. Sepioni, I-Ling Tsai, O. Lehtinen, J. Keinonen, A. V. Krasheninnikov, T. Thomson, A. K. Geim, and I. V. Grigorieva, 2012, "Spin-half paramagnetism in graphene induced by point defects," Nat. Phys. **8**, 199.

Nakada, Kyoko, Mitsutaka Fujita, Gene Dresselhaus, and Mildred S. Dresselhaus, 1996, "Edge state in graphene ribbons: Nanometer size effect and edge shape dependence," Phys. Rev. B **54**, 17 954.

Nandkishore, Rahul, and Leonid Levitov, 2010a, "Dynamical Screening and Excitonic Instability in Bilayer Graphene," Phys. Rev. Lett. **104**, 156803.

Nandkishore, Rahul, and Leonid Levitov, 2010b, "Quantum anomalous Hall state in bilayer graphene," Phys. Rev. B **82**, 115124.

Nandkishore, Rahul, and Leonid Levitov, 2011, "Polar Kerr Effect and Time Reversal Symmetry Breaking in Bilayer Graphene," Phys. Rev. Lett. **107**, 097402.

N'Diaye, Alpha T., Sebastian Bleikamp, Peter J. Feibelman, and Thomas Michely, 2006, "Two-Dimensional Ir Cluster Lattice on a Graphene Moiré on Ir(111)," Phys. Rev. Lett. **97**, 215501.

Newaz, A. K. M., Yevgeniy S. Puzyrev, Bin Wang, Sokrates T. Pantelides, and Kirill I. Bolotin, 2012, "Probing charge scattering mechanisms in suspended graphene by varying its dielectric environment," Nat. Commun. **3**, 734.

Newson, Ryan W., Jesse Dean, Ben Schmidt, and Henry M. van Driel, 2009, "Ultrafast carrier kinetics in exfoliated graphene and thin graphite films," Opt. Express **17**, 2326.

Ni, Z. H., H. M. Wang, J. Kasim, H. M. Fan, T. Yu, Y. H. Wu, Y. P. Feng, and Z. X. Shen, 2007, "Graphene Thickness Determination Using Reflection and Contrast Spectroscopy," Nano Lett. **7**, 2758.

Ni, Zhenhua, Yingying Wang, Ting Yu, and Zexiang Shen, 2008, "Raman spectroscopy and imaging of graphene," Nano Res. **1**, 273.

Ni, Zhen Hua, Ting Yu, Yun Hao Lu, Ying Ying Wang, Yuan Ping Feng, and Ze Xiang Shen, 2008, "Uniaxial Strain on Graphene: Raman Spectroscopy Study and Band-Gap Opening," ACS Nano **2**, 2301.

Ni, Zhen Hua, Ting Yu, Yun Hao Lu, Ying Ying Wang, Yuan Ping Feng, and Ze Xiang Shen, 2009, "Uniaxial Strain on Graphene: Raman Spectroscopy Study and Band-Gap Opening," ACS Nano **3**, 483.

Ni, Zhen Hua, Ting Yu, Zhi Qiang Luo, Ying Ying Wang, Lei Liu, Choun Pei Wong, Jianmin Miao, Wei Huang, and Ze Xiang Shen, 2009, "Probing Charged Impurities in Suspended Graphene Using Raman Spectroscopy," ACS Nano **3**, 569.

Nikitin, A. Yu., F. Guinea, F. J. García-Vidal, and L. Martín-Moreno, 2011, "Edge and Waveguide THz Surface Plasmon Modes in GrapheneMicro-Ribbons," Phys. Rev. B **84**, 161407.

Nilsson, Johan, A. H. Castro Neto, F. Guinea, and N. M. R. Peres, 2007, "Transmission through a biased graphene bilayer barrier," Phys. Rev. B **76**, 165416.

Nilsson, Johan, A. H. Castro Neto, F. Guinea, and N. M. R. Peres, 2008, "Electronic properties of bilayer and multilayer graphene," Phys. Rev. B **78**, 045405.

Nilsson, Johan, A. H. Castro Neto, N. M. R. Peres, and F. Guinea, 2006, "Electron-electron interactions and the phase diagram of a graphene bilayer," Phys. Rev. B **73**, 214418.

Novoselov, K. S., A. K. Geim, S. V. Morozov, D. Jiang, M. I. Katsnelson, I. V. Grigorieva, S. V. Dubonos, and A. A. Firsov, 2005, "Two-Dimensional Gas of Massless Dirac Fermions in Graphene," Nature (London) **438**, 197.

Novoselov, K. S., D. Jiang, F. Schedin, T. J. Booth, V. V. Khotkevich, S. V. Morozov, and A. K. Geim, 2005, "Two-dimensional atomic crystals," Proc. Natl. Acad. Sci. U.S.A. **102**, 10 451.

Nozieres, P., and D. Pines, 1999, *Theory Of Quantum Liquids*, Advanced Book Classics (Perseus Books, Cambridge, MA).

Ohta, Taisuke, Aaron Bostwick, Thomas Seyller, Karsten Horn, and Eli Rotenberg, 2006, "Controlling the Electronic Structure of Bilayer Graphene," Science **313**, 951.

Oksanen, Mika, Andreas Uppstu, Antti Laitinen, Daniel J. Cox, Monica Craciun, Saverio Russo, Ari Harju, and Pertti Hakonen, 2014, "Single- and multi-mode Fabry-Pérot interference in suspended graphene," Phys. Rev. B **89**, 121414(R).

Oostinga, Jeroen B., Hubert B. Heersche, Xinglan Liu, Alberto F. Morpurgo, and Lieven M. K. Vandersypen, 2007, "Gate-induced insulating state in bilayer graphene devices," Nat. Mater. **7**, 151.

Oostinga, Jeroen B., Benjamin Sacépé, Monica F. Craciun, and Alberto F. Morpurgo, 2010, "Magnetotransport through graphene nanoribbons," Phys. Rev. B **81**, 193408.

Orlita, M, and M. Potemski, 2010, "Dirac electronic states in graphene systems: optical spectroscopy studies," Semicond. Sci. Technol. **25**, 063001.

Oshima, Chuhei, and Ayato Nagashima, 1997, "Ultra-thin epitaxial films of graphite and hexagonal boron nitride on solid surfaces," J. Phys. Condens. Matter **9**, 1.

Papagno, Marco, Stefano Rusponi, Polina Makarovna Sheverdyaeva, Sergio Vlaic, Markus Etzkorn, Daniela Pacilé, Paolo Moras, Carlo Carbone, and Harald Brune, 2012, "Large Band Gap Opening between Graphene Dirac Cones Induced by Na Adsorption onto an Ir Superlattice," ACS Nano **6**, 199.

Park, Cheol-Hwan, Feliciano Giustino, Marvin L. Cohen, and Steven G. Louie, 2007, "Velocity Renormalization and Carrier Lifetime in Graphene from the Electron-Phonon Interaction," Phys. Rev. Lett. **99**, 086804.

Park, Cheol-Hwan, Feliciano Giustino, Marvin L. Cohen, and Steven G. Louie, 2008, "Electron Phonon Interactions in Graphene, Bilayer Graphene, and Graphite," Nano Lett. **8**, 4229.

Park, Cheol-Hwan, Feliciano Giustino, Jessica L. McChesney, Aaron Bostwick, Taisuke Ohta, Eli Rotenberg, Marvin L. Cohen, and Steven G. Louie, 2008, "Van Hove singularity and apparent

anisotropy in the electron-phonon interaction in graphene," Phys. Rev. B **77**, 113410.
Park, Cheol-Hwan, Li Yang, Young-Woo Son, Marvin L. Cohen, and Steven G. Louie, 2008a, "New Generation of Massless Dirac Fermions in Graphene under External Periodic Potentials," Phys. Rev. Lett. **101**, 126804.
Park, Cheol-Hwan, Li Yang, Young-Woo Son, Marvin L. Cohen, and Steven G. Louie, 2008b, "Anisotropic behaviours of massless Dirac fermions in graphene under periodic potentials," Nat. Phys. **4**, 213.
Pereira, Vitor M., and A. H. Castro Neto, 2009, "Strain Engineering of Graphene's Electronic Structure," Phys. Rev. Lett. **103**, 046801.
Peres, N. M. R., 2010, "*Colloquium*: The transport properties of graphene: An introduction," Rev. Mod. Phys. **82**, 2673.
Peres, N. M. R., F. Guinea, and A. H. Castro Neto, 2006, "Electronic properties of disordered two-dimensional carbon," Phys. Rev. B **73**, 125411.
Peres, N. M. R., R. M. Ribeiro, and A. H. Castro Neto, 2010, "Excitonic Effects in the Optical Conductivity of Gated Graphene," Phys. Rev. Lett. **105**, 055501.
Peres, N. M. R., T. Stauber, and A. H. Castro Neto, 2008, "The infrared conductivity of graphene on top of silicon oxide," Europhys. Lett. **84**, 38 002.
Petković, I., F. I. B. Williams, K. Bennaceur, F. Portier, P. Roche, and D. C. Glattli, 2013, "Carrier Drift Velocity and Edge Magnetoplasmons in Graphene," Phys. Rev. Lett. **110**, 016801.
Pfnür, H, T. Langer, J. Baringhaus, and C. Tegenkamp, 2011, "Multiple plasmon excitations in adsorbed two-dimensional systems," J. Phys. Condens. Matter **23**, 112204.
Pisana, Simone, Michele Lazzeri, Cinzia Casiraghi, Kostya S. Novoselov, A. K. Geim, Andrea C. Ferrari, and Francesco Mauri, 2007, "Breakdown of the adiabatic Born-Oppenheimer approximation in graphene," Nat. Mater. **6**, 198.
Piscanec, S., M. Lazzeri, Francesco Mauri, A. C. Ferrari, and J. Robertson, 2004, "Kohn Anomalies and Electron-Phonon Interactions in Graphite," Phys. Rev. Lett. **93**, 185503.
Pletikosić, I., M. Kralj, P. Pervan, R. Brako, J. Coraux, A. T. N'Diaye, C. Busse, and T. Michely, 2009, "Dirac Cones and Minigaps for Graphene on Ir(111)," Phys. Rev. Lett. **102**, 056808.
Polini, Marco, Reza Asgari, Yafis Barlas, T. Pereg-Barnea, and A. H. MacDonald, 2007, "Graphene: A pseudochiral Fermi liquid," Solid State Commun. **143**, 58.
Polini, Marco, Reza Asgari, Giovanni Borghi, Yafis Barlas, T. Pereg-Barnea, and A. H. MacDonald, 2008, "Plasmons and the spectral function of graphene," Phys. Rev. B **77**, 081411(R).
Ponomarenko, L. A., R. Yang, R. V. Gorbachev, P. Blake, A. S. Mayorov, K. S. Novoselov, M. I. Katsnelson, and A. K. Geim, 2010, "Density of States and Zero Landau Level Probed through Capacitance of Graphene," Phys. Rev. Lett. **105**, 136801.
Ponomarenko, L. A., *et al.*, 2011, "Tunable metal-insulator transition in double-layer graphene heterostructures," Nat. Phys. **7**, 958.
Ponomarenko, L. A., *et al.*, 2013, "Cloning of Dirac fermions in graphene superlattices," Nature (London) **497**, 594.
Principi, A., Marco Polini, Reza Asgari, and A. H. MacDonald, 2012, "The tunneling density-of-states of interacting massless Dirac fermions," Solid State Commun. **152**, 1456.
Principi, Alessandro, Giovanni Vignale, Matteo Carrega, and Marco Polini, 2013a, "The impact of disorder on Dirac plasmon losses," Phys. Rev. B **88**, 121405(R).
Principi, Alessandro, Giovanni Vignale, Matteo Carrega, and Marco Polini, 2013b, "Intrinsic lifetime of Dirac plasmons in graphene," Phys. Rev. B **88**, 195405.
Proctor, John E., Eugene Gregoryanz, Konstantin S. Novoselov, Mustafa Lotya, Jonathan N. Coleman, and Matthew P. Halsall, 2009, "High-pressure Raman spectroscopy of graphene," Phys. Rev. B **80**, 073408.
Qazilbash, M. M., J. J. Hamlin, R. E. Baumbach, Lijun Zhang, D. J. Singh, M. B. Maple, and D. N. Basov, 2009, "Electronic correlations in the iron pnictides," Nat. Phys. **5**, 647.
Rader, O., A. Varykhalov, J. Sánchez-Barriga, D. Marchenko, A. Rybkin, and A. M. Shikin, 2009, "Is There a Rashba Effect in Graphene on 3*d* Ferromagnets?" Phys. Rev. Lett. **102**, 057602.
Ren, Lei, *et al.*, 2012, "Terahertz and Infrared Spectroscopy of Gated Large-Area Graphene," Nano Lett. **12**, 3711.
Riedl, C., C. Coletti, T. Iwasaki, A. A. Zakharov, and U. Starke, 2009, "Quasi-Free-Standing Epitaxial Graphene on SiC Obtained by Hydrogen Intercalation," Phys. Rev. Lett. **103**, 246804.
Roddaro, S., P. Pingue, V. Piazza, V. Pellegrini, and F. Beltram, 2007, "The Optical Visibility of Graphene: Interference Colors of Ultrathin Graphite on SiO_2," Nano Lett. **7**, 2707.
Roldán, R. R., J.-N. Fuchs, and M. O. Goerbig, 2009, "Collective modes of doped graphene and a standard two-dimensional electron gas in a strong magnetic field: Linear magnetoplasmons versus magnetoexcitons," Phys. Rev. B **80**, 085408.
Rollings, E., G.-H. Gweon, S. Y. Zhou, B. S. Mun, J. L. McChesney, B. S. Hussain, A. V. Fedorov, P. N. First, W. A. de Heer, and A. Lanzara, 2006, "Synthesis and characterization of atomically thin graphite films on a silicon carbide substrate," J. Phys. Chem. Solids **67**, 2172.
Rossi, Enrico, and Sankar Das Sarma, "Ground State of Graphene in the Presence of Random Charged Impurities," Phys. Rev. Lett. **101**, 166803 (2008).
Rouhi, Nima, Santiago Capdevila, Dheeraj Jain, Katayoun Zand, Yung Wang, Elliott Brown, Lluis Jofre, and Peter Burke, 2012, "Terahertz graphene optics," Nano Res. **5**, 667.
Rutter, G. M., J. N. Crain, N. P. Guisinger, T. Li, P. N. First, and J. A. Stroscio, 2007, "Scattering and Interference in Epitaxial Graphene," Science **317**, 219.
Sabio, J., J. Nilsson, and A. H. Castro Neto, 2008, "f-sum rule and unconventional spectral weight transfer in graphene," Phys. Rev. B **78**, 075410.
Sadowski, M. L., G. Martinez, M. Potemski, C. Berger, and W. A. de Heer, 2006, "Landau Level Spectroscopy of Ultrathin Graphite Layers," Phys. Rev. Lett. **97**, 266405.
Santoso, I., *et al.*, 2011, "Observation of room-temperature high-energy resonant excitonic effects in graphene," Phys. Rev. B **84**, 081403.
Sasaki, Ken-ichi, Yoshiyuki Kawazoe, and Riichiro Saito, 2005, "Local Energy Gap in Deformed Carbon Nanotubes," Prog. Theor. Phys. **113**, 463.
Scharf, Benedikt, Vasili Perebeinos, Jaroslav Fabian, and Phaedon Avouris, 2013, "Effects of optical and surface polar phonons on the optical conductivity of doped graphene," Phys. Rev. B **87**, 035414.
Schedin, F., A. K. Geim, S. V. Morozov, E. W. Hill, P. Blake, M. I. Katsnelson, and K. S. Novoselov, 2007, "Detection of individual gas molecules adsorbed on graphene," Nat. Mater. **6**, 652.
Schmidt, Manuel. J., and Daniel Loss, 2010, "Edge states and enhanced spin-orbit interaction at graphene/graphane interfaces," Phys. Rev. B **81**, 165439.
Shallcross, S., S. Sharma, E. Kandelaki, and O. A. Pankratov, 2010, "Electronic structure of turbostratic graphene," Phys. Rev. B **81**, 165105.
Sheehy, Daniel E., and Jörg Schmalian, 2007, "Quantum Critical Scaling in Graphene," Phys. Rev. Lett. **99**, 226803.
Sheehy, Daniel E., and Jörg Schmalian, 2009, "Optical transparency of graphene as determined by the fine-structure constant," Phys. Rev. B **80**, 193411.

Shin, S. Y., N. D. Kim, J. G. Kim, K. S. Kim, D. Y. Noh, Kwang S. Kim, and J. W. Chung, 2011, "Control of the π-plasmon in a single layer graphene by charge doping," Appl. Phys. Lett. **99**, 082110.

Shirley, Eric L., L. J. Terminello, A. Santoni, and F. J. Himpsel, 1995, "Brillouin-zone-selection effects in graphite photoelectron angular distributions," Phys. Rev. B **51**, 13 614.

Shklovskii, B. I., 2007, "Simple model of Coulomb disorder and screening in graphene," Phys. Rev. B **76**, 233411.

Siegel, D. A., C. Hwang, A. V. Fedorov, and A. Lanzara, 2012, "Electron-Phonon Coupling in Highly-Screened Graphene," New J. Phys. **14**, 095006.

Siegel, D. A., C. G. Hwang, A. V. Fedorov, and A. Lanzara, 2010, "Quasifreestanding multilayer graphene films on the carbon face of SiC," Phys. Rev. B **81**, 241417.

Siegel, D. A., S. Y. Zhou, F. El Gabaly, A. V. Fedorov, A. K. Schmid, and A. Lanzara, 2008, "Self-doping effects in epitaxially grown graphene," Appl. Phys. Lett. **93**, 243119.

Siegel, David A., Cheol-Hwan Park, Choongyu Hwang, Jack Deslippe, Alexei V. Fedorov, Steven G. Louie, and Alessandra Lanzara, 2011, "Many-body interactions in quasi-freestanding graphene," Proc. Natl. Acad. Sci. U.S.A. **108**, 11 365.

Siegel, David A., William Regan, Alexei V. Fedorov, A. Zettl, and Alessandra Lanzara, 2013, "Charge-Carrier Screening in Single-Layer Graphene," Phys. Rev. Lett. **110**, 146802.

Sławińska, J., I. Zasada, and Z. Klusek, 2010, "Energy gap tuning in graphene on hexagonal boron nitride bilayer system," Phys. Rev. B **81**, 155433.

Sodemann, I., and M. M. Fogler, 2012, "Interaction corrections to the polarization function of graphene," Phys. Rev. B **86**, 115408.

Son, D. T., 2007, "Quantum critical point in graphene approached in the limit of infinitely strong Coulomb interaction," Phys. Rev. B **75**, 235423.

Song, Young Jae, *et al.*, 2010, "High-resolution tunnelling spectroscopy of a graphene quartet," Nature (London) **467**, 185.

Sprinkle, M., *et al.*, 2009, "First Direct Observation of a Nearly Ideal Graphene Band Structure," Phys. Rev. Lett. **103**, 226803.

Stampfer, C., J. Güttinger, S. Hellmüller, F. Molitor, K. Ensslin, and T. Ihn, 2009, "Energy Gaps in Etched Graphene Nanoribbons," Phys. Rev. Lett. **102**, 056403.

Starodub, Elena, Aaron Bostwick, Luca Moreschini, Shu Nie, Farid El Gabaly, Kevin F. McCarty, and Eli Rotenberg, 2011, "In-plane orientation effects on the electronic structure, stability, and Raman scattering of monolayer graphene on Ir(111)," Phys. Rev. B **83**, 125428.

Stauber, T., N. M. R. Peres, and A. H. Castro Neto, 2008, "Conductivity of suspended and non-suspended graphene at finite gate voltage," Phys. Rev. B **78**, 085418.

Stauber, T., N. M. R. Peres, and A. K. Geim, 2008, "Optical conductivity of graphene in the visible region of the spectrum," Phys. Rev. B **78**, 085432.

Stöhr, Rainer J., Roman Kolesov, Jens Pflaum, and Jörg Wrachtrup, 2010, "Fluorescence of laser-created electron-hole plasma in graphene," Phys. Rev. B **82**, 121408(R).

Strait, Jared H., Haining Wang, Shriram Shivaraman, Virgil Shields, Michael Spencer, and Farhan Rana, 2011, "Very Slow Cooling Dynamics of Photoexcited Carriers in Graphene Observed by Optical-Pump Terahertz-Probe Spectroscopy," Nano Lett. **11**, 4902.

Sun, Dong, Charles Divin, Claire Berger, Walt A. de Heer, Phillip N. First, and Theodore B. Norris, 2010, "Spectroscopic Measurement of Interlayer Screening in Multilayer Epitaxial Graphene," Phys. Rev. Lett. **104**, 136802.

Sun, Dong, Zong-Kwei Wu, Charles Divin, Xuebin Li, Claire Berger, Walt A. de Heer, Phillip N. First, and Theodore B. Norris, 2008, "Ultrafast Relaxation of Excited Dirac Fermions in Epitaxial Graphene Using Optical Differential Transmission Spectroscopy," Phys. Rev. Lett. **101**, 157402.

Sun, Zhipei, Tawfique Hasan, Felice Torrisi, Daniel Popa, Giulia Privitera, Fengqiu Wang, Francesco Bonaccorso, Denis M. Basko, and Andrea C. Ferrari, 2010, "Graphene Mode-Locked Ultrafast Laser," ACS Nano **4**, 803.

Sutter, P., M. S. Hybertsen, J. T. Sadowski, and E. Sutter, 2009, "Electronic Structure of Few-Layer Epitaxial Graphene on Ru (0001)," Nano Lett. **9**, 2654.

Suzuura, Hidekatsu, and Tsuneya Ando, 2002, "Phonons and electron-phonon scattering in carbon nanotubes," Phys. Rev. B **65**, 235412.

Szafranek, B. N., D. Schall, M. Otto, D. Neumaier, and H. Kurz, 2010, "Electrical observation of a tunable band gap in bilayer graphene nanoribbons at room temperature," Appl. Phys. Lett. **96**, 112103.

Tan, Y.-W., Y. Zhang, K. Bolotin, Y. Zhao, S. Adam, E. H. Hwang, S. Das Sarma, H. L. Stormer, and P. Kim, 2007, "Measurement of Scattering Rate and Minimum Conductivity in Graphene," Phys. Rev. Lett. **99**, 246803.

Tang, Tsung-Ta, *et al.*, 2010, "A tunable phonon-exciton Fano system in bilayer graphene," Nat. Nanotechnol. **5**, 32.

Tao, Chenggang, *et al.*, 2011, "Spatially resolving edge states of chiral graphene nanoribbons," Nat. Phys. **7**, 616.

Tapasztó, Levente, Péter Nemes-Incze, Gergely Dobrik, Kwon Jae Yoo, Chanyong Hwang, and László P. Biró, 2012, "Mapping the electronic properties of individual graphene grain boundaries," Appl. Phys. Lett. **100**, 053114.

Tassin, Philippe, Thomas Koschny, Maria Kafesaki, and Costas M. Soukoulis, 2012, "A comparison of graphene, superconductors and metals as conductors for metamaterials and plasmonics," Nat. Photonics **6**, 259.

Tegenkamp, C., H. Pfnür, T. Langer, J. Baringhaus, and H. W. Schumacher, 2011, "Plasmon electron-hole resonance in epitaxial graphene," J. Phys. Condens. Matter **23**, 012001.

Todd, Kathryn, Hung-Tao Chou, Sami Amasha, and David Goldhaber-Gordon, 2009, "Quantum Dot Behavior in Graphene Nanoconstrictions," Nano Lett. **9**, 416.

Trambly de Laissardiére, G., D. Mayou, and L. Magaud, 2010, "Localization of Dirac Electrons in Rotated Graphene Bilayers," Nano Lett. **10**, 804.

Trauzettel, Bjorn, Denis V. Bulaev, Daniel Loss, and Guido Burkard, 2007, "Spin qubits in graphene quantum dots," Nat. Phys. **3**, 192.

Tsoukleri, Georgia, John Parthenios, Konstantinos Papagelis, Rashid Jalil, Andrea C. Ferrari, Andre K. Geim, Kostya S. Novoselov, and Costas Galiotis, 2009, "Subjecting a Graphene Monolayer to Tension and Compression," Small **5**, 2397.

Tudorovskiy, T., and S. A. Mikhailov, 2010, "Intervalley plasmons in graphene," Phys. Rev. B **82**, 073411.

Vafek, Oskar, and Kun Yang, 2010, "Many-body instability of Coulomb interacting bilayer graphene: Renormalization group approach," Phys. Rev. B **81**, 041401(R).

Vakil, Ashkan, and Nader Engheta, 2011, "Transformation Optics Using Graphene," Science **332**, 1291.

Valla, T., A. V. Fedorov, P. D. Johnson, and S. L. Hulbert, 1999, "Many-Body Effects in Angle-Resolved Photoemission: Quasiparticle Energy and Lifetime of a Mo(110) Surface State," Phys. Rev. Lett. **83**, 2085.

van Bommel, A. J., J. E. Crombeen, and A. van Tooren, 1975, "LEED and Auger electron observations of the SiC(0001) surface," Surf. Sci. **48**, 463.

Varykhalov, A., J. Sánchez-Barriga, A. M. Shikin, C. Biswas, E. Vescovo, A. Rybkin, D. Marchenko, and O. Rader, 2008, "Electronic and Magnetic Properties of Quasifreestanding Graphene on Ni," Phys. Rev. Lett. **101**, 157601.

Velasco, J., *et al.*, 2012, "Transport spectroscopy of symmetry-broken insulating states in bilayer graphene," Nat. Nanotechnol. **7**, 156.

Volkov, V. A., and S. A. Mikhailov, 1988, "Edge Magnetoplasmons: low frequency weakly damped excitations in inhomogeneoustwo-dimensional electron systems," Zh. Eksp. Teor. Fiz. **94**, 217 [Sov. Phys. JETP **67**, 1639 (1988)].

Wallace, P. R., 1947, "The Band Theory of Graphite," Phys. Rev. **71**, 622.

Wallbank, J. R., A. A. Patel, M. Mucha-Kruczyński, A. K. Geim, and V. I. Fal'ko, 2013, "Generic miniband structure of graphene on a hexagonal substrate," Phys. Rev. B **87**, 245408.

Walter, Andrew L., Shu Nie, Aaron Bostwick, Keun Su Kim, Luca Moreschini, Young Jun Chang, Davide Innocenti, Karsten Horn, Kevin F. McCarty, and Eli Rotenberg, 2011a, "Electronic structure of graphene on single-crystal copper substrates," Phys. Rev. B **84**, 195443.

Walter, Andrew L., *et al.*, 2011b, "Effective screening and the plasmaron bands in graphene," Phys. Rev. B **84**, 085410.

Walter, Andrew L., *et al.*, 2011c, "Highly *p*-doped epitaxial graphene obtained by fluorine intercalation," Appl. Phys. Lett. **98**, 184102.

Wang, B., M.-L. Bocquet, S. Marchini, S. Gunther, and J. Wintterlin, 2008, "Chemical origin of a graphene moiré overlayer on Ru (0001)," Phys. Chem. Chem. Phys. **10**, 3530.

Wang, Feng, Yuanbo Zhang, Chuanshan Tian, Caglar Girit, Alex Zettl, Michael Crommie, and Y. Ron Shen, 2008, "Gate-Variable Optical Transitions in Graphene," Science **320**, 206.

Wang, Y., *et al.*, 2013, "Observing Atomic Collapse Resonances in Artificial Nuclei on Graphene," Science **340**, 734..

Wang, Y., V. W. Brar, A. V. Shytov, Q. Wu, W. Regan, H.-Z. Tsai, A. Zettl, L. S. Levitov, and M. F. Crommie, 2012, "Mapping Dirac Quasiparticles near a Single Coulomb Impurity on Graphene," Nat. Phys. **8**, 653.

Wang, Ying Ying, Zhen Hua Ni, Ting Yu, Ze Xiang Shen, Hao Min Wang, Yi Hong Wu, Wei Chen, and Andrew Thye Shen Wee, 2008, "Raman Studies of Monolayer Graphene: The Substrate Effect," J. Phys. Chem. C **112**, 10 637.

Weeks, Conan, Jun Hu, Jason Alicea, Marcel Franz, and Ruqian Wu, 2011, "Engineering a Robust Quantum Spin Hall State in Graphene via Adatom Deposition," Phys. Rev. X **1**, 021001.

Wehling, T. O., K. S. Novoselov, S. V. Morozov, E. E. Vdovin, M. I. Katsnelson, A. K. Geim, and A. I. Lichtenstein, 2008, "Molecular Doping of Graphene," Nano Lett. **8**, 173.

Weitz, R. T., M. T. Allen, B. E. Feldman, J. Martin, and A. Yacoby, 2010, "Broken-Symmetry States in Doubly Gated Suspended Bilayer Graphene," Science **330**, 812.

Wintterlin, J., and M.-L. Bocquet, 2009, "Graphene on metal surfaces," Surf. Sci. **603**, 1841.

Wright, A. R., X. G. Xu, J. C. Cao, and C. Zhang, 2009, "Strong nonlinear optical response of graphene in the terahertz regime," Appl. Phys. Lett. **95**, 072101.

Wunsch, B., F. Guinea, and F. Sols, 2008, "Dirac-point engineering and topological phase transitions in honeycomb optical lattices," New J. Phys. **10**, 103027.

Wunsch, B., T. Stauber, F. Sols, and F. Guinea, 2006, "Dynamical Polarization of Graphene at Finite Doping," New J. Phys. **8**, 318.

Xia, Fengnian, Damon B. Farmer, Yu-Ming Lin, and Phaedon Avouris, 2010, "Graphene Field-Effect Transistors with High On/Off Current Ratio and Large Transport Band Gap at Room Temperature," Nano Lett. **10**, 715.

Xia, Fengnian, Thomas Mueller, Yu-Ming Lin, Alberto Valdes-Garcia, and Phaedon Avouris, 2009, "Ultrafast graphene photodetector," Nat. Nanotechnol. **4**, 839.

Xia, Jilin, Fang Chen, Jinghong Li, and Nongjian Tao, 2009, "Measurement of the quantum capacitance of graphene," Nat. Nanotechnol. **4**, 505.

Xue, Jiamin, Javier Sanchez-Yamagishi, Danny Bulmash, Philippe Jacquod, Aparna Deshpande, K. Watanabe, T. Taniguchi, Pablo Jarillo-Herrero, and Brian J. LeRoy, 2011, "Scanning tunnelling microscopy and spectroscopy of ultra-flat graphene on hexagonal boron nitride," Nat. Mater. **10**, 282.

Xue, Jiamin, Javier Sanchez-Yamagishi, K. Watanabe, T. Taniguchi, Pablo Jarillo-Herrero, and Brian J. LeRoy, 2012, "Long-Wavelength Local Density of States Oscillations Near Graphene Step Edges," Phys. Rev. Lett. **108**, 016801.

Yan, Hugen, Zhiqiang Li, Xuesong Li, Wenjuan Zhu, Phaedon Avouris, and Fengnian Xia, 2012, "Infrared Spectroscopy of Tunable Dirac Terahertz Magneto-Plasmons in Graphene," Nano Lett. **12**, 3766.

Yan, Hugen, Tony Low, Wenjuan Zhu, Yanqing Wu, Marcus Freitag, Xuesong Li, Francisco Guinea, Phaedon Avouris, and Fengnian Xia, 2013, "Damping pathways of mid-infrared plasmons in graphene nanostructures," Nat. Photonics **7**, 394.

Yan, Hugen, Daohua Song, Kin Fai Mak, Ioannis Chatzakis, Janina Maultzsch, and Tony F. Heinz, 2009, "Time-resolved Raman spectroscopy of optical phonons in graphite: Phonon anharmonic coupling and anomalous stiffening," Phys. Rev. B **80**, 121403(R).

Yan, Hugen, Fengnian Xia, Zhiqiang Li, and Phaedon Avouris, 2012, "Plasmonics of coupled graphene micro-structures," New J. Phys. **14**, 125001.

Yan, Jun, Yuanbo Zhang, Philip Kim, and Aron Pinczuk, 2007, "Electric Field Effect Tuning of Electron-Phonon Coupling in Graphene," Phys. Rev. Lett. **98**, 166802.

Yang, Li, Jack Deslippe, Cheol-Hwan Park, Marvin L. Cohen, and Steven G. Louie, 2009, "Excitonic Effects on the Optical Response of Graphene and Bilayer Graphene," Phys. Rev. Lett. **103**, 186802.

Yang, Wei, *et al.*, 2013, "Epitaxial growth of single-domain graphene on hexagonal boron nitride," Nat. Mater. **12**, 792.

Yankowitz, Matthew, Jiamin Xue, Daniel Cormode, Javier D. Sanchez-Yamagishi, K. Watanabe, T. Taniguchi, Pablo Jarillo-Herrero, Philippe Jacquod, and Brian J. LeRoy, 2012, "Emergence of superlattice Dirac points in graphene on hexagonal boron nitride," Nat. Phys. **8**, 382.

Yu, G. L., *et al.*, 2013, "Interaction phenomena in graphene seen through quantum capacitance," Proc. Natl. Acad. Sci. U.S.A. **110**, 3282.

Yu, P. Y., and M. Cardona, 1999, *Fundamentals of Semiconductors: Physics and Materials Properties* (Springer, Berlin).

Yu, Ting, Zhenhua Ni, Chaoling Du, Yumeng You, Yingying Wang, and Zexiang Shen, 2008, "Raman Mapping Investigation of Graphene on Transparent Flexible Substrate: The Strain Effect," J. Phys. Chem. C **112**, 12 602.

Zhang, Han, Dingyuan Tang, R. J. Knize, Luming Zhao, Qiaoliang Bao, and Kian Ping Loh, 2010, "Graphene mode locked, wavelength-tunable, dissipative soliton fiber laser," Appl. Phys. Lett. **96**, 111112.

Zhang, L. M., and M. M. Fogler, 2008, "Nonlinear Screening and Ballistic Transport in a Graphene *p–n* Junction," Phys. Rev. Lett. **100**, 116804.

Zhang, L. M., Z. Q. Li, D. N. Basov, M. M. Fogler, Z. Hao, and M. C. Martin, 2008, "Determination of the electronic structure of bilayer graphene from infrared spectroscopy," Phys. Rev. B **78**, 235408.

Zhang, Lingfeng M., Michael M. Fogler, and Daniel P. Arovas, 2011, "Magnetoelectric coupling, Berry phase, and Landau level dispersion in a biased bilayer graphene," Phys. Rev. B **84**, 075451.

Zhang, Y., J. P. Small, M. E. S. Amori, and P. Kim, 2005, "Electric Field Modulation of Galvanomagnetic Properties of Mesoscopic Graphite," Phys. Rev. Lett. **94**, 176803.

Zhang, Yuanbo, Victor W. Brar, Caglar Girit, Alex Zettl, and Michael F. Crommie, 2009, "Origin of spatial charge inhomogeneity in graphene," Nat. Phys. **5**, 722.

Zhang, Yuanbo, Victor W. Brar, Feng Wang, Caglar Girit, Yossi Yayon, Melissa Panlasigui, Alex Zettl, and Michael F. Crommie, 2008, "Giant phonon-induced conductance in scanning tunnelling spectroscopy of gate-tunable graphene," Nat. Phys. **4**, 627.

Zhang, Yuanbo, Tsung-Ta Tang, Caglar Girit, Zhao Hao, M. C. Martin, A. Zettl, M. F. Crommie, Y. R. Shen, and F. Wang, 2009, "Direct observation of a widely tunable bandgap in bilayer graphene," Nature (London) **459**, 820.

Zhang, Yuanbo, Yan-Wen, Tan Horst L. Stormer, and Philip Kim, 2005, "Experimental observation of the quantum Hall effect and Berry's phase in graphene," Nature (London) **438**, 201.

Zhou, S. Y., G.-H. Gweon, A. V. Fedorov, P. N. First, W. A. de Heer, D.-H. Lee, F. Guinea, A. H. Castro Neto, and A. Lanzara, 2007, "Substrate-induced bandgap opening in epitaxial graphene," Nat. Mater. **6**, 770.

Zhou, S. Y., G.-H. Gweon, and A. Lanzara, 2006, "Low energy excitations in graphite: The role of dimensionality and lattice defects," Ann. Phys. (N.Y.) **321**, 1730.

Zhou, S. Y., D. A. Siegel, A. V. Fedorov, F. El Gabaly, A. K. Schmid, A. H. Castro Neto, D.-H. Lee, and A. Lanzara, 2008, "Origin of the energy bandgap in epitaxial graphene," Nat. Mater. **7**, 259.

Zhou, S. Y., D. A. Siegel, A. V. Fedorov, and A. Lanzara, 2008a, "Metal to Insulator Transition in Epitaxial Graphene Induced by Molecular Doping," Phys. Rev. Lett. **101**, 086402.

Zhou, S. Y., D. A. Siegel, A. V. Fedorov, and A. Lanzara, 2008b, "Kohn anomaly and interplay of electron-electron and electron-phonon interactions in epitaxial graphene," Phys. Rev. B **78**, 193404.

Zhou, S. Y., D. A. Siegel, A. V. Fedorov, and A. Lanzara, 2008c, "Departure from the conical dispersion in epitaxial graphene," Physica E (Amsterdam) **40**, 2642.

Ziegler, K., 2007, "Minimal conductivity of graphene: Nonuniversal values from the Kubo formula," Phys. Rev. B **75**, 233407.